Molecular, Cellular, and Circuit Analysis of *C. elegans* Spitting Behavior

by

Steven R. Sando

B.A. Biochemistry
Grinnell College, 2011

Submitted to the Department of Biology
in Partial Fulfillment of the Requirements for the Degree of

Doctor of Philosophy

at the

Massachusetts Institute of Technology

February 2020

Signature redacted

Signature of Author: __ _____
Department of Biology
September 12, 2019

Signature redacted

Certified by: _____ _____
H. Robert Horvitz
Professor of Biology
Thesis Supervisor

Signature redacted

Accepted by: _____ _____
Stephen Bell
Professor of Biology
Co-Chair, Biology Graduate Committee

Molecular, Cellular, and Circuit Analysis of a *C. elegans* Spitting Behavior

by Steven R. Sando

Submitted to the MIT Department of Biology

On September 17, 2019 in Partial Fulfillment of the Requirements

For the Degree of Doctor of Philosophy in Biology

Abstract

To identify the neural and molecular substrates of animal behavior and understand the principles by which they function is a major goal in neurobiology. One simple system for such behavioral studies is the pharynx of the nematode worm *C. elegans*, which contracts rhythmically (pumps) to ingest food. The connectivity (connectome) of the 20 pharyngeal neurons has been completely determined, making the pharynx one of the anatomically simplest and best-defined neuromuscular systems known to science. Previous work showed that ultraviolet (UV) light interrupts and modulates the pharyngeal pumping rhythm. This modulation requires the gustatory receptor orthologs *lite-1* and *gur-3.* Because *lite-1* and *gur-3* control a similar pharyngeal response to hydrogen peroxide, the pharyngeal response to light was proposed to be a gustatory response to noxious chemical products of photooxidation (Bhatla and Horvitz, 2015).

Here, we report that UV light induces a novel pharyngeal behavior: the spitting of the pharyngeal contents from the pharynx. Using this behavior as a model to study how a simple nervous system encodes an inversion of function (i.e., switching from feeding to spitting), we identified biomechanical mechanisms of and neural circuitry for spitting. Spitting results from the sustained contraction of pharyngeal muscles pm1, pm2, and/or pm3. This contraction opens the food-trapping pharyngeal valve that normally captures food during feeding, resulting in spitting. Spatially restricted calcium increases in pm1, pm2, and/or pm3 colocalize with the site of contraction. As reported previously (Bhatla *et al.*, 2015), spitting requires the M1 pharyngeal neuron, which directly innervates pm1, pm2, and pm3. M1 responds to UV light with calcium increases, and activation of M1 produces spitting. UV light-induced spitting requires *lite-1* and *gur-3*. *gur-3* functions in the I2 and I4 pharyngeal neurons and at least one other undetermined location to produce M1-dependent spitting. We propose that M1 acts as a functional hub for spitting, upon which multiple other neurons in the pharyngeal nervous system converge. Our work identifies a simple motif that controls an inversion of behavioral function and suggests that the M1 neuron is an important point of control in the pharyngeal network.

Thesis advisor: H. Robert Horvitz
Title: Professor of Biology

Biographical Note

Education:

Ph.D. Candidate in Biology, Horvitz laboratory, MIT, Cambridge, MA *2011-2019*
B.A. Biochemistry, Grinnell College, Grinnell, IA *2011*
IES Freiburg and Albert-Ludwigs-Universität, Freiburg, Germany *2010*

Research Experience:

Amgen Neuroscience Department, Cambridge, MA
Intern: *2017*
Used immunofluorescence and confocal microscopy to visualize cellular localization of CGRP-pathway components in trigeminal ganglia. Mentor: Jacinthe Gingras, PhD.

Levandoski laboratory, Department of Chemistry, Grinnell College, Grinnell, IA
Student Research Project: *2009-2011*
Used site-directed mutagenesis to help identify the binding site of an allosteric modulator of the nicotinic acetylcholine receptor (see publications below).

Gygi Laboratory, Department of Cell Biology, Harvard Medical School, Boston, MA
Summer Student: *2008*
HPLC purification and TNBS quantification of peptides used in Kubota *et al.,* Sensitive multiplexed analysis of kinase activities and activity-based kinase identification. Nature Biotechnology, 2009;27:933-942.
Basic Science Partnership Fellow: *2007*
Optimized sample preparation methods for mass spectrometry proteomic analysis.

Academic Achievements and Awards:

MIT
Conference Poster Prize: CeNeuro 2018 *2018*
Friends of the McGovern Institute Student Fellow, McGovern Institute *2017-2018*
Gene Brown-Merck Graduate Teaching Award, Department of Biology *2015*
Honorable Mention: NSF Graduate Research Fellowship *2012*

Grinnell College
Trustee Honor Scholarship *2007-2011*
Thomas and Charlotte Taylor Scholarship *2008-2009*

Publications:

Bhatla N, Droste R, Sando S, Huang H, and Horvitz HR. Distinct neural circuits control rhythm inhibition and spitting by the myogenic pharynx of *C. elegans.* Current Biology, 2015;25(16):2075-89.

Cesa LC, Higgins CA, Sando SR, Kuo DW, and Levandoski MM. Specificity determinants of allosteric modulation in the neuronal nicotinic acetylcholine receptor: a fine line between inhibition and potentiation. Mol Pharmacol., 2012;81(2):239-49.

Presentations:

Talks

MIT Building 68 Retreat, June 2018. Sando SR, Bhatla N, Horvitz HR. Analyzing a Novel *C. elegans* Spitting Behavior.

Boston Area Worm Meeting, March 2018. Sando SR, Bhatla N, Lee ELQ, Horvitz HR. Opposing behaviors driven by a single pharyngeal neuron.

CeNeuro2016, *C. elegans* Topic Meeting: Neuronal Development, Synaptic Function, and Behavior, 2016. Sando SR, Bhatla B, and Horvitz HR. Abstract O-28: The Pharyngeal I2 Neurons Are Multifunctional Command Neurons that Respond to Noxious Stimuli by Reducing Food Intake via Inhibition of Feeding and Stimulation of Spitting.

20th International *C. elegans* Meeting, 2015. Plenary section: Sando SR, Bhatla B, and Horvitz HR. Abstract #193: Noxious Stimuli Induce Spitting by *C. elegans* via Spatially-Restricted Calcium Increases in Pharyngeal Muscle.

Posters

CeNeuro2018, *C. elegans* Topic Meeting: Neuronal Development, Synaptic Function, and Behavior, 2018. Sando SR, Lee ELQ, Horvitz HR. Abstract #158: Spitting and Gulping: Opposite Feeding Behaviors Produced by the Graded Activity of a Single Pharyngeal Neuron.

C. elegans Topic Meeting: Neuronal Development, Synaptic Function, and Behavior, 2014. Sando SR, Bhatla N, and Horvitz HR. Abstract #100: Light Induces a Pharyngeal Gag Reflex by *C. elegans*.

19th International *C. elegans* Meeting, 2013. Sando SR and Horvitz HR. Abstract #589: *lgc-40* Encodes a Choline-Gated Chloride Channel Subunit Expressed in Neurons and Muscles.

Conference of the Society for Neuroscience 2010: MM Levandoski, CA Higgins, SR Sando, LC Cesa, DW Kuo. Abstract 39.14: Defining a Positive-Negative Allosteric Modulator Switch in Nicotinic Receptors.

Teaching Experience:

MIT

Invited speaker, Milton Academy, Milton MA	*4/5/2018*
Guest lecturer, Fitchburg State University, Fitchburg MA	*3/19/2018*
Teaching Assistant, 7.29/9.01 Cellular Neurobiology	*2015*
Teaching Assistant, 7.52 Graduate Genetics	*2012*
Biology teacher, English as a Second Language (ESL) Program, MIT:	*2014-2015*

Developed and taught a course for two MIT employees speaking English as a second language to prepare them for the Massachusetts MCAS Biology standardized test as part of obtaining a GED.

Tutor, English as a Second Language (ESL) Program, MIT	*2013, 2018-2019*
Tutor, 7.52 Graduate Genetics	*2013-2015*

Grinnell College

Teaching Assistant, Biochemistry	*2011*
Teaching Assistant, Molecular Biology Laboratory	*2009-2010*
Tutor, Organic Chemistry	*2009-2010*

Acknowledgments

The work described in this thesis would have been impossible without the mentorship and support of many people over the years.

First, I want to thank my thesis advisor, Bob Horvitz. Bob has created a rigorous and inspiring environment in which to do science, and I have been continuously challenged to learn and grow over the course of my time here. Bob has also brought an incredible group of people together and led by example to create a wonderful research community: in addition to being intellectually exciting and fulfilling, the Horvitz lab is a kind, supportive, and fun place. Bob has taught me how to think about science and genetics in a rigorous way, and his high standards have always driven me to improve. In particular, he has instilled in me an infinite optimism that any idea, no matter how nuanced, complex, or abstract, can be expressed clearly and unambiguously using the written word, all while remaining below the relevant character limit. Bob gave me the freedom to pursue my curiosity and learn first-hand through experience how to approach a problem in biology. However, he was always available to give me a nudge in the right direction when I became stuck or lost my way. I also remember fondly times when I had the opportunity to work closely with Bob, in particular while TAing the graduate genetics course and working on grant writing, experiences that led me to learn and grow tremendously. Bob has also been very supportive of me throughout my time in the lab, for which I am very grateful.

I also want to thank my thesis committee members, Troy Littleton and Peter Reddien, for being on my thesis committee and sharing their input and feedback over the years. Troy has probably taught me more about neuroscience than any other person, and his insightful and critical comments have continuously improved the project in numerous ways. I especially valued and grew during the opportunity to TA his cellular neurobiology course. Peter has always amazed me with his creativity, logic, and ability to think outside the box, and has been a constant source of encouragement and inspiration in my explorations. I also thank Eve Marder for serving on my thesis defense committee and providing insightful comments and criticisms.

The Horvitz lab has been a second family to me over the course of my time at MIT. My baymate Nikhil Bhatla influenced my path more than anybody else at MIT and has been a generous mentor and kind friend over the years. In addition to laying the foundations of my studies via his work and collaborating with me in a number of experiments, Nikhil has been an endless source of encouragement, discussions, critiques, suggestions, wisdom, and inspiration. I consider myself very fortunate to have had the opportunity to work with Nikhil so closely. I am also especially grateful to Na An, our lab manager and adoptive mother, without whose constant and tireless support none of my work would have been possible. Nick Anisimov and Rita Droste provided essential support and have been close friends over the years. Cory Pender was my lab twin and responsible for endless fun, adventure, and scientific growth over the years. Vivek Dwivedi has been

my lab brother and in particular has been my go-to man for all things related to cloning and molecular biology. I also give special thanks to everyone I had the great pleasure of sharing 68-417 with: Kostas Boulias, Holly Johnsen, Nikhil Bhatla, Eugene Lee, and Marco Suarez. I thank Eugene especially for his enormous contributions to data analysis in the later stages of my project. Dipon Ghosh has been a generous and insightful labmate upon whom I have often depended, and Dan Denning and Dengke Ma were early sources of inspiration in the lab. Finally, Kaitlin Driscoll, Anna Corrionero, Akiko Doi, and Kirk Burkhart accompanied me through all or most of my Horvitz lab journey as kind friends and insightful colleagues.

It would be impossible to imagine working with *C. elegans* at MIT without our neighbors the Kim Lab, who have been incredible peers and colleagues. In particular, I thank Josh Meisel, Dan Pagano, and Doug Cattie for years of friendship and various adventures inside and outside the world of *C. elegans*.

I am also deeply grateful to the many teachers and mentors who supported and encouraged my path in science before my graduate studies. I am particularly indebted to Linde Eyster, my high school biology teacher, who first awakened my fascination with the workings of biological systems and subsequently gave me the tools to start thinking about such systems rigorously. After I graduated from high school, Steve Gygi took me on in his lab as a summer student, which gave me my first thrilling experiences with real biological research. In the Gygi lab, Don Kirkpatrick and Kazu Kubota mentored me and taught me almost everything I learned there. During my studies at Grinnell College, Mark Levandoski was an inspiration, bringing science and biochemistry to life and encouraging me to journey deeper into the world of science.

My work would have been impossible without the work of many other people at MIT who supported me in a number of capacities. Betsey Walsh, Janice Chang, and Maggie Cabral have all played indispensable roles in making the grad program and Building 68 run smoothly. I am especially indebted to Stephen Goldman, who led us safely through many issues with our lab servers and computer systems that I would have been unable to resolve on my own. Ike Brochu, Kate Quinn, Kathleen Cahill, Shawn Ferullo, and Xiaolu Hsi all provided essential support in a variety of ways. I also thank the many professors who taught, encouraged, inspired, and/or supported me at MIT, in particular Frank Solomon, Dennis Kim, Chip Quinn, Wendy Gilbert, Steve Flavell, and Amy Keating. Jacinthe Gingras mentored me in my internship at Amgen and in doing so gave me a peek into a very different and equally fascinating world of science.

I am deeply grateful for the wonderful people I have had the good fortune to call my friends in this part of my life and who have enriched my years here in so many ways. I thank my fellow biograds who accompanied me through the various ups and downs of my journey through MIT, especially Audra Amasino, Paggard Champasa, Grace Chen, Jonathon Coravos, Kunle Demuren, Alex Godfrey, Aaron Hosios, Kellie Kravarik, Sean McGeary, Dave Phizicky, Laura Frawley, and Eugene Serebryany, and Faye Vassel. I am also grateful for my friendships with others in the greater community of MIT biology

and beyond - Tom O'Grady, Stephen Eichhorn, Jamie Kwasnieski, Mark Mimee, Mike Erickson, and Shu Dar Yao. Xenia Ferran has been and stayed a close friend in spite of living ~4,000 miles away. Jared and Laurie Berezin get special thanks for their continuous support and facilitating many musical adventures, most especially those with Nick Anisimov and Dave Darmofal. Finally, Stephanie Kinkle has been a close friend and support for so many of my years at MIT that I can't imagine what things would have been like without her.

I have been fortunate to live with many incredible people who have enhanced my life here immeasurably as housemates: Adi Jaishankar, Leo Banchik, Cory Pender, Aaron Hosios, and Andrea Hirbst. I am also grateful for the friendships I found outside of MIT, and in particular thank Matt and Marissa Cruz and the amazing friend-family I have gotten to know through them: Jill Barry, Kevin Wessel, Dave Pezzano, Kristen Salerno, Dan Wallach, Megan Brasch, Matt Vick, Kathryn Milograno, Kyle Rundles, and Jordan Garfinkle. I have also found myself in grateful possession of an extended rock-climbing family, namely my top-rope buddies Jon Elliot, Lawrence Li, TK Mosher, Chris Bridge, and Chelsea Rosenberg and my Sunday morning bouldering buddies Ash Wilsily, Jacob Reyna, Paul Murray, Lekha, Emily, and Anders Simpson-Wolf. I also thank the college friends who have continued to be a big part of my life in my years at MIT: Adam Wert, Brita Higgins, Bianca Silva, Kevin Parker, Seth Treber, Ben Flebbe, Jakob Gowell, Sara Woolery, Alex Cohn, and Stephanie Cheung. I have had the great fortune to enjoy many long and rewarding years of friendship with those who knew me in high school or before and who continuously reenergize and reorient me: Nick and Kaylee Dougherty, Veronika Sykorova, Mariya Shapiro, Hanna Tonegawa, Matt Schoen, and Ivan Kozyryev. I've also had the lucky windfall of being able grow into friendships with many of the people I looked up to as my seniors at the time – Neil Katuna, Andrew Pinkham, Julia Kingsdale, Matt Miller, Clara Kim and John Mussman. None of that would have been possible without Lee Seymour, one of the rare people who brings the best out of anybody and everybody, for bringing everyone together. I am particularly thankful for many years of friendship with my all-but-brother Jono Forbes, who is a source of constant support and inspiration to me. Finally, I am grateful for the support and friendship of Anna Ford, who has accompanied and supported me through many of the longest years of my thesis work.

The foundation for my relationships with everyone above and everything that follows in this thesis is my family: my parents, my grandmother, and my two sisters, who I thank for a literal lifetime of unflagging love, support, encouragement, and fun. I count myself very fortunate, and look forward to many more years of continued journey together.

Table of Contents

Chapter 1

Introduction

I. Overview

Light is essential for most life on earth and has major effects on living organisms. Thus, animals have evolved a variety of adaptations to detect and respond to light. This thesis describes aspects of a behavioral response of the *C. elegans* pharynx to ultraviolet light. In this introductory chapter, I will provide context for these studies by briefly reviewing general aspects of the molecular and cellular adaptations used by animals to detect light. I will also review previous studies of the *C. elegans* response to ultraviolet light.

II. The detection of ultraviolet light by animals

The great majority of organisms depend directly or indirectly on light for life, using it for vision, navigation, and the anticipation of seasonal changes, amongst other things (Cronin and Bok, 2016; Pérez *et al.*, 2019). Ultraviolet (UV) light, which is conventionally divided into UVA (315-400 nm), UVB (280-315 nm), and UVC (100-280 nm), is an important component of light with significant impacts on life. While UVC is blocked by the atmosphere, UVB and UVA light reach and impact organisms living on Earth's surface. Although it is imperceptible to humans, many animals can perceive light in the UVA range (Cronin and Bok, 2016). This ability can be useful simply because it expands the range of colors that organisms can detect. Furthermore, UVA light's scattering properties in the atmosphere and water make it useful for the detection of prey and predators, while many insects can utilize the constant polarization pattern of UVA light in the sky for orientation during navigation (Cronin and Bok, 2016). Conversely, UV light can also be hazardous. In particular, the high-energy UVA and UVB components of sunlight can damage biological tissue and DNA (Hockberger, 2012; Cronin and Bok, 2016; Schuch *et al.*, 2017). Thus, animals have developed a variety of cellular, anatomical, and molecular systems for light detection, and the sensitivity of many of these systems extends into the UV spectrum (Hockberger, 2012; Cronin and Bok, 2016).

III. Cellular, anatomical, and molecular adaptations for the detection of light

At the cellular level, animals have evolved specialized photoreceptor cells to efficiently capture photons from the environment. Two major classes of photoreceptor cells are found in animals, named based on their characteristic cellular morphologies. Both photoreceptor types enhance their light-detecting properties by increasing the surface area of the pigment-bearing membranes used for light capture. Rhabdomeric photoreceptor cells expand their light-sensing membranes' area by folding the apical cell surface, while the ciliary photoreceptors do so by folding membrane drawn from the cilium (Arendt, 2003; Lamb *et al.*, 2007). Molecular comparison of genes that function in photoreceptor development suggest rhabdomeric and ciliated photoreceptors likely evolved from a single progenitor cell (Arendt, 2003). Historically, rhabdomeric and ciliary photoreceptors were believed to be specific to protostomes and deuterostomes respectively; however, it is now known that both types occur in both clades, sometimes in the same animal (Arendt, 2003; Lamb *et al.*, 2007).

At the anatomical level, light-sensing organs often take the form of eyes, which allow measurements of light intensity and, to varying degrees, localization to be combined into vision. In addition to functioning in vision, photoreceptor cells in the eye can also contribute to non-visual processes – for example, the entrainment of circadian rhythms and the vertebrate pupillary light reflex that adjusts the aperture size of the pupil (Fu *et al.*, 2005; Pickard and Sollars, 2011).

Photoreceptor cells also commonly occur outside of or in the absence of eyes to influence various aspects of animal physiology and behavior (Yoshida, 1979; Pérez *et al.*, 2019). For example, many eyeless animals possess "shadow reflexes" by which

they withdraw in response to sudden reductions in illumination, presumably to avoid a looming predator (Steven, 1963), while other organisms exhibit eye-independent locomotory increases in the presence of light (Currie *et al.*, 2016). In addition to controlling acutely light-responsive behaviors, extraocular photoreceptors can also regulate responses to chronic light exposure. For example, extraocular photoreceptors control pigmentation changes (for fish, see Pérez *et al.*, 2019; for melanin changes in humans, see Lin and Fisher, 2007; Wicks *et al.*, 2011) and alter reproductive behavior in response to seasonal changes in the duration of the day (Pérez *et al.*, 2019).

Photoreceptor cells can occur not only in rhabdomeric or ciliary form but also in the absence of any of the ultrastructural features described above (Wilkens, 1988; Yoshida, 1979; Gotow and Nishi, 2008; Gotow and Nishi, 2009). Interestingly, some of these "simple photoreceptors" are known to be interneurons or motor neurons that control other behaviors or respond to non-light sensory stimuli, allowing information about surrounding natural light levels to modulate existing reflexes (Wilkens, 1988; Gotow and Nishi, 2009).

While anatomical light-sensing structures exist in near-endless variations, molecular solutions for light-sensing are more limited. To date, seven types of light-sensing proteins have been discovered and characterized: BLUF proteins, cryptochromes, phototropins, phytochromes, rhodopsins, xanthopsins, and UVR8 (van der Horst and Hellingwerf, 2003; O'Hara and Jenkins, 2012). The first six of these proteins use photosensitive chromophores to absorb and detect light (van der Horst and Hellingwerf, 2003), while UVR8's photosensitivity is mediated by tryptophan residues (Christie *et al.*, 2012). With the exception of several cases noted below, animals detect

light almost exclusively via the opsins, G protein-coupled receptors (GPCRs) that use photoisomerizable chromophores derived from vitamin A.

The majority of opsins fall into two phylogenetic groups, the r-opsins and c-opsins, named after the rhabdomeric and ciliated photoreceptor cell types with which they are commonly associated (Arendt, 2003; Yau and Hardie, 2009). As with rhabdomeric and ciliated photoreceptor cells, r-type and c-type opsin photoreceptor molecules predominate in protostomes and deuterostomes respectively. Protostomes and deuterostomes likely shared a common ancestor possessing both c- and r-opsin types, and it is thus not uncommon for both types to be present together in a single organism (Yau and Hardie, 2009). For example, in the vertebrate retina the ciliated rods and cones utilize c-opsins, while the intrinsically photosensitive retinal ganglion cells use the r-type opsin melanopsin (Arendt 2003; Yau and Hardie, 2009; Pickard and Sollars, 2011).

Although all opsins are GPCRs, the r- and c-type opsins utilize distinct second messenger systems, the precise details of which vary from organism to organism (Yau and Hardie, 2009). Briefly, in the ciliated rods of the vertebrate retina, activated rhodopsin produces hyperpolarizing currents. Specifically, rhodopsin activates transducin, which activates cGMP phosphodiesterases. Active phosophodiesterases then reduce intracellular cGMP levels, which closes constitutively active cyclic-nucleotide-gated (CNG) channels, resulting in hyperpolarization. Thus, the effect of phototransduction is to terminate constitutive neuronal signaling in the presence of light. Conversely, photostimulation of rhabdomeric opsins activates a phospholipase C

cascade that opens a TRP channel, resulting in the depolarization of the photoreceptor cell and transduction of the light signal.

Examples of non-opsin light detection systems in animals exist. Animals possess blue light-sensing cryptochromes, which evolved from the photolyase class of light-dependent DNA repair enzymes (Michael *et al.*, 2017). In at least some animals, including *D. melanogaster*, cryptochromes function as blue-light receptors to entrain circadian rhythms. In an interesting evolutionary twist, vertebrate cryptochromes appear to function in circadian rhythms as well, but are not directly involved in the detection of light itself (Michael *et al.,* 2017), this function being filled by melanopsin (Pickard and Sollars, 2011; Michael *et al.*, 2017). In another example, the eponymous sensory organs ("pits") present on the face of pit vipers are sensitive to infrared light, and pit vipers combine thermal imagery derived from these organs with visual information in the brain to track and strike warm-blooded prey in the dark. These unusual sensory organs are derived from the trigeminal nerve and sense infrared light via warmth-sensitive TRPA1 channels (Gracheva *et al.*, 2010). Thus, while uncommon, opsin-independent light-detection systems in animals do exist.

IV. Discovery of an opsin- and cryptochrome-independent light-avoidance behavior by *C. elegans*

In 2008, two groups reported a novel *C. elegans* light-avoidance behavior. Specifically, they discovered that illumination of the worm's head or tail with short-wavelength light drives reverse or forward locomotion, respectively (Edwards *et al.*,

2008; Ward *et al.*, 2008). Worms avoid UV, violet, and blue light. Shorter-wavelength UV light is more aversive, ruling out a possible effect of temperature, which is produced more prominently by longer wavelengths of light. Given that no known light-sensing proteins are encoded by the *C. elegans* genome (Bargmann, 1998; Terakita, 2005; Romanowski, 2014), these findings raised the interesting possibility that worms might detect light through previously uncharacterized molecular mechanisms. As described below, these studies identified a novel potential photoreceptor molecule named LITE-1 and sought to characterize the LITE-1 signal transduction pathway.

Both groups sought to define the opsin-independent molecular phototransduction pathways controlling nematode light avoidance. One group performed an EMS mutagenesis screen to identify mutant animals unable to detect or respond to light (Edwards *et al.,* 2008). This screen identified 20 strains defective in the avoidance of light, 18 of which were found to carry mutations in a previously uncharacterized gene that was subsequently named *lite-1.* These *lite-1* mutants were severely and specifically defective in the avoidance of light. Surprisingly, *lite-1* was found to be similar in sequence to genes from the insect gustatory receptor (*Gr*) family, with the greatest similarity to the *D. melanogaster* gene *Gr28b* (see below for discussion of *Gr28b* specifically and the *Gr*-family generally). Consistent with *lite-1* being actively involved in photo-detection/transduction, heterologous expression of *lite-1* cDNA in the body-wall and egg-laying muscles endowed them with responsiveness to light. Because *lite-1* lacks any known chromophore-binding domain, Edwards *et al.* (2008) proposed that *lite-1* might either possess a chromophore permanently bound via a novel domain or that it

might function without a chromophore, perhaps detecting acutely generated photooxidation products.

The other group identified a potential photoreceptor neuron and characterized components of the putative phototransduction pathway in this cell (Ward *et al.*, 2008). Laser ablations identified a set of 7 pairs of ciliated sensory neurons in the *C. elegans* head that are redundantly required for light avoidance: ASJ, AWB, ASK, ASH, ASI, AWC, and ADL (Ward *et al.*, 2008). Consistent with a ciliary-like phototransduction pathway functioning in all or some of these cells, Ward *et al.* found that avoidance behavior depends on *tax-2*, which encodes a CNG channel subunit. By expressing a wild-type copy of *tax-2* in subsets of the above neurons, they found that expression of wild-type *tax-2* specifically in the ASJ neuron pair of *tax-2* mutants gave the strongest rescue of any single candidate neuron (~55%). Given this major contribution of the ASJs to the behavior, they focused on the ASJ response to light. Using perforated whole-cell recording techniques, they found that light induces a depolarizing, *tax-2*-dependent current in the ASJs. Consistent with the requirement for the CNG channel-encoding *tax-2*, cGMP delivered by dialysis activated ASJ, and chemical inhibition of cGMP-producing guanylate cyclases eliminated the response of the ASJs to light.

Subsequent work on the ciliated ASJ neurons by the same group identified additional components of the putative phototransduction cascade, which was shown to depend on *lite-1*, expression of which in the ASJs restored light-induced currents (Liu *et al.*, 2010). Through a combination of pharmacological and genetic analyses, Liu *et al.* (2010) showed that activation of the ASJs by light depends on signaling via $G_{i/o}$ family G

proteins and specifically depends upon the G_α subunits encoded by *goa-1* and *gpa-3.* Photocurrents required the guanylate cyclases encoded by *daf-11* and *odr-1*.

While the ASJs' ciliated sensory endings and molecular second-messenger system are similar to those of the rods and cones of the vertebrate retina, the ASJs behave unlike canonical ciliated photoreceptors in that they respond to light with depolarization rather than hyperpolarization. This feature of the *lite-1* phototransduction cascade in the ASJs is reminiscent of the unusual phototransduction system of the lizard parietal (or "third") eye, in that light increases, rather than decreases, intracellular cGMP (Xiong *et al.*, 1998). cGMP increases in the parietal eye photoreceptor likely occurs via inhibition of cGMP phosphodiesterases, leading to depolarization of the photoreceptor cell via CNG channels (Xiong *et al.*, 1998). However, the extent of the similarity between the lizard and the worm pathways is unclear: cGMP in the ASJs could be increased either via inhibition of phosphodiesterases or by the activation of guanylate cyclases and Liu *et al.* (2010) were unable to distinguish between these possibilities. Thus, examination of the ASJs' photocurrents suggest that some aspects of the putative *LITE-1* phototransduction pathway are similar to the canonical pathway found in vertebrate rods and cones, while others are distinct.

Shortly thereafter, a third group reported that *D. melanogaster* larvae avoid short-wavelength UV, violet, and blue light in a manner independent of their light-sensing Bolwig organ (Xiang *et al.*, 2010). Avoidance of UV light requires *Gr28b,* the closest *D. melanogaster* homolog to *lite-1. Gr28b* is expressed in the larval class IV dendritic arborization (ddaC) neurons, the dendrites of which branch across the entirety of the larva's surface and are believed to function as nociceptors (Hwang *et al.*, 2007).

Extracellular recordings and calcium imaging of these cells *in vivo* indicate that they are acutely activated by short-wavelength light. Furthermore, this response was preserved when these cells were dissociated and grown in culture, suggesting that they are able to detect light directly. Additionally, genetic ablation and optogenetic activation experiments confirmed the role of the ddaC neurons in light avoidance. Thus, *D. melanogaster* also requires a gustatory receptor paralog to respond to short-wavelength light (Xiang *et al.*, 2010).

V. The gustatory receptor gene family

The insect gustatory receptor (*Gr*) family was originally identified via bioinformatic searches for 7-transmembrane proteins in the *D. melanogaster* genome (Clyne *et al.*, 2000) and was incrementally expanded to ultimately include 68 members (Clyne *et al.*, 2000; Dunipace *et al.*, 2001; Scott *et al.*, 2001; Robertson *et al.*, 2003). *Gr*-family genes are expressed in various taste organs and control behavioral responses to sweet and bitter tastes (Vosshall and Stocker, 2007) and to CO_2 (Kwon *et al.*, 2007). As described above, *Gr28b*, the closest *D. melanogaster* homolog to *lite-1,* was previously shown to function in larval avoidance of short-wavelength light (Xiang *et al.*, 2010). More recently, specific isoforms of *Gr28b* have also been shown to control responses to heat (*Gr28b.d* and perhaps *Gr28b.b*; Ni *et al.*, 2013; Mishra *et al.*. 2018) and the bitter plant-derived insecticide saponin (*Gr28b.c*; Sang *et al.*, 2019).

What is the GR sensory transduction mechanism? By virtue of their predicted 7-transmembrane topology, GRs were initially assumed to be GPCRs, and several G

protein subunits that are expressed in gustatory receptor neurons and required for taste responses were accordingly identified (Ishimoto *et al.*, 2005; Ueno *et al.*, 2006; Yao and Carlson, 2010). Additional evidence, however, has challenged the GPCR model. First, the *Gr*-family genes are distantly related to genes of the insect-specific odorant receptor (*Or*) family (Vosshall and Stocker, 2007). OR-family receptors have been shown to have an inverted membrane topology with the C-terminus facing the extracellular side and the N-terminus facing the cytosol, inconsistent with such receptors being GPCRs (Benton *et al.*, 2006). Consistent with this, Zhang *et al.* (2011) have shown an inverted membrane topology for certain insect GRs (Zhang *et al.*, 2011), and a recent study of *C. elegans* LITE-1 expressed ectopically in cultured muscle cells indicated that LITE-1 adopts this membrane orientation as well (Gong *et al.*, 2016). Second, several groups have succeeded in expressing individual *Gr* genes heterologously in the oocytes of *Xenopus laevis* and found that at least some *Gr* genes, including isoforms of *Gr28b*, confer ligand-induced currents consistent with their encoding nonselective cation channels (Sato *et al.*, 2011; Mishra *et al.*, 2018). GR function as ion channels is also difficult to reconcile with their functioning as GPCRs, although it is possible that GPCRs might function permissively for, upstream of, downstream of, or in parallel to GRs. Thus, despite progress, many aspects of the molecular mechanisms of GR signal transduction remain unclear.

Although the evolution and function of *Gr* genes has not been studied extensively outside of insects, *Gr*-superfamily members have been identified in genomes of organisms across Protostomia, non-Bilateria, and Deuterostomia (chordates excepted) (Saina *et al.*, 2015). Thus, the family likely orginates from before the split of Bilateria

and non-Bilateria (Saina *et al.*, 2015). Intriguingly, a cnidarian *Gr*-family homolog was shown to be expressed in early development, but not in subsequent stages in which the sensory system is fully formed. Surprisingly, morpholino-knockdown of this gene not only produced developmental patterning defects, but also resulted in the disappearance of an apical sensory organ, suggesting that this *Gr* gene might control sensory system development rather than function. Thus, *Gr* family genes might also function in processes other than chemosensation.

VI. Discovery of a *C. elegans* pharyngeal response to light

In a separate line of inquiry, Horvitz lab graduate student Nikhil Bhatla discovered that shining bright violet light inhibits the ingestive pumping rhythm of the *C. elegans* pharynx (Bhatla and Horvitz, 2015). This light-induced inhibition of feeding shares the same wavelength-dependency as the *C. elegans* and *D. melanogaster* light-induced avoidance behaviors described above (Ward *et al.*, 2008; Edwards *et al.*, 2008; Xiang e*t al.*, 2010). Indeed, light-induced inhibition of feeding was found to require both *lite-1* and *lite-1*'s closest *C. elegans* paralog, *gur-3*, a gene of previously unknown function (Bhatla and Horvitz, 2015). *lite-1* mutants were found to be defective in the amplitude of their pumping inhibition (i.e., they do not completely inhibit pumping), while *gur-3* mutants were found to be defective in the latency of inhibition (i.e., they inhibit pumping a few seconds later than wild-type animals). *lite-1* was found to be expressed in four pharyngeal neuron classes (MI, M1, M4, and M5), eleven pairs of extra-pharyngeal neurons, and several hypodermal and glial-like cells, while *gur-3* was found to be expressed in three neuron classes, including the paired pharyngeal I2 neurons

(Bhatla and Horvitz, 2015). These sites of *lite-1* expression partially overlapped with the subset of the ciliated neuron classes previously found by Ward *et al.* to function in light avoidance, specifically ASK, ASH, ASI, and ADL but not ASJ, AWB, and AWC (Ward *et al.*, 2008; Bhatla and Horvitz, 2015). The lack of *lite-1* expression in the ASJ neurons was surprising, as they were previously shown to respond to light and used to identify the putative *lite-1* signal transduction pathway in *C. elegans* (Ward *et al.*, 2008; Liu *et al.*, 2010). This discrepancy observed by Bhatla and Horvitz (2015) might be explained by incomplete capture of the endogenous expression pattern by the reporters used or due to ASJ being downstream of a *lite-1*-expressing cell rather than being directly photosensitive itself.

VII. *C. elegans* might sense light via light's generation of reactive oxygen species

gur-3 was found to function in the I2 neurons, which were shown to be rapidly activated by light and inhibit feeding via glutamate signaling and the glutamate-gated chloride channel encoded by *avr-15* (Bhatla and Horvitz, 2015; Bhatla *et al.*, 2015). Similarly to *lite-1*, *gur-3* was found to confer light sensitivity when ectopically expressed in other cells (Bhatla and Horvitz, 2015).

The evolutionary advantage of expressing light receptors in the mouth and using them to inhibit feeding was unclear. Furthermore, the intensity of light required to activate the *gur-3*-dependent component of the response to light was unnaturally bright. *lite-1* and *gur-3*'s pharyngeal expression pattern and homology to gustatory receptors suggested they might encode chemoreceptors, and Bhatla and Horvitz

(2015) hypothesized that *lite-1* and *gur-3* might detect a chemical or chemicals generated by light, perhaps products of photooxidation, rather than light itself.

Light is known to produce reactive oxygen species (ROS) when shined on biological tissues (Hockberger, 2002). One such photooxidation product is hydrogen peroxide (H_2O_2) (Richardson, 1893; Bedford, 1927; McCormick, 1976; Hockberger *et al.*, 1999). ROS and H_2O_2 can occur environmentally (ECETOC, 1996), but are also generated internally both as aerobic waste products and as participants in specific signaling pathways (Finkel, 2011), with a variety of impacts on biological function (Sundaresan *et al.*, 1995; Salmeen *et al.*, 2003; Niethammer *et al.*, 2009).

Consistent with the hypothesis that worms detect light via an H_2O_2 intermediate, *C. elegans* inhibit pharyngeal pumping when exposed to H_2O_2 vapors (Bhatla and Horvitz, 2015). Furthermore, a variety of other oxidizing substances were also found to activate the I2s (Bhatla and Horvitz, 2015). As with light-mediated pumping inhibition, H_2O_2-mediated pumping inhibition depends on *lite-1* and *gur-3*. This result suggests that *lite-1* and *gur-3* might confer sensitivity to light and H_2O_2 via a common mechanism – consistent with the hypothesis that worms detect light via the generation of H_2O_2. Riboflavin has been shown to function as a photosensitizer for the production of H_2O_2 by light (McCormic *et al.*, 1976), and RNAi against either of *rft-1* or *rft-2*, which encode the *C. elegans* riboflavin transporters, attenuated the response to light (Bhatla and Horvitz, 2015), also consistent with the hypothesis that the response to light might be a response to photooxidation.

Two of the studies described previously also considered and tested the hypothesis that worms and flies detect light via its production of H_2O_2 (Liu *et al.*, 2010;

Xiang *et al.*, 2010). Xiang *et al.* tested 10 μM H_2O_2 and found no effect on the larval class IV dendritic arborization neurons (Xiang *et al.*, 2010). It is possible that this concentration of H_2O_2 was not high enough to elicit a response; for comparison, *lite-1*-dependent pharyngeal and locomotory responses by *C. elegans* were observed starting in the 1-10 mM range (Bhatla and Horvitz, 2015). Secondly, Liu *et al.* (2010) found that perfusion of the ASJ neuron with 1 mM H_2O_2 did indeed induce inward currents, but these currents did not depend on *lite-1*. At the time, *gur-3*'s control of light- and H_2O_2-induced behaviors was not appreciated, so Liu *et al.* (2010) concluded that *lite-1* was likely not involved in H_2O_2-sensing. In hindsight, this result could also be explained by *lite-1* and *gur-3* functioning redundantly to activate the ASJs. It would be interesting to determine the ASJs' response to H_2O_2 in each of *lite-1*, *gur-3,* and *lite-1 gur-3* animals.

Interestingly, Bhatla and Horvitz (2015) showed that *lite-1* and *gur-3* contribute differentially to the pharyngeal responses to light and H_2O_2,, with *lite-1* required for high-affinity light-sensing function and *gur-3* required for high-affinity H_2O_2-sensing function. While *lite-1* mutants are severely defective in the pharyngeal response to light, their pharyngeal response to H_2O_2 is indistinguishable from wild-type animals. Conversely, while *gur-3* mutants are only subtly defective in their pharyngeal response to light, their pharyngeal response to H_2O_2 is severely defective. Mutations in *lite-1* completely eliminate the residual response of *gur-3* mutants to H_2O_2, and *gur-3* mutations conversely eliminate the residual responsiveness of *lite-1* mutants to light, indicating that each gene contributes to the pharyngeal sensing of both stimuli. Furthermore, while the *gur-3*-dependent pharyngeal response requires unnaturally bright light, *lite-1*-dependent inhibition was evoked by direct sunlight in the field and by light powers

approximating the intensity of sunlight in the lab (Bhatla and Horvitz, 2015). The behavioral avoidance of both light and H_2O_2 depends only on *lite-1*. Thus, the ethological function of *gur-3* is likely to detect noxious oxidants and inhibit feeding, while the likely ethological function of *lite-1* seems to be to detect both light (possibly via detection of a photooxidant) and H_2O_2 (or other oxidants) and inhibit feeding and induce avoidance behavior. Each of these behaviors make sense: sustained short-wavelength light kills worms (Ward *et al.*, 2008; Edwards *et al.*, 2008), while H_2O_2 is toxic to worms and has been shown to be released with lethal effects by worm-killing pathogens (Jansen *et al.*, 2002; Bolm *et al.*, 2004; Moy *et al.*, 2004).

VIII. Purification and spectrophotometric characterization of LITE-1

To further explore *lite-1*'s function, Gong *et al.* (2016) expressed *lite-1* transgenically in *C. elegans* muscles and measured the absorbance profile of purified LITE-1 protein using spectrophotometry, reasoning that absorption of UV light would, together with the other evidence presented above, indicate that LITE-1 is a direct photoreceptor (Gong *et al.,* 2016). *lite-1*-expressing muscles robustly increased calcium levels and became paralyzed in response to light. Gong *et al.* (2016) found that purified LITE-1 strongly absorbed UVB and UVA light, with absorbance peaks at 280 and 320 nm, respectively, and that LITE-1's extinction coefficient of light absorption at these wavelengths was 1-2 orders of magnitude greater than those of other opsin photoreceptors characterized previously (Gong *et al.*, 2016). However, while absorbing light is consistent with function as a photoreceptor, this property does not necessitate that a given protein is a photoreceptor, as absorbance simply reflects that ability of a

protein to block light. Gong *et al.* (2016) thus sought evidence for a functional role of the absorbance peaks they detected. To this end, they turned to the *lite-1* mutants they obtained previously in their screen for animals that failed to avoid UVA light (Liu *et al.*, 2010). Two mutations, *lite-1* missense alleles *xu8* and *xu10,* result in respective amino acid changes A332V and S226F in the LITE-1 transmembrane domain regions. Gong *et al.* (2016) purified these proteins and measured their absorbances. As expected, these mutant LITE-1 proteins no longer absorbed UVA. Functional assays of mutant *lite-1* in muscle indicated that they no longer conferred light-induced paralysis and that muscle calcium response to light was greatly diminished, although not eliminated completely. Interestingly, UVB absorbance by these LITE-1 variants was unchanged. Given that UVB but not UVA absorbance was spared, Gong *et al.* (2016) wondered whether the UVB response of these UVA-insensitive mutants might be intact. To test LITE-1 function in vivo, they assayed the response of *lite-1*-expressing body wall muscles to UVA and UVB light. Indeed, *lite-1(xu8)* and *lite-1(xu10)* mutants exhibited wild-type responses to UVB light, as measured by light-induced muscle calcium signals and paralysis. Thus, Gong *et al.* (2016) were able to show a correlation between the absorbance properties of purified LITE-1 and the behavioral responses that *lite-1* controls. This is not biophysical proof that LITE-1 detects light via direct absorption of a photon, but it does suggest that LITE-1's absorbance can be correlated with its function, which implies a close association between LITE-1's absorbance properties and the wavelength-dependencies of *lite-1* mutant animals' responses to light. An additional study subsequently implicated *lite-1* in a color discrimination behavior (Ghosh *et al.*, posted

2017). All of the above taken together, *lite-1*'s involvement in the sensation of light and hydrogen peroxide is unclear.

IX. *dTrpA1*-dependent responses to photooxidation in *D. melanogaster*

LITE-1 is not the first protein suggested to detect light via light's generation of ROS. Contemporarily to Bhatla and Horvitz (2015), several groups reported examples of *D. melanogaster* behavioral responses to light which appear to depend on the detection of photooxidation. Additionally, these studies provided evidence that dTRPA1 TRP channels are capable of responding to H_2O_2 and/or ROS produced by UV light in a way potentially analogous to *lite-1* and *gur-3*.

Kim and Johnson (2014) investigated a previously reported UV-induced writhing behavior of *D. melanogaster*, which occurs independently of the visual system (Baden *et al.*, 1996). This response to light was shown to depend on the mdIV nociceptive neurons that innervate the larval body wall, which were acutely activated by UVC illumination (Kim and Johnson, 2014). Because these neurons were previously shown to be highly responsive to H_2O_2 (Kim *et al.*, 2013), Kim and Johnson (2014) hypothesized that the writhing response might be induced by light-produced H_2O_2. Consistent with this hypothesis, overexpression of catalase or other antioxidant enzymes suppressed UVC-induced writhing. Subsequent studies also observed physiological and behavioral responses to UV and succeeded in blocking them in a similar manner by manipulating ROS production or consumption (Guntur *et al.*, 2015; Guntur *et al.*, 2017).

Additionally, some of these studies implicated the TRP channel dTRPA1 in behavioral responses to light-induced ROS (Guntur *et al.*, 2015; Guntur *et al.*, 2017). Specific isoforms of dTRPA1 were previously implicated in responding to ROS, and mammalian TRPA1 was shown to confer UV light- and H_2O_2-responsiveness when expressed in heterologous systems (Hill and Schaefer, 2008). TRPA1 was subsequently shown to confer light- and H_2O_2-sensitivity to HEK cells and heterologous neurons of *D. melanogaster* larvae and adults (Guntur *et al.*, 2015; Du *et al.*, 2016). Du *et al.* (2016) found endogenous TRPA1(A) conferred UV-sensitivity to labellum taste neurons (Du *et al.*, 2016), while Guntur *et al.* further found that the corpus cardiacum (CC) cells of *D. melanogaster* larvae endogenously express *dTrpA1* and respond to UV light in a *dTrpA1*-dependent manner (Gunter *et al.*, 2015); this response could be blocked with catalase. The response of the CC cells did not depend on *Gr28b*, suggesting that TRPA1 is not simply a *Gr28b* effector (Guntur *et al.*, 2015). Interestingly, while *Gr28b* mutant larvae were partially defective in light avoidance, *dTrpA1* mutant larvae were completely defective (Xiang *et al.*, 2010). Thus, it is possible *dTrpA1* might be responsible for the residual light sensitivity of *Gr28b* mutants that Xiang *et al.* (2010) described. Importantly, the light powers used to evoke these behaviors were comparable to the light of the sun, indicating that these phenomena are likely ethologically significant (Guntur *et al.*, 2015; Du *et al.*, 2016; Gunter *et al.*, 2017). In total, *D. melanogaster* likely use TRPA1 to detect short-wavelength light via light's production of H_2O_2, supporting the hypothesis that ROS-mediated light-detection occurs in nature.

Acknowledgments:

Vivek Dwivedi, Calista Diehl, and Catherine Olsen provided comments on this section.

References

Arendt, D. (2003). Evolution of eyes and photoreceptor cell types. Int. J. Dev. Biol. *47*, 563–571.

Baden, H.P., Kollias, N., Anderson, R.R., Hopkins, T., and Raftery, L. (1996). *Drosophila melanogaster* larvae detect low doses of UVC radiation as manifested by a writhing response. Arch. Insect Biochem. Physiol. *32*, 187–196.

Bargmann, C.I. (1998). Neurobiology of the *Caenorhabditis elegans* genome. Science *282*, 2028–2033.

Bedford, T.H.B. (1927). The nature of the action of ultra-violet light on micro-organisms. Br J Exp Pathol *8*, 437–441.

Benton, R., Sachse, S., Michnick, S.W., and Vosshall, L.B. (2006). Atypical membrane topology and heteromeric function of *Drosophila* odorant receptors in vivo. PLOS Biology *4*, e20.

Bhatla, N., and Horvitz, H.R. (2015). Light and hydrogen peroxide inhibit *C. elegans* feeding through gustatory receptor orthologs and pharyngeal neurons. Neuron *85*, 804–818.

Bhatla, N., Droste, R., Sando, S.R., Huang, A., and Horvitz, H.R. (2015). Distinct neural circuits control rhythm inhibition and spitting by the myogenic pharynx of *C. elegans*. Current Biology *25*, 2075–2089.

Bolm, M., Jansen, W.T.M., Schnabel, R., and Chhatwal, G.S. (2004). Hydrogen peroxide-mediated killing of *Caenorhabditis elegans:* a common feature of different *Streptococcal* species. Infection and Immunity *72*, 1192–1194.

Christie, J.M., Arvai, A.S., Baxter, K.J., Heilmann, M., Pratt, A.J., O'Hara, A., Kelly, S.M., Hothorn, M., Smith, B.O., Hitomi, K., et al. (2012). Plant UVR8 photoreceptor senses UV-B by tryptophan-mediated disruption of cross-dimer salt bridges. Science *335*, 1492–1496.

Clyne, P.J., Warr, C.G., and Carlson, J.R. (2000). Candidate taste receptors in *Drosophila*. Science *287*, 1830–1834.

Cronin, T.W., and Bok, M.J. (2016). Photoreception and vision in the ultraviolet. Journal of Experimental Biology *219*, 2790–2801.

Du, E.J., Ahn, T.J., Wen, X., Seo, D., Na, D.L., Kwon, J.Y., Choi, M., Kim, H., Cho, H., and Kang, K. (2016). Nucleophile sensitivity of *Drosophila* TRPA1 underlies light-induced feeding deterrence. Elife *5*, e18425.

Dunipace, L., Meister, S., McNealy, C., and Amrein, H. (2001). Spatially restricted expression of candidate taste receptors in the *Drosophila* gustatory system. Current Biology *11*, 822–835.

ECETOC (1996). Special Report 10 - Hydrogen Peroxide OEL Criteria Document. (Brussels, Belgium: ECETOC).

Edwards, S.L., Charlie, N.K., Milfort, M.C., Brown, B.S., Gravlin, C.N., Knecht, J.E., and Miller, K.G. (2008). A novel molecular solution for ultraviolet light detection in *Caenorhabditis elegans*. PLOS Biology *6*, e198.

Finkel, T. (2011). Signal transduction by reactive oxygen species. The Journal of Cell Biology *194*, 7–15.

Fu, Y., Liao, H., Do, M.T.H., and Yau, K. (2005). Non-image-forming ocular photoreception in vertebrates. Current Opinion in Neurobiology *15*, 415–422.

Ghosh, D.D., Jin, X., and Nitabach, M. (2017). *C. elegans* discriminate colors without eyes or opsins. BioRxiv 092072.

Gong, J., Yuan, Y., Ward, A., Kang, L., Zhang, B., Wu, Z., Peng, J., Feng, Z., Liu, J., and Xu, X.Z.S. (2016). The *C. elegans* taste receptor homolog LITE-1 is a photoreceptor. Cell *167*, 1252-1263.e10.

Gotow, T., and Nishi, T. (2008). Simple photoreceptors in some invertebrates: Physiological properties of a new photosensory modality. Brain Research *1225*, 3–16.

Gotow, T., and Nishi, T. (2009). A new photosensory function for simple photoreceptors, the intrinsically photoresponsive neurons of the sea slug *Onchidium*. Front Cell Neurosci *3*.

Gracheva, E.O., Ingolia, N.T., Kelly, Y.M., Cordero-Morales, J.F., Hollopeter, G., Chesler, A.T., Sánchez, E.E., Perez, J.C., Weissman, J.S., and Julius, D. (2010). Molecular basis of infrared detection by snakes. Nature *464*, 1006–1011.

Guntur, A.R., Gu, P., Takle, K., Chen, J., Xiang, Y., and Yang, C. (2015). *Drosophila* TRPA1 isoforms detect UV light via photochemical production of H_2O_2. Proc Natl Acad Sci USA *112*, E5753–E5761.

Guntur, A.R., Gou, B., Gu, P., He, R., Stern, U., Xiang, Y., and Yang, C. (2017). H_2O_2-sensitive isoforms of *Drosophila melanogaster* TRPA1 act in bitter-sensing gustatory neurons to promote avoidance of UV during egg-laying. Genetics *205*, 749–759.

Hill, K., and Schaefer, M. (2009). Ultraviolet light and photosensitising agents activate TRPA1 via generation of oxidative stress. Cell Calcium *45*, 155–164.

Hockberger, P.E. (2002). A history of ultraviolet photobiology for humans, animals and microorganisms. Photochemistry and Photobiology *76*, 561–579.

Hockberger, P.E., Skimina, T.A., Centonze, V.E., Lavin, C., Chu, S., Dadras, S., Reddy, J.K., and White, J.G. (1999). Activation of flavin-containing oxidases underlies light-induced production of H_2O_2 in mammalian cells. PNAS *96*, 6255–6260.

van der Horst, M.A., and Hellingwerf, K.J. (2004). Photoreceptor proteins, "star actors of modern times": A review of the functional dynamics in the structure of representative members of six different photoreceptor families. Acc. Chem. Res. *37*, 13–20.

Hwang, R.Y., Zhong, L., Xu, Y., Johnson, T., Zhang, F., Deisseroth, K., and Tracey, W.D. (2007). Nociceptive neurons protect *Drosophila* larvae from parasitoid wasps. Current Biology *17*, 2105–2116.

Ishimoto, H., Takahashi, K., Ueda, R., and Tanimura, T. (2005). G-protein gamma subunit 1 is required for sugar reception in *Drosophila*. The EMBO Journal *24*, 3259–3265.

Jansen, W.T.M., Bolm, M., Balling, R., Chhatwal, G.S., and Schnabel, R. (2002). Hydrogen peroxide-mediated killing of *Caenorhabditis elegans* by *Streptococcus pyogenes*. Infection and Immunity *70*, 5202–5207.

Kim, M.J., and Johnson, W.A. (2014). ROS-mediated activation of *Drosophila* larval nociceptor neurons by UVC irradiation. BMC Neurosci *15*, 14.

Kim, M.J., Ainsley, J.A., Carder, J.W., and Johnson, W.A. (2013). Hyperoxia-triggered aversion behavior in *Drosophila* foraging larvae is mediated by sensory detection of hydrogen peroxide. Journal of Neurogenetics *27*, 151–162.

Kwon, J.Y., Dahanukar, A., Weiss, L.A., and Carlson, J.R. (2007). The molecular basis of CO_2 reception in Drosophila. PNAS *104*, 3574–3578.

Lamb, T.D., Collin, S.P., and Pugh Jr, E.N. (2007). Evolution of the vertebrate eye: opsins, photoreceptors, retina and eye cup. Nature Reviews Neuroscience *8*, 960–976.

Lin, J.Y., and Fisher, D.E. (2007). Melanocyte biology and skin pigmentation. Nature *445*, 843–850.

Liu, J., Ward, A., Gao, J., Dong, Y., Nishio, N., Inada, H., Kang, L., Yu, Y., Ma, D., Xu, T., et al. (2010). *C. elegans* phototransduction requires a G protein–dependent cGMP pathway and a taste receptor homolog. Nature Neuroscience *13*, 715–722.

McCormick, J., Fischer, Pachlatko, J., and Eisenstark, A. (1976). Characterization of a cell-lethal product from the photooxidation of tryptophan: hydrogen peroxide. Science *191*, 468–469.

Michael, A.K., Fribourgh, J.L., Gelder, R.N.V., and Partch, C.L. (2017). Animal cryptochromes: divergent roles in light perception, circadian timekeeping and beyond. Photochemistry and Photobiology *93*, 128–140.

Mishra, A., Salari, A., Berigan, B.R., Miguel, K.C., Amirshenava, M., Robinson, A., Zars, B.C., Lin, J.L., Milescu, L.S., Milescu, M., et al. (2018). The *Drosophila Gr28bD* product is a non-specific cation channel that can be used as a novel thermogenetic tool. Scientific Reports *8*, 901.

Moy, T.I., Mylonakis, E., Calderwood, S.B., and Ausubel, F.M. (2004). Cytotoxicity of hydrogen peroxide produced by *Enterococcus faecium*. Infection and Immunity *72*, 4512–4520.

Ni, L., Bronk, P., Chang, E.C., Lowell, A.M., Flam, J.O., Panzano, V.C., Theobald, D.L., Griffith, L.C., and Garrity, P.A. (2013). A gustatory receptor paralogue controls rapid warmth avoidance in *Drosophila*. Nature *500*, 580–584.

Niethammer, P., Grabher, C., Look, A.T., and Mitchison, T.J. (2009). A tissue-scale gradient of hydrogen peroxide mediates rapid wound detection in zebrafish. Nature *459*, 996–999.

O'Hara, A., and Jenkins, G.I. (2012). *In vivo* function of tryptophans in the *Arabidopsis* UV-B photoreceptor UVR8. The Plant Cell *24*, 3755–3766.

Pérez, J.H., Tolla, E., Dunn, I.C., Meddle, S.L., and Stevenson, T.J. (2019). A comparative perspective on extra-retinal photoreception. Trends in Endocrinology & Metabolism *30*, 39–53.

Pickard, G.E., and Sollars, P.J. (2011). Intrinsically Photosensitive Retinal Ganglion Cells. In Reviews of Physiology, Biochemistry and Pharmacology 162, B. Nilius, S.G. Amara, T. Gudermann, R. Jahn, R. Lill, S. Offermanns, and O.H. Petersen, eds. (Berlin, Heidelberg: Springer Berlin Heidelberg), pp. 59–90.

Richardson, A. (1893). The action of light in preventing putrefactive decomposition; and in inducing the formation of hydrogen peroxide in organic liquids. J. Chem. Soc., Trans. *63*, 1109–1130.

Robertson, H.M., Warr, C.G., and Carlson, J.R. (2003). Molecular evolution of the insect chemoreceptor gene superfamily in *Drosophila melanogaster*. PNAS *100*, 14537–14542.

Romanowski, A., Garavaglia, M.J., Goya, M.E., Ghiringhelli, P.D., and Golombek, D.A. (2014). Potential conservation of circadian clock proteins in the phylum Nematoda as revealed by bioinformatic searches. PLoS One *9*.

Saina, M., Busengdal, H., Sinigaglia, C., Petrone, L., Oliveri, P., Rentzsch, F., and Benton, R. (2015). A cnidarian homologue of an insect gustatory receptor functions in developmental body patterning. Nat Commun *6*, 6243.

Salmeen, A., Andersen, J.N., Myers, M.P., Meng, T., Hinks, J.A., Tonks, N.K., and Barford, D. (2003). Redox regulation of protein tyrosine phosphatase 1B involves a sulphenyl-amide intermediate. Nature *423*, 769–773.

Sang, J., Rimal, S., and Lee, Y. (2019). *Gustatory receptor 28b* is necessary for avoiding saponin in *Drosophila melanogaster*. EMBO Rep. *20*, e47328.

Sato, K., Tanaka, K., and Touhara, K. (2011). Sugar-regulated cation channel formed by an insect gustatory receptor. PNAS *108*, 11680–11685.

Schuch, A.P., Moreno, N.C., Schuch, N.J., Menck, C.F.M., and Garcia, C.C.M. (2017). Sunlight damage to cellular DNA: Focus on oxidatively generated lesions. Free Radical Biology and Medicine *107*, 110–124.

Scott, K., Brady, R., Cravchik, A., Morozov, P., Rzhetsky, A., Zuker, C., and Axel, R. (2001). A chemosensory gene family encoding candidate gustatory and olfactory receptors in *Drosophila*. Cell *104*, 661–673.

Sundaresan, M., Yu, Z.X., Ferrans, V.J., Irani, K., and Finkel, T. (1995). Requirement for generation of H_2O_2 for platelet-derived growth factor signal transduction. Science *270*, 296–299.

Terakita, A. (2005). The opsins. Genome Biology *6*, 213.

Ueno, K., Kohatsu, S., Clay, C., Forte, M., Isono, K., and Kidokoro, Y. (2006). Gsα is involved in sugar perception in *Drosophila melanogaster*. J. Neurosci. *26*, 6143–6152.

Vosshall, L.B., and Stocker, R.F. (2007). Molecular architecture of smell and taste in *Drosophila*. Annual Review of Neuroscience *30*, 505–533.

Ward, A., Liu, J., Feng, Z., and Xu, X.Z.S. (2008). Light-sensitive neurons and channels mediate phototaxis in *C. elegans*. Nature Neuroscience *11*, 916–922.

Wicks, N.L., Chan, J.W., Najera, J.A., Ciriello, J.M., and Oancea, E. (2011). UVA phototransduction drives early melanin synthesis in human melanocytes. Current Biology *21*, 1906–1911.

Wilkens, L.A. (1988). The crayfish caudal photoreceptor: advances and questions after the first half century. Comparative Biochemistry and Physiology Part C: Comparative Pharmacology *91*, 61–68.

Xiang, Y., Yuan, Q., Vogt, N., Looger, L.L., Jan, L.Y., and Jan, Y.N. (2010). Light-avoidance-mediating photoreceptors tile the *Drosophila* larval body wall. Nature *468*, 921–926.

Xiong, W., Solessio, E.C., and Yau, K. (1998). An unusual cGMP pathway underlying depolarizing light response of the vertebrate parietal-eye photoreceptor. Nature Neuroscience *1*, 359.

Yao, C.A., and Carlson, J.R. (2010). Role of G-proteins in odor-sensing and CO_2-sensing neurons in Drosophila. J. Neurosci. *30*, 4562–4572.

Yau, K., and Hardie, R.C. (2009). Phototransduction motifs and variations. Cell *139*, 246–264.

Yoshida, M. (1979). Extraocular photoreception. In Comparative Physiology and Evolution of Vision in Invertebrates, p. 60.

Zhang, H., Anderson, A.R., Trowell, S.C., Luo, A.R., Xiang, Z., and Xia, Q. (2011). Topological and functional characterization of an insect gustatory receptor. PLOS ONE *6*, e24111.

Chapter 2

The M1 neuron functions as a hub to control flow reversal in a simple neuromuscular pump via spatially restricted calcium increases in muscle

Steven R. Sando, Nikhil Bhatla*, Eugene L.Q. Lee, H. Robert Horvitz

To be submitted to a neuroscience journal.

Author contributions

Nikhil Bhatla performed all laser ablation surgeries except for those shown in Figure 2.2, B-D. In the course of analyzing the activity of another set of neurons, Nikhil generated the *gpa-16*$_{promoter}$*::gcamp3* transgene used to perform calcium imaging of pharyngeal muscle introduced in Figure 2.3, C, and noted the spatially restricted calcium increases in pharyngeal muscle in this strain.

Eugene Lee analyzed the behavioral videos used to make Figure 2.2, A-H and Figure 2.4, A-F, and contributed to cloning reagents.

*University of California, Berkeley, Berkeley, United States

Abstract

A major goal in the study of animal behavior is to identify the neural and molecular substrates of behavior and understand the principles by which these substrates function. One simple system for the mechanistic study of animal behavior is the pharynx of the nematode worm *C. elegans*, which contracts rhythmically (pumps) to ingest food. Previous work showed that short-wavelength violet or ultraviolet (UV) light interrupts and modulates the pharyngeal pumping rhythm. Most strikingly, light reverses the flow of material in the pharynx, causing the pharynx to spit food into the environment. We analyzed the biomechanical, molecular, and cellular bases of this behavior to identify principles by which nervous systems encode opposing behaviors. We report that spitting is accomplished by the sustained contraction of the subset of pharyngeal muscles that control the food-trapping pharyngeal valve, and that these contractions are accompanied by sustained, spatially restricted increases calcium levels in those muscle subregions only. Spitting is controlled by the M1 neuron, which responds to light and drives spitting when activated. M1 directly innervates the pharyngeal muscles involved in spitting and receives synaptic input from a broad set of pharyngeal neurons, suggesting it might play a central role in coordinating spitting behavior. Spitting depends on the gustatory receptor orthologs *lite-1* and *gur-3.* We use laser ablations and cell-specific rescue to show that *gur-3* functions in the I2 and I4 neurons to promote spitting via M1. We propose that the M1 pharyngeal neuron acts as a hub for the control of spitting behavior.

Introduction

Animals are capable of many behaviors but perform only one or a small subset of those behaviors in any given circumstance. How animals process internal and external sensory information to generate context-appropriate behavior is a fundamental problem in neuroscience. To address this problem, connectomics, the graph theoretical analysis of connectivity maps derived from micro-, meso-, and/or macro-scale measurements of neural connectivity, has emerged as an area of active inquiry (Bullmore and Sporns, 2009; van den Heuval *et al.*, 2016; Schröter *et al.*, 2017; van den Heuvel and Yeo, 2017) . Connectomic analyses have been applied to or suggested as analytical frameworks for a wide variety of theoretical and applied problems in neurobiology (Bassett and Bullmore, 2009; Buckholtz and Meyer-Lindenberg, 2012; Grefkes and Fink, 2014; van den Heuval and Fornito, 2014; Van Essen and Barch, 2015; Hannawi and Stevens, 2016; Kral *et al.*, 2016; van den Heuval *et al.*, 2016; Yan *et al.*, 2017). However, studies of a variety of organisms, and in particular of invertebrates with comparatively simple nervous systems, have highlighted significant practical limitations to the connectomic method (Bargmann, 2012; Marder, 2012; Griffith, 2012). Thus, theoretical connectomic analyses will require integration with experimental studies of simple systems.

The nematode worm *C. elegans* possesses several advantages for behavioral studies, including its genetic accessibility, transparency, and the small size of its nervous system, which is composed of 302 neurons of defined morphology and connectivity (Albertson and Thomson, 1976; White *et al.*, 1986). Despite this relative

simplicity, worms possess a rich behavioral repertoire (Bono and Villu, 2005; Rengarajan and Hallem, 2016; Emmons, 2018), the neural basis of which is incompletely understood.

The worm's feeding organ, the pharynx (Figure 2.1, A) contracts rhythmically (pumps) to generate suction (contraction opens the lumen of the pharynx) and ingest bacterial food (Avery and You, 2012). The anatomy of the pharynx is simple and has been intensively characterized: it contains only 20 neurons of 14 classes, 20 muscles, 4 glands, and 16 structural cells (Albertson and Thomson, 1976). The pharyngeal connectome has been precisely and completely defined by serial section electron microscopy (Albertson and Thomson, 1976), and, with the exception of a single pair of synapses, is isolated in synaptic connectivity from the main somatic nervous system.

Two important stimuli to which animals in nature must respond are light and reactive oxygen species. Light is essential for life but can also damage biological tissues (Hockberger, 2012; Cronin and Bok, 2016; Schuch *et al.*, 2017) and thus poses a potentially lethal threat to unpigmented animals like *C. elegans* (Ward *et al.*, 2008; Edwards *et al.*, 2008). Reactive oxygen species such as hydrogen peroxide can be encountered environmentally (ECETOC, 1996) or be generated internally via a variety of physiological or pathological processes (Rhee, 1999; Finkel, 2011). Because of the photooxidative properties of light, these stimuli can overlap in their effects (Hockberger, 2012; Cronin and Bok, 2016; Schuch *et al.*, 2017).

C. elegans avoids short-wavelength blue, violet, or ultraviolet light (Ward *et al.*, 2008; Edwards *et al.*, 2008; Liu *et al.*, 2010). This response to light is intriguing, as no known molecular photoreceptors are encoded by the *C. elegans* genome (Bargmann,

1998; Terakita, 2005; Romanowski, 2014). Genetic screens for *C. elegans* mutants defective in the avoidance of light identified a gene subsequently named *lite-1*, which encodes a transmembrane protein of the gustatory receptor (Gr) family (Edwards *et al.*, 2008; Liu *et al.*, 2010). Subsequent studies found that a *lite-1* homolog, *Gr28.b*, controls a similar light-avoidance response by the larvae of the fruit fly *D. melanogaster* (Xiang *et al.*, 2010). Because *lite-1* can confer sensitivity to light when expressed in otherwise light-unresponsive cells (Edwards *et al.*, 2008; Liu *et al.*, 2010; Gong *et al.*, 2016), it was proposed to encode a photoreceptor (Edwards *et al.*, 2008).

Short-wavelength light not only stimulates an avoidance response but also interrupts and modulates the pumping rhythm of the *C. elegans* pharynx (Bhatla and Horvitz, 2015; Bhatla *et al.*, 2015). Upon exposure to violet or ultraviolet light, pumping rapidly stops (acute inhibition), and then transiently increases (burst pumping; Figure 2.1, B). After the light stimulus is removed, the pumping rate remains depressed and slowly recovers (recovery) to the 4-5 Hz of normal feeding over about a minute.

The pharyngeal response to light requires *lite-1* and the *lite-1* paralog *gur-3,* which together are expressed in six of the 14 pharyngeal neuron classes (I2, I4, MI, M1, M4, and M5) as well as in a number of extra-pharyngeal neuron classes (Bhatla and Horvitz, 2015). Short-wavelength light can produce hydrogen peroxide in biological tissues and fluids (Richardson, 1893; Bedford, 1927; McCormick, 1976; Hockberger *et al.*, 1999; Hockberger, 2002). Given their expression in pharyngeal neurons and their sequence similarity to chemosensory GR-family receptors, Bhatla and Horvitz (2015) proposed that LITE-1 and GUR-3 might detect light via the generation by light of reactive oxygen species, i.e., that LITE-1 and GUR-3 might be gustatory receptors that

detect reactive oxygen species. Consistent with this hypothesis, Bhatla and Horvitz (2015) showed that worms inhibit pumping in response to the odor of hydrogen peroxide and that this inhibition depends on *lite-1* and *gur-3*. Interestingly, purified LITE-1 strongly absorbs UVA and UVB ultraviolet light, consistent with the hypothesis that LITE-1 can function as a photoreceptor (Gong *et al.*, 2016). Furthermore, *lite-1* can function in a color discrimination behavior (Ghosh *et al.*, posted 2017). In short, *lite-1*'s function in the detection of light and hydrogen peroxide is incompletely understood.

Because we have observed significant overlap between the pharyngeal response to light and to hydrogen peroxide (Bhatla and Horvitz, 2015), as others have in other systems (Hill and Schaefer, 2009; Kim *et al.*, 2013b; Kim and Johnson, 2014; Gunter *et al.*, 2015; Du *et al.*, 2016; Gunter *et al.*, 2017), we used light as a tool to probe the function of neural circuits controlling gustatory responses to noxious tastants such as hydrogen peroxide.

Previous studies implicated four classes of pharyngeal neurons in the pumping response to light (Bhatla and Horvitz, 2015; Bhatla *et al.*, 2015). The I2 neurons likely detect light directly and control the latency of acute inhibition (Bhatla and Horvitz, 2015; Bhatla *et al.*, 2015). The I1 neurons control the amplitude of acute pumping inhibition and likely transduce a *lite-1*-dependent signal from outside the pharynx via the pharyngeal MC neurons (Bhatla *et al.*, 2015). Finally, the M1 neuron is required for the burst pumping phase, which constitutes a spitting behavior that interrupts feeding and ejects material from the anterior pharynx (Bhatla *et al.*, 2015).

We further analyzed the pharyngeal response to light, focusing on the M1 neuron. Using spitting behavior by the *C. elegans* pharynx as a model for how a simple

connectome encodes a transition between opposing behaviors (i.e., switching from feeding to spitting), we traced the flow of light-evoked information backward through the connectome from motor outputs to putative sensory neurons. We find that spitting is accomplished by sustained contraction of the subset of pharyngeal muscles that control the food-trapping pharyngeal valve, and that these contractions are accompanied by sustained, spatially restricted increases in calcium levels in those muscle regions only. Together, our functional data suggest that the pharyngeal M1 neuron receives input from multiple other pharyngeal neurons and functions as a central hub for spitting behavior.

Results

We defined the burst pumping phase as the transient increase in pumping rate that follows the acute inhibition phase of the response to light (Figure 2.1, B) (Bhatla *et al.*, 2015). We scored burst pumping by eye, based on the contractions ("pumps") of the grinder (Figure 2.1, A) (Bhatla and Horvitz, 2015). To distinguish feeding and spitting pumps, we recorded high-speed videos of worms feeding on 1 μM polystyrene beads. We then analyzed these videos and designated pumps that trapped ingested material in the anterior pharynx as feeding pumps and pumps that ejected or failed to trap material as spitting pumps.

UV light, like the violet light used previously, induces spitting (Figure 2.1, C,D). Because burst pumping was most robustly evoked by 365 nm (UV) light (Bhatla and Horvitz, 2015), we used this wavelength in our experiments (Figure 2.1, B). Similarly to UV light, the odor of hydrogen peroxide also induced spitting (Supplemental Figure 2.1, A)

Spitting Is Produced via the Sustained Opening of the Pharyngeal Valve

First, we sought to determine the biomechanical mechanism by which particle flow in the anterior pharynx is reversed during spitting behavior. In normal feeding, contraction of the pharyngeal muscles opens the lumen of the pharynx, generating suction and drawing food and fluid inwards. Food is trapped by the pharyngeal valve

(Figure 2.1, A), a cuticular structure that projects from the anterior tip of pharyngeal muscle 3 (pm3). Prior to the onset of pharyngeal muscle relaxation, the pharyngeal valve closes, sealing the anterior end of the lumen and acting as a filter to retain bacteria while fluid is ejected (Fang-Yen *et al.*, 2009). Given the importance of the pharyngeal valve in feeding, we hypothesized that the spitting mechanism must include some alteration in the position or motion of the pharyngeal valve. Therefore, we sought to compare the motions of the anteriormost pharyngeal muscle regions during feeding and UV light-induced spitting. We recorded worms pumping under a coverslip, such that the opening of the lumen appeared as a light space in our videos. As reported previously, feeding pumps involved the closure of the pharyngeal valve occurring shortly before the relaxation of the rest of the lumen, thus trapping food (Figure 2.1, E). By contrast, spitting pumps were characterized by a strikingly different motion: rather than contracting and relaxing with the rest the pharynx, the anterior tip of the pharynx remained open throughout the pumping cycle (Figure 2.1, E). This sustained contraction prevented the pharyngeal valve from closing and capturing food at the end of the pump. Instead, the pharyngeal contents were expelled as the pharynx relaxed and the lumen closed. As with spitting pumps defined by the release of polystyrene beads (Figure 2.1, D), these open-ended pumping motions occurred specifically in the burst pumping phase (Figure 2.1, F,G).

In short, while the pharyngeal valve closes at the conclusion of feeding pumps, thereby trapping food, spitting pumps are characterized by sustained contraction of the muscles operating the pharyngeal valve, such that the relaxation of the rest of the

pharynx at the end of the pump ejects the contents of the pharynx into the environment (Figure 2.1, H).

The M1 Neuron Innervates the Pharyngeal Valve and Functions in UV Light-Induced Spitting

The pharyngeal neuron M1 is required for spitting induced by violet light (Bhatla and Horvitz, 2015; Bhatla *et al.*, 2015). The pharyngeal connectome indicates that M1 has several interesting attributes. First, M1 directly innervates the pharyngeal muscle that controls the pharyngeal valve, suggesting that it might be directly involved in generating spitting behavior. Second, M1 is the most diversely connected neuron in the pharynx, making and receiving unique connections with a greater number of other cell classes than any other neuron (Albertson and Thomson, 1976; Supplemental Figure 2.2, A). Third, it receives input from each of the other five classes of pharyngeal neurons expressing *lite-1* (M4, M5, MI) or *gur-3* (the I2s, I4). Together, these properties led us to hypothesize that M1 might function as a hub in the pharyngeal connectome, controlling the decision to spit based on inputs from the rest of the network.

Since M1 is necessary for violet light-induced spitting, we asked whether M1 is also necessary for spitting induced by UV light (henceforth "light"). We killed M1 using a laser microbeam and also generated an M1 genetic-ablation strain (*lury-1*$_{promoter}$*::ICE::SL2::mCherry)* in which the mammalian caspase ICE (Cerretti *et al.*, 1992; Thornberry *et al.*, 1992; Zheng *et al.,* 1999) is overexpressed in M1 via the *lury-1* promoter (Ohno *et al.*, 2017) (Supplemental Figure 2.3, A,B). Both laser and genetic

ablation of M1 eliminated light-induced spitting (Figure 2.2, A,B; E,F). Thus, M1 is required for light-induced spitting. In analyzing these videos, we observed two additional effects of M1 ablation that have not been previously reported. First, while wild-type animals largely inhibited pumping during the recovery phase that follows stimulation with light, M1-ablated animals engaged in significant pumping (Figure 2.2, C,G). Thus, in addition to promoting spitting, the M1 neuron inhibits grinder pumping as the pharynx recovers from illumination. Second, we noticed that the contractions of the grinder and procorpus (Figure 2.1, A) of M1-ablated animals became uncoupled from each other during the pumping that occurred in the recovery phase, such that many of the extra pumps consisted of contractions of the grinder but not of the procorpus (Figure 2.2, D,H). These observations indicate that the different compartments of pharyngeal muscle are capable of contracting independently of each other and imply that the pharynx might be capable of a finer degree of behavioral control than previously appreciated.

Given the necessity of M1 in light-induced spitting, we wondered whether M1 is acutely activated by light. We generated transgenic animals expressing the calcium reporter GCaMP6s (Chen *et al.*, 2013) in M1 using the *glr-2* promoter (Brockie *et al.*, 2001) and measured light-induced calcium changes. As indicated by increases in GCaMP6s fluorescence, light robustly increased M1 somatic calcium signals, consistent with an acute function for M1 in spitting (Figure 2.2, I-K).

M1 expresses *lite-1* (Bhatla and Horvitz, 2015), which controls behavioral responses to light and hydrogen peroxide (Ward *et al.*, 2008; Edwards *et al.*, 2008; Bhatla and Horvitz, 2015; Gong *et al.*, 2016). We wondered whether M1 might be activated directly by light, or whether it is instead activated by input from other light-

sensitive cells via synaptic, humoral (i.e., dense core vesicle), or gap junction inputs. Synaptic and humoral signaling require *unc-13* (Maruyama and Brenner, 1991; Richmond *et al.*, 1999; Richmond *et al.*, 2001) and *unc-31* (Berwin *et al.*, 1998), respectively, so we examined light-induced M1 calcium signals in these mutants. In both *unc-13* and *unc-31* mutants, M1's calcium response was reduced in magnitude, but still significant (Figure 2.2, L,M). These results are consistent with M1's being capable of functioning as a cellular photoreceptor, but they do not preclude the possibility that the *unc-13* and/or *unc-31*-independent activation of M1 occurs via gap junctions, redundant signals that utilize both *unc-13* and *unc-31,* or some combination thereof. The reduced calcium responses of *unc-13* and *unc-31* mutants suggest that M1 receives input from other cells, consistent with M1's acting as a hub in the pharyngeal network. To determine whether acute activation of M1 is sufficient to produce spitting, we expressed Channelrhodopsin 2 (ChR2) (Nagel *et al.*, 2003; Boyden *et al.*, 2005) specifically in M1 using the *lury-1* promoter (Ohno *et al.*, 2017). We performed these experiments using *lite-1 gur-3* mutant animals, which lack endogenous pharyngeal responses to light (Bhatla and Horvitz, 2015). While no animals grown in the absence of the ChR2 cofactor all-*trans* retinal (ATR) spat in response to optogenetic stimulation with 470 nm light, 25% of animals grown with ATR spat when illuminated (Figure 2.2, N,O). Thus, optogenetic activation of M1 can produce spitting behavior, although perhaps not as efficiently as light does in the wild-type background.

Spatially Restricted Calcium Increases in Pharyngeal Muscle Underlie the Sustained Opening of the Pharyngeal Valve During Spitting

M1's anatomy strongly suggests that it controls spitting directly: it extends a process to the anterior end of the pharynx, where it is the only neuron to form neuromuscular junctions with pm1, pm2, and/or the anterior tip of pm3 (Albertson and Thomson, 1976). These neuromuscular junctions are found in the same location as the pharyngeal valve and as the sustained contraction of pharyngeal muscle we observed to occur during spitting (Figure 2.3, A). Because the muscles of the *C. elegans* pharynx are thought to be connected via gap junctions (Avery and Horvitz, 1989; Starich *et al.*, 1996; Bhattacharya *et al.*, 2019), we found it surprising that some or all of pm1, pm2, and/or the anteriormost end of pm3 could remain contracted while the rest of the corpus underwent cyclical contraction and relaxation. We thus wondered by what physiological mechanism M1 produces these sustained and spatially restricted muscle contractions. Because muscle contractions are acutely triggered by increases in intracellular calcium, we expressed the calcium reporter GCaMP3 (Tian *et al.*, 2009) in pharyngeal muscle using the *gpa-16* promoter (Jansen *et al.*, 1999) and observed calcium changes during light-induced spitting pumps. When we stimulated pumps with light, we detected calcium increases across all regions of the pharynx, including the terminal bulb, procorpus, and anterior muscle region innervated by M1 (Figure 2.3, B-D). Interestingly, we noticed that the anterior muscle region responded to light with calcium increases more quickly than other compartments of the pharynx (Figure 2.3, C,D). Additionally, while calcium in these compartments rose and fell over the course of the pump, GCaMP3 signals at the tip of the pharynx were sustained continuously through the

pump cycle (Figure 2.3, C). These sustained signals were restricted to the anterior tip of the pharynx, and did not occur in adjacent regions of the procorpus (Figure 2.3, C,E). Importantly, laser ablation of M1 eliminated these spatially restricted calcium signals (Figure 2.3, F), consistent with their resulting from M1 activation. We did not observe spatially restricted calcium signals in feeding pumps, suggesting this phenomenon is specific to spitting (data not shown). The location and temporal dynamics of these sustained calcium signals coincide precisely with the sustained muscle contractions that we observed during spitting behavior, suggesting that they might be part of the physiological mechanism driving sustained contraction.

Pharyngeally-Expressed Gustatory Receptor Orthologs *lite-1* and *gur-3* Control UV Light-Induced Spitting and Activation of M1 and Pharyngeal Muscle

The *C. elegans* locomotory and pharyngeal responses to light described previously depend on the gustatory receptor orthologs *lite-1* and *gur-3* (Ward *et al.*, 2008; Edwards *et al.*, 2008; Bhatla and Horvitz, 2015). *gur-3* is required for the short latency of pumping inhibition, while *lite-1* controls the amplitude of inhibition in both the acute and recovery phase. To determine whether *lite-1* and/or *gur-3* function in spitting, we assayed light-induced spitting in single and double null mutant animals carrying the alleles *lite-1(ce314)* and/or *gur-3(ok2245)*. While the spitting behavior of *gur-3* mutants was comparable to wild-type animals, *lite-1* mutants were partially defective in spitting: not only was the peak spitting rate reduced in *lite-1* mutants (Figure 2.4, A-C), but these animals also intermixed feeding and spitting pumps when stimulated with light (data not

shown). The partial spitting defect of *lite-1* mutants was enhanced by mutation of *gur-3*, such that *lite-1 gur-3* double mutants were completely defective in light-induced spitting (Figure 2.4, D). We also examined *lite-1 gur-3* double mutants expressing wild-type copies of *lite-1* or *gur-3* under their endogenous promoters (Bhatla and Horvitz, 2015). In both cases, the rescue transgenes restored light-induced spitting to *lite-1 gur-3* double mutants (Figure 2.4, D-F). Together, these results indicate that *lite-1* and *gur-3* function in light-induced spitting.

Next, we tested the requirement of *lite-1* and *gur-3* in M1 light-induced calcium increases (Figure 2.4, G-J). *gur-3* mutants generally resembled the wild type, with the exception that they were activated with a short but significant delay (Figure 2.4, K). Conversely, *lite-1* mutants were almost completely defective in the calcium response to light, with the exception of a weak, fast response (Figure 2.4, L). The fast response depended on *gur-3* because *lite-1 gur-3* double mutants were completely defective in the calcium response to light (Figure 2.4, M). Thus, *lite-1* and *gur-3* make complementary contributions to M1's light-induced calcium increases: *lite-1* is required for the great majority of the calcium response to light, with the exception of the weak, fast component of the response, which depends on *gur-3*.

We note that *gur-3* accounts for only ~1% of M1 calcium increases in response to light yet is sufficient to maintain a peak spitting rate of about 50% that of the wild type (Figure 2.4, C, L). This discrepancy might be explained by the fact that the limited brightness of our M1 calcium-imaging transgene restricted our analysis to the M1 soma. Calcium dynamics might differ in the distal regions closer to M1's neuromuscular junctions (NMJs) with pharyngeal muscle.

The requirement of *lite-1* and *gur-3* in light-induced calcium increases in the anterior tip of pharyngeal muscle was similar to their requirement in M1's light-induced calcium increases (Figure 2.4, N-P). We noticed that fluorescence levels in *lite-1* mutants declined during the course of the imagining experiment, while the fluorescence levels in *lite-1 gur-3* double mutants did not change (Figure 2.4, O,P). Given that loss of *gur-3* eliminates this decline in muscle fluorescence, we conclude that *gur-3* has an inhibitory effect on pharyngeal muscle. This *gur-3*-dependent inhibition of pharyngeal muscle is likely due to the activity of the *gur-3*-expressing I2 neurons, which inhibit the procorpus when activated by light (Bhatla and Horvitz, 2015; Bhatla *et al.*, 2015).

Taken together, these results suggest that *lite-1* and *gur-3* both promote light-induced spitting and calcium increases in M1 and pharyngeal muscle, with *lite-1* playing a major role and *gur-3* making a smaller, albeit functionally significant, contribution.

lite-1, but Not *gur-3*, Controls the Rate of Pumping During M1-Dependent Spitting

M1 increases the rate of pumping during the burst pumping phase. Given the role of *lite-1* and *gur-3* in light-induced spitting, we wondered whether gustatory receptor orthologs might also be required for this M1-dependent pumping rate increase during burst pumping (Figure 2.1, A). Burst pumping behavior was wild-type in animals mutant for *gur-3* or its paralogs *egl-47/gur-1, gur-4,* and *gur-5* (Figure 2.5, A; Supplemental Figure 2.4, A-D). The role of *lite-1* could not be assayed directly, however, because *lite-1* mutants are significantly defective in the acute and sustained light-induced inhibition of pumping, obscuring the burst pumping phase (Figure 2.5, B,C).

We therefore sought a way to circumvent the issue of pumping inhibition in *lite-1* mutants. The fast 5 Hz on-food pumping rate is controlled by the pharyngeal MC neurons, ablation of which reduces the on-food pumping rate to 1 Hz (Raizen *et al.*, 1995). We hypothesized that mutants defective in the function of the MCs but not M1 might exhibit slow 1 Hz on-food pumping and wild-type 3.5 Hz M1-dependent pumping rate increases. Thus, the burst pumping rate would rise above the background pumping rate and could be scored regardless of whether inhibition occurred. In search of such MC-defective animals, we screened a set of mutants known to be defective in pharyngeal function, the *eat* mutants (Avery, 1993). We hypothesized the existence of four possible mutant classes: mutants defective in the rate of feeding but not the rate of burst pumping (class I), mutants defective in the rate of burst pumping but not the rate of feeding (class II), mutants generally defective in pumping (class III), and mutants wild-type in the rate of both feeding and burst pumping (class IV). The 18 mutants we examined fell roughly equally into these four classes (Supplemental Table 2.1; Supplemental Figure 2.5, A-X). Five mutants fit the criteria for class I (feeding-defective, burst pumping-normal), and we selected one of these mutants, *eat-2,* for further investigation (Figure 2.5, D). *eat-2* encodes a subunit of a nicotinic acetylcholine receptor required for the excitation of pharyngeal muscle downstream of the MCs (Raizen *et al.*, 1995; McKay *et al.*, 2004). To verify that the burst pumping behavior observed in *eat-2* mutants depends on M1, we crossed our M1 genetic-ablation transgene into the *eat-2* mutant background. Genetic ablation of M1 eliminated light-induced pumping increases (Figure 2.5, E). We then assayed the burst pumping rate of *lite-1, gur-3*, and *lite-1 gur-3* double mutants in the *eat-2* background and found that *lite-*

1 but not *gur-3* was required for burst pumping (Figure 2.5, F-H). Transgenic expression of wild-type *lite-1* under the endogenous *lite-1* promoter rescued the burst pumping defect of *eat-2*; *lite-1 gur-3* mutants (Figure 2.5, I). Thus, while both *lite-1* and *gur-3* promote spitting (i.e., the opening of the pharyngeal valve), *lite-1* but not *gur-3* is responsible for the increase in pumping rate that occurs during the burst pumping phase.

gur-3 Function in the I2 Neurons Is Sufficient for M1-Dependent UV Light-Induced Spitting

As discussed above, we believe that *lite-1* might function both in M1 and in other cells. *gur-3* also promotes light-induced spitting and M1 calcium increases but is not expressed in M1 (Bhatla and Horvitz, 2015). Rather, g*ur-3* is expressed in two pharyngeal neuron classes, the paired I2s and the unpaired I4 neuron (Figure 2.6, A) (Bhatla and Horvitz, 2015), both of which form synapses and gap junctions with M1 (Albertson and Thomson, 1976). Therefore, we wondered whether the I2s and/or I4 provide input to M1. The pharyngeal I2 neurons were previously shown to express *gur-3* and to be rapidly activated by light in a *gur-3* dependent manner, resulting in the inhibition of pumping (Bhatla and Horvitz, 2015; Bhatla *et al.*, 2015). We hypothesized that the I2s might also provide input to M1's activation by light and tested this hypothesis by expressing a wild-type copy of *gur-3* specifically in the I2 neurons of otherwise light-insensitive *lite-1 gur-3* double mutants (Figure 2.6, B). I2-specific rescue of *gur-3* restored robust light-induced spitting and M1 calcium increases to *lite-1 gur-3* double mutants, indicating that the I2 neurons are capable of providing input to M1 in

response to light via *gur-3* (Figure 2.6, B-D). Importantly, laser ablation of M1 suppressed this *gur-3*-dependent spitting (Figure 2.6, E,F), indicating that the I2s act through or in parallel to M1.

As mentioned above, previous work showed that the I2 neurons inhibit pumping in response to light (Bhatla and Horvitz, 2015; Bhatla *et al.*, 2015). For this reason, we were initially surprised to see that *lite-1 gur-3*; $I2_{promoter}$*::gur-3(+)* animals inhibited pumping very weakly if at all (Figure 2.6, C,E). Interestingly, after we ablated M1 in *lite-1 gur-3;* $I2_{promoter}$*::gur-3(+)* animals, we observed robust light-induced pumping inhibition (Figure 2.6, G). This finding suggested that, in addition to inhibiting pumping, the I2 neurons promote pumping via M1, and this stimulatory effect overpowers and masks the I2s' inhibitory input in the *lite-1 gur-3* double mutant background. Initially, it seemed paradoxical that the I2s would simultaneously inhibit and stimulate pumping. However, this result makes sense when one considers the rate of feeding pumps, defined as the subset of pumps that intake food. When we compared the rate of feeding pumps in M1- or mock-ablated *lite-1 gur-3; pI2::gur-3* animals, it was clear that the I2s' activation of M1 actually serves to reduce the overall feeding rate, because activated M1 eliminates feeding pumps by turning them into spits (Figure 2.6, H). Thus, rather than simply acting as nonspecific inhibitors of pumping rate generally, the I2s' function is specifically to reduce food intake, and they accomplish this task by two mechanisms: direct inhibition of feeding via the hyperpolarization of pharyngeal muscles (Bhatla and Horvitz, 2015) and indirect conversion of feeding pumps into spits via activation of M1 (Figure 2.6, I).

Given that the I2 neurons strongly stimulate spitting, we next wondered whether they could increase pumping rates in the slow-pumping *eat-2* mutant background

(Figure 2.5, D). We found that activating the I2 neurons via *gur-3* did not increase pumping rate in *eat-2* mutants (Figure 2.6, J). Thus, while the *gur-3*-expressing I2 neurons can activate M1 and thus open the pharyngeal valve, they are unable to activate M1 so strongly that it drives pumping rate increases in the slow-pumping *eat-2* mutant background. This finding is consistent with our observation that *gur-3* is insufficient for burst pumping in the absence of *lite-1* in the slow-pumping *eat-2* mutant background (Figure 2.5, G). The I2s do, however, produce enough excitation via M1 to obscure their own inhibitory effects on pumping in the *lite-1 gur-3* mutant background.

We used an I2-specific genetic-ablation transgene to kill the I2 neurons and confirmed (Bhatla *et al.*, 2015) that the I2s are not necessary for spitting in the wild-type background (Figure 2.6, K). To determine whether the I2s are the necessary site of *gur-3* action in *gur-3*-dependent spitting, we also killed the I2s in a *lite-1* mutant background. Spitting persisted after ablation of the I2s in *lite-1* mutant animals (Figure 2.6, L), indicating that *gur-3*-expressing neurons other than the I2s can produce spits.

The *gur-3*-Expressing I4 Neuron Acts with the I2 Neurons to Promote Spits

In addition to the I2 neurons, *gur-3* is also expressed in the pharyngeal I4 neuron (Figure 2.6, A), which can be activated by light but is of unknown function (Bhatla and Horvitz, 2015). We killed the I2 and I4 neurons of *lite-1* mutants singly and in combination and assayed spitting behavior. While *lite-1* animals in which either the I2s or I4 were ablated alone spat in response to light, I2/I4 double-ablated animals exhibited significantly delayed spitting (Figure 2.7, A-D), suggesting that the I2 and I4 neurons are

required redundantly for fast light-induced spitting. We detected small light-induced increases in M1 calcium in *lite-1*, *lite-1*; I2-ablated, and *lite-1*; I4-ablated animals but not in the *lite-1*; I2/I4 double-ablated animals, consistent with these neurons acting together to promote activation of M1 (Figure 2.7, E). However, ablating the I2s and I4 together failed to completely eliminate spitting, suggesting *gur-3* functions somewhere else in addition to in the I2s and I4. The redundancy of *gur-3*-dependent inputs into M1 is consistent with M1's functioning as a hub, receiving information from many other neurons in the pharyngeal network.

To verify that the spitting we observed in these experiments was M1-dependent, we killed M1 in combination with the I2 and I4 neurons of *lite-1* mutants. As expected, ablation of M1 eliminated spitting in all conditions (Figure 2.7, F-J). Interestingly, we observed that the ablation of the I2 neurons did not completely eliminate pumping inhibition in *lite-1*; M1-ablated animals, suggesting that the I4 neuron might also inhibit pumping. Consistent with this hypothesis, killing I4 in *lite-1*; M1/I2-ablated animals completely eliminated pumping inhibition (Figure 2.7, J). This result indicates that, like the I2 neurons, I4 both promotes spits and inhibits pumping.

Discussion

We identified biomechanical, molecular, and neural circuit mechanisms by which the *C. elegans* pharynx, a simple neuromuscular pump with a defined connectome, produces spitting behavior, an inversion of its typical ingestive function. Together, our functional data suggest that the pharyngeal M1 neuron functions as a central hub for the control spitting behavior, receiving input from multiple other pharyngeal neurons (Figure 2.8, A). Spitting results from the sustained contraction of pharyngeal muscles pm1, pm2, and/or pm3. This contraction opens the food-trapping pharyngeal valve that captures food during feeding, resulting in spitting (Figure 2.8, B). As reported previously (Bhatla *et al.*, 2015), spitting requires the M1 neuron, which directly innervates pm1, pm2, and pm3. M1 responds to UV light with calcium increases and activation of M1 is sufficient to produce spitting. The sustained contraction of pharyngeal muscle that produces spitting uncouples the contraction-relaxation cycle of pm1, pm2, and/or pm3 from the rest of the pharynx and appears to be generated via spatially restricted calcium increases in pm1, pm2, and/or pm3. UV light-induced spitting and M1 calcium increases require the gustatory receptor orthologs *lite-1* and *gur-3*. Light-induced M1-dependent increases in pumping rate depend on *lite-1* but not *gur-3*. *lite-1* likely functions in M1 and additional unidentified neurons, while *gur-3* functions in the I2 and I4 pharyngeal neurons and at least one other undetermined location.

Sustained Contraction of a Subcompartment of Pharyngeal Muscle Converts Feeding Motions into Spitting Motions

The conversion of feeding motions into spitting motions is controlled by the M1 neuron, which innervates the pharyngeal valve. During a feeding pump, closure of the pharyngeal valve at the end of the pump traps food in the pharynx (Fang-Yen *et al.*, 2009). Activation of M1 results in the sustained contraction of the muscles that control the valve, holding the valve constitutively open and causing material in the procorpus to be expelled at the pump's conclusion. Interestingly, this strategy requires that the motions of the pharyngeal muscles become uncoupled from each other during spitting. While the muscles of the procorpus and terminal bulb continue to contract and relax, pm1, pm2, and the anterior end of pm3 undergo sustained contraction throughout the pumping cycle. This result was unexpected, as the pharyngeal muscles are believed to be functionally coupled to each other via gap junctions (Avery and Horvitz, 1989; Starich *et al.*, 1996; Bhattacharya *et al.*, 2019).

We identified a physiological process that likely participates in this decoupling: during light stimulation, spatially restricted calcium signals occur in the same muscle region that is innervated by M1 and that undergo sustained contraction in spitting. We speculate that these signals contribute to the sustained contraction of the subset of pharyngeal muscles driving spitting. Although considerable attention has been given to spatially restricted calcium signaling in neurons and in particular in dendrites (Euler *et al.*, 2002; Higley and Sabatini, 2008; Hendricks *et al.*, 2012; Yang *et al.*, 2016), less is known about such spatially restricted calcium signals in muscle and their contribution to behavior. We propose that spatially restricted calcium signaling in muscle, whether

achieved via influx of calcium into a specific subset of muscle cells in an organ or a subcellular compartment of a single cell, might be a general mechanism for the control of motor behavior.

We identified a second condition in which pharyngeal muscle segments become uncoupled from each other: killing M1 increased the contraction rate of the grinder in the recovery phase of the light response, and grinder contractions frequently occurred in the absence of contractions of the procorpus. These results indicate that the contractions of the procorpus can become uncoupled from those of the grinder. Because the procorpus is the compartment that first ingests food, this uncoupling might allow the worm to prevent further food intake while it uses the grinder to chew and swallow whatever material it has already ingested. Thus, the uncoupling of muscle contractions between groups of coupled muscle seems to be a theme of the pharyngeal response to light. We suggest that the pharynx possesses a finer degree of behavioral control than previously appreciated.

The Apparent Dual Function of *lite-1* and *gur-3* in Response to UV Light and Hydrogen Peroxide is Reminiscent of that of *dTrpA1*

lite-1 was first identified in genetic screens for animals defective in the avoidance of light (Edwards *et al.*, 2008; Liu *et al.*, 2010). Because of its function in light avoidance and its ability to confer sensitivity to light when expressed ectopically, *lite-1* was proposed to encode a light receptor (Edwards *et al.*, 2008).

Based on *lite-1* and *gur-3*'s pharyngeal expression, their function in light-induced feeding inhibition, and their similarity to known chemoreceptors, Bhatla and Horvitz

(2015) hypothesized that *lite-1* and *gur-3* might control the chemosensation of products of photooxidation and function as gustatory receptors (Bhatla and Horvitz, 2015). Consistent with this hypothesis, *lite-1* and *gur-3* are required for hydrogen peroxide-induced avoidance and feeding inhibition (Bhatla and Horvitz, 2015). Here, we additionally report that *lite-1* and *gur-3* function in light-induced spitting behavior. Although we cannot rule out the possibility that there is an ethological reason for worms to spit in the presence of UV light, we suggest that light-induced spitting can be understood as an aversive gustatory response to noxious chemical products of photooxidation.

Other studies support the hypothesis that animals can detect light via the detection of products of photooxidation. Unnaturally bright 254 nm UVC light has been shown to induce a writhing behavior by *Drosophila* larvae that is likely mediated by light-generated hydrogen peroxide (Kim and Johnson, 2014). UVA and UVB light of ethologically relevant intensity can elicit behaviors from *Drosophila* larvae and adults, likely via the production of hydrogen peroxide (Gunter *et al.*, 2015; Du *et al.*, 2016; Gunter *et al.*, 2017). Interestingly, these UVA and UVB responses depend on *dTrpA1*, which encodes a nociceptive TRP channel. Heterologously-expressed mammalian TRPA1 was previously proposed to act as a detector of UV-induced photooxidation (Hill and Schaefer, 2008), and subsequent work has shown that dTRPA1 functions in this manner as well (Gunter *et al.*, 2015; Du *et al.*, 2016; Gunter *et al.*, 2017). *dTrpA1* isoforms known to confer nociceptive chemosensation are expressed in *D. melanogaster* chemosensory neurons that can produce regurgitation when activated (Kang *et al.*, 2012; Guntur *et al.*, 2017). Taken together, the parallels between *lite-1* and

dTrpA1 are striking: both encode putative chemoreceptors, both control responsivity to hydrogen peroxide and ethologically significant doses of UVA light, and both are expressed in gustatory neurons that produce egestive behaviors when activated (Kang *et al.*, 2012; Bhatla and Horvitz; Bhatla *et al.*, 2015). We speculate that molecular and cellular systems functioning in the detection of both light and reactive oxygen species might have originated as chemosensory systems and subsequently evolved to respond to photooxidation. We further speculate that such systems could later be stepping stones in the evolution of more sophisticated photosensory systems. Given the striking similarities between the *lite-1* and *dTrpA1* systems, such an occurrence might reflect a general evolutionary trajectory in sensory neurobiology.

The M1 Neuron Controls UV Light-Induced Spitting Behavior via a Hub-Like Circuit Motif

We identified a convergent, hub-like circuit motif that controls a *C. elegans* spitting behavior, centered on the M1 neuron, which the pharyngeal connectome suggested might be important for the control of light-induced spitting. M1 is highly connected with the rest of the pharyngeal nervous system, specifically receives synaptic input from each of the *lite-1*- or *gur-3*-expressing and therefore likely light-responsive neurons in the pharynx, and is directly connected to the muscles that produce spitting. These properties led us to hypothesize that M1 might act as a hub upon which the rest of the pharyngeal nervous system converges to control spitting. Consistent with this hypothesized role, our functional data indicate that spitting requires M1 and that M1's activation is sufficient for spitting. M1 expresses *lite-1* and responds to light in the

absence of synaptic or humoral inputs, suggesting that it might detect light directly. Additionally, multiple *lite-1*- and *gur-3*-expressing neurons can promote M1-dependent spitting.

We used genetic and cellular analysis to identify neurons that can provide functional input to M1. We found that the *gur-3*-expressing I2 and I4 neurons can activate M1 and produce M1-dependent spitting. The I2 and I4 neurons together tile the length of the pharynx (Figure 2.6, A), presumably allowing the pharyngeal nervous system to detect hydrogen peroxide anywhere along its length. Interestingly, while activation of M1 in wild-type animals produces strong M1 calcium responses, spits, and increases in pumping rate, the *gur-3*- and I2/I4-dependent inputs we identified can activate M1 only very weakly, opening the pharyngeal valve and producing spits but not increasing the rate of pharyngeal pumping. *gur-3* controls high-affinity responses to micromolar levels of hydrogen peroxide, while *lite-1* controls low-affinity responses to millimolar hydrogen peroxide levels (Bhatla and Horvitz, 2015). We speculate that the *gur-3*-expressing I2 and I4 neurons might function in the spitting circuit as high-affinity cellular receptors for micromolar levels of hydrogen peroxide. Thus, when the worm encounters a mildly noxious taste, I2 and/or I4 could weakly stimulate M1 and produce spits, but not pumping rate increases. Conversely, we speculate that *lite-1*-expressing neurons such as M1 might function as low-affinity cellular receptors for millimolar levels of hydrogen peroxide or other noxious oxidants, which could strongly activate M1 via *lite-1* and produce a more vigorous spitting behavior characterized by increases in the rate of pumping so as to flush material from the pharynx. In other words, we propose that the I2s and I4 evoke an attenuated form of spitting, while other cells and/or M1

produce spitting in a more robust manner, enabling the pharyngeal nervous system to produce graded variations of the spitting reflex.

Notably, all the neurons we found to promote spitting also promote the inhibition of pumping. In the case of M1, these outputs were temporally distinct: in the burst pumping phase, M1 promotes spitting and burst pumping, and in the recovery phase, M1 inhibits pumping. In the case of the I2s and I4, pumping inhibition occurred simultaneously with the induction of spitting and was evident only after M1 was killed. We note that, while all stimulation of spitting passes through M1, pumping inhibition occurred M1-independently, indicating that M1's hub-like properties are specific to spitting.

Overall, the various stimulatory and inhibitory functions we observed for M1, the I2s, and I4 serve a single purpose: to reduce food intake. M1, the I2s, and I4 all inhibit pumping rate independently of each other, and all can produce spits via M1. In addition, strong activation of M1 can also increase pumping rate, as in the burst pumping phase. These M1-stimulated pumps might allow the worm to rinse its pharynx more vigorously when it encounters a sustained noxious stimulation. We speculate that these various functions might allow the pharynx to generate a sequence of actions, first inhibiting pumping and/or spitting, then increasing pumping rate in the burst pumping phase if noxious stimulation continues, and finally inhibiting all pumping, including spitting, as it flees the site of the noxious encounter. Taken together, our results demonstrate how a simple neuromuscular system encodes an inversion of behavioral function in the context of a simple, well-defined connectome.

Experimental Procedures

C. elegans strains and transgenes (listed in order of appearance)

N2 (wild type)

CB1072 *unc-29(e1072)*

MT25631 *lin-15(n765ts); nIs864 [glr-2$_{promoter}$::gfp::unc-54 3' UTR; lin-15(+)]* (6x outcrossed)

MT25732 *lin-15(n765ts); nIs864; nEx2905 [lury-1$_{promoter}$::ICE::SL2::mCherry::unc-54 3' UTR; ttx-3$_{promoter}$::mCherry]*

MT23192 *lin-15(n765ts); nIs678 [glr-2$_{promoter}$::gcamp6s::unc-54 3' UTR; lin-15(+)]* (5x outcrossed)

MT23343 *unc-13(s69); lin-15(n765ts); nIs678*

MT23410 *unc-31(u280); lin-15(n765ts); nIs678*

MT25468 *lite-1(ce314) gur-3(ok2245) lin-15(n765ts); nEx2815 [lury-1$_{promoter}$::ChR2::SL2::mCherry::unc-54 3'UTR]*

MT23338 *nIs686 [gpa-16$_{promoter}$::gcamp3::unc-54 3' UTR] III* (5x outcrossed*); lin-15AB(n765ts)*

MT21783 *gur-3(ok2245)* (1x outcrossed)

KG1180 *lite-1(ce314)*

MT21793 *lite-1(ce314) gur-3(ok2245)*

MT25810 *lite-1(ce314) gur-3(ok2245) lin-15(n765ts); nEx2157 [gur-3 genomic; lin-15(+)]*

MT25809 *lite-1(ce314) gur-3(ok2245) lin-15(n765ts); nEx2281 [lite-1$_{promoter}$::lite-1::gfp; lin-15(+)]*

MT23250 *gur-3(ok2245) lin-15(n765ts); nIs678*

MT23230 *lite-1(ce314) lin-15(n765ts); nIs678*

MT23369 *lite-1(ce314) gur-3(ok2245) lin-15(n765ts); nIs678*

MT23415 *lite-1(ce314) gur-3(ok2245) lin-15(n765ts); nIs678*

MT23415 *nIs686 III; gur-3(ok2245) lin-15(n765ts)*

MT23370 *nIs686 III; lite-1(ce314) gur-3(ok2245) lin-15(n765ts)*

DA1113 *eat-2(ad1113)*

MT25950 *eat-2(ad1113); nIs865 [integration of nEx2905: lury-1$_{promoter}$::ICE::SL2::mCherry::unc-54 3' UTR; ttx-3$_{promoter}$::mCherry]* (8x outcrossed)

MT25982 *eat-2(ad1113); gur-3(ok2245)*

MT22899 *eat-2(ad1113); lite-1(ce314)*

MT25983 *eat-2(ad1113); lite-1(ce314) gur-3(ok2245)*

MT25999 *eat-2(ad1113); lite-1(ce314) gur-3(ok2245); nIs687 [lite-1$_{promoter}$::lite-1::gfp]* (8x outcrossed)

MT23606 lite-1(ce314) gur-3(ok2245) lin-15AB(n765ts); nEx2144 [flp-15$_{promoter}$::mCherry::gur-3, lin-15(+)]

MT23545 lite-1(ce314) gur-3(ok2245) lin-15AB(n765ts); nIs678 ; nEx2144

MT26001 eat-2(ad1113); lite-1(ce314) gur-3(ok2245) nIs791 X [integration of nEx2144: flp-15$_{promoter}$::mCherry::gur-3, lin-15(+)]

MT21421 *nIs569 [flp-15$_{promoter}$::csp-1b; ges-1$_{promoter}$::gfp]* (1x outcrossed)

MT21791 *lite-1(ce314) nIs569*

Supplemental strains:

MT25804 *oxIs322 [myo-2$_{promoter}$::mcherry::H2B; myo-3$_{promoter}$::mcherry::H2B] II ; nIs310 [nlp-13$_{promoter}$::gfp] V ; nEx2905*

MT2249 *egl-47(n1082dm)*

RB850 *egl-47(ok677)*

RB845 *gur-4(ok672)*

FX06169 *gur-5(tm6169)*

DA531 *eat-1(ad427)*

FX14669 *eat-3(tm1107)*

MT6308 *eat-4(ky5)*

DA464 *eat-5(ad464)*

DA1402 *eat-5(ad1402)*

DA467 *eat-6(ad467)*

DA792 *eat-6(ad792)*

MT1073 *egl-4(n478)*

DA599 *eat-8(ad599)*

DA563 *eat-9(e2337); him-8(e1489)*

DA606 *grld-1/eat-10(ad606)*

TV10239 *grld-1/eat-10(wy225)*

TV8888 *grld-1/eat-10(wy655)* (2x outcrossed)

DA541 *gpb-2(ad541)*

MT1212 *egl-19(n582)*

MT6129 *egl-19(n2368sd)*

DA522 *eat-13(ad522)*

DA573 *eat-14(ad573)*

DA602 *eat-15(ad602)*

JT609 *eat-16(sa609)*

DA707 *eat-17(ad707)*

DA1110 *eat-18(ad1110)*

Molecular biology

Transgenes were generated by standard cloning methods. DNA sequences used in the generation of transgenes were amplified with the following primers.

Generated using the infusion cloning technique (Clontech) and injected as plasmids:

nIs864 - pSS028 [glr-2$_{promoter}$::gfp::unc-54 3' UTR]

nEx2905 and nIs865 - pSS042 [lury-1$_{promoter}$::ICE::SL2::mCherry::unc-54 3' UTR]

nEx2815 - pSS034 [lury-1$_{promoter}$::ChR2::SL2::mCherry::unc-54 3'UTR]

glr-2$_{promoter}$: TTGGGACAAATGTGGAAACGA,

TTCGCTTTTTACAGAGTTAACTCTGC

lury-1$_{promoter}$: TTCATTAAGTAATCCGTTTAGGGCAAAT,

GATTGGATTTTCTGGAATAATCGGGT

ICE: ATGGCCGACAAGGTCCTGA,

TTAATGTCCTGGGAAGAGGTAGAAACATC

Generated and injected as PCR product:

nIs678 - [glr-2$_{promoter}$::gcamp6s::unc-54 3' UTR]

nIs686 - pcNB1 [gpa-16$_{promoter}$::gcamp3::unc-54 3' UTR]

gcamp6s: ATGGGTTCTCATCATCATCATCATC,

GCCCGTACGGCCGACTAGTAGG

gpa-16$_{promoter}$: ACCAACCTGAACAGCGAATC

AAAGGGAATTTTATGTGAATAATATCG

Behavioral response to light

Previously, we used a xenon bulb to deliver 365 nm light through an inverted microscope to individual worms on an agar pad. Due to the low throughput of this approach, we designed a device to deliver 365 nm light to standard petri dishes used for culturing worms. The apparatus consists of a UV light-emitting LED (Thorlabs 365 nm M365F1) coupled by a fiber-optic cable to a collimating lens. This system delivers 365 nm UV light in a 3-4 mm spot at a power of ~1.5mW/mm^2 to worms moving freely on a petri dish, producing a burst pumping response indistinguishable from those obtained previously (Bhatla and Horvitz, 2015).

Pharyngeal transport assay

Pharyngeal transport assays were performed as described previously (Bhatla et al., 2015). To visualize the direction of flow in the pharynx for each pump, worms were fed a 50% dilution of 1 µm polystyrene beads (Polysciences) in M9. One-day-old adults were placed with bacteria on an NGM agar pad on a coverslip and observed with a 20x objective on an inverted microscope (Zeiss Axiovert S100). Videos were recorded at 1000 fps using a high-speed video camera (Photron Fastcam Mini). 365 nm light was presented to the worm for 10 seconds (Till Photonics Polychrome V, 150 W xenon bulb). Videos were viewed and manually annotated, using custom Matlab software, for specific behavioral events: ingestion (beads being retained in the corpus after corpus

relaxation), spitting (beads flowing out of the corpus), and pumping (movement of the grinder). In some cases, the worm moved out of the focal plane of the microscope or field-of-view of the camera, in which case those frames were annotated as "missing" and excluded from further analysis.

Behavioral videos of muscle motions

To visualize the timing of muscle motions in the pharynx for each pump, one-day-old adults were placed with bacteria on an NGM agar pad underneath a coverslip and observed with a 20x objective on an inverted microscope (Zeiss Axiovert S100). Videos were recorded at 86 fps using an EMCCD camera (Andor iXon^{+}). 365 nm light was presented to the worm for 10 seconds (Till Photonics Polychrome V, 150 W xenon bulb). *unc-29(e1072)* animals were filmed to facilitate video capture. Videos were viewed and manually annotated based on whether the anterior tip of the pharynx closed or remained open at the end of each pump.

Laser ablations

We used a pulsed nitrogen laser (Andor MicroPoint coupled to a Zeiss Axioplan microscope) to conduct laser microsurgery of individual pharyngeal neurons, as previously described (Bargmann and Avery, 1995; Fang-Yen et al., 2012). Briefly, worms were immobilized by 10 mM sodium azide and mounted for viewing through a 100x oil objective. Ablations were performed on larvae of stage 1 or 2 (L1 or L2), with cells identified by nucleus location visualized with either Nomarski differential

interference contrast optics or a cell-specific GFP reporter. Ablations were confirmed the following day by appearance under Nomarski optics or by the loss of cell-specific fluorescence. On day 3 or 4, adults were assayed for their response to light.

Genetic ablation

For all animals assayed, genetic ablation of M1 was confirmed beforehand using an M1-specific GFP marker (nIs864). The *nEx2905* genetic ablation transgene also killed the M2 neurons in approximately 50% of animals assayed, confirmed via an M2-specific GFP marker (*nIs310*) (Supplementary Figure 2.1, A). The *SL2::mCherry* sequence used drove varying degrees of mCherry expression in the intestine, and we found that the brightness of this intestinal mCherry expression correlated with the rate of M2-killing, such that selecting animals with dim intestinal mCherry expression reduced the rate of M2-killing to 1-2% (Supplementary Figure 2.1, C). Animals assayed in Figure 2.2, E-H were not selected in this way. We did not determine the rate of M1 or M2 killing in *nIs865* animals.

Optogenetic depolarization

Optogenetic manipulations were performed as described before (Bhatla et al., 2015). Cultivation plates were seeded with 300 µl of OP50 *E. coli* mixed with 0.5 µl of 100 mM all-*trans* retinal (ATR+) or ethanol alone (ATR-) and stored in the dark. Transgenic worms carrying channelrhodopsin (ChR2) (Boyden et al., 2005: Nagel et al., 2005) fused to an SL2::mCherry sequence were cultivated on these plates in the dark

from egg to adulthood. For behavioral assays, one-day old animals were analyzed as described above ('Pharyngeal Transport Assay'), except that 470 nm light was used in the place of 365 nm light. *nEx2815 [lury-1$_{promoter}$::ChR2::SL2::mCherry::unc-54 3'UTR]* was expressed in both M1 and the M2s. To avoid confounding optogenetic activation of the M2s, we assayed only animals pre-selected for expression of mCherry in M1 but not the M2s.

Calcium imaging

Calcium imaging was performed as described previously (Bhatla and Horvitz, 2015). Cellular calcium changes were monitored using either GCaMP3 or GCaMP6s (Tian et al., 2009; Chen et al., 2013) transgenically expressed in the cell of interest. Adult worms were immobilized using polystyrene beads on 10% agarose pads under a coverslip (Kim et al., 2013a), and neurons were imaged using an inverted microscope with a 40x air objective. To stimulate animals with UV light and image GCaMP fluorescence simultaneously, light was flickered between 365 nm UV and 485 nm light at a rate of 2 Hz. Videos were recorded using an EMCCD camera (Andor iXon^{+}) and analyzed using custom Matlab software as described previously (Bhatla and Horvitz, 2015; Bhatla et al., 2015).

Acknowledgments

Kirk Burkhart, Eugene Lee, Dipon Ghosh, Josh Saul, and Catherine Olsen provided comments on this section.

Figure 2.1

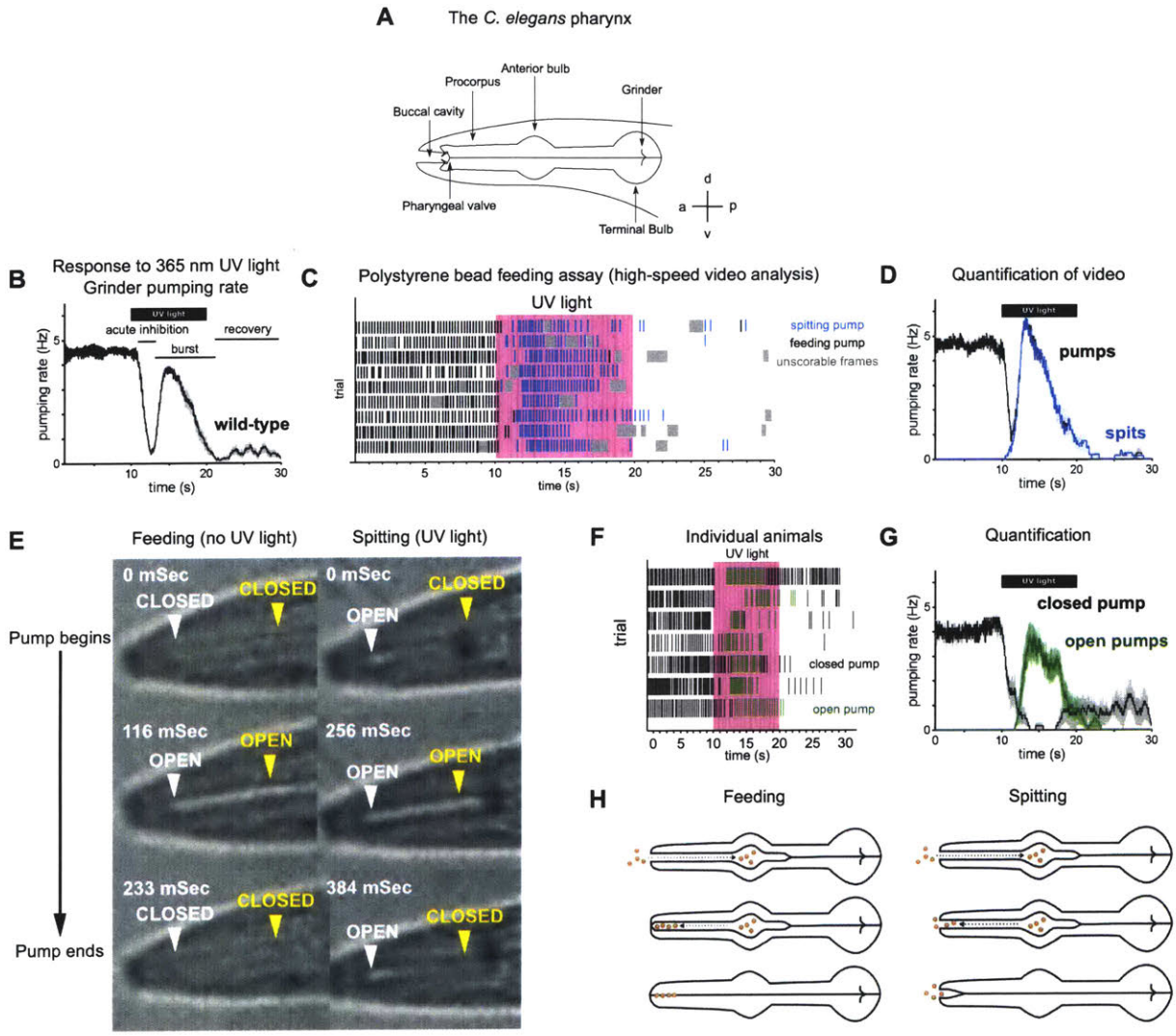
A
The C. elegans pharynx
Anterior bulb
Procorpus
Grinder
Buccal cavity
Pharyngeal valve
Terminal Bulb
d
a
p
v
B
Response to 365 nm UV light
Grinder pumping rate
UV light
acute inhibition
recovery
burst
wild-type
pumping rate (Hz)
time (s)
C
Polystyrene bead feeding assay (high-speed video analysis)
UV light
spitting pump
feeding pump
unscorable frames
trial
time (s)
D
Quantification of video
UV light
pumps
spits
pumping rate (Hz)
time (s)
E
Feeding (no UV light)
Spitting (UV light)
Pump begins
Pump ends
0 mSec
CLOSED
CLOSED
0 mSec
CLOSED
OPEN
116 mSec
OPEN
OPEN
256 mSec
OPEN
OPEN
233 mSec
CLOSED
CLOSED
384 mSec
CLOSED
OPEN
F
Individual animals
UV light
trial
closed pump
open pump
time (s)
G
Quantification
UV light
closed pump
open pumps
pumping rate (Hz)
time (s)
H
Feeding
Spitting

Figure 2.1: Worms spit via sustained contraction of the anterior pharynx.

(A) Anatomy of the *C. elegans* pharynx.

(B) The pharyngeal response to 365 nm UVA light. Line is a backward moving average of the pumping rate of 20 animals; labels indicate the "acute inhibition", "burst", and "recovery" phases of the response. Data recorded by eye in real time. This result was originally reported by Bhatla and Horvitz (2015).

(C) Raster plot of representative results from polystyrene bead feeding assay. Pumps were scored as "feeding" if they concluded in the retention of particles in the anterior pharynx, while pumps were scored as "spitting" if they released beads from the corpus into the environment or if beads ingested during corpus contraction were not retained. Video segments which were unscorable (e.g. due to poor visibility, the worm moving out of frame, etc.) were excluded from the analysis and are shown as grey boxes. n = 9 worms. Data derived from analysis of behavioral videos.

(D) Quantification of average grinder pumping and spitting rates of animals from in (B). The burst pumping phase is composed entirely of spits.

(E) Representative images of the pumping cycle of feeding (left column) and spitting worms (right column). The lumen of the pharynx (yellow arrowheads) is visible as a white line. The food-trapping pharyngeal valve (white arrowheads) is located at the anterior end of the lumen. During feeding (left column), "closed" pumps occur and the lumen and pharyngeal valve open and close nearly synchronously, enabling the trapping and eventual ingestion of food (Fang-yen *et al.*, 2009). By contrast, the opening of the lumen and the pharyngeal valve become uncoupled in spitting ("open" pumps). While the lumen continues to open and close, the muscles at the site of the pharyngeal

valve undergo sustained contraction, such that the conclusion of a pump ejects material from the pharynx. Animals are *unc-29(e1072)* to facilitate video capture (see experimental procedures).

(F) Raster plot showing induction of "closed" (i.e., feeding) and "open" (i.e., spitting) pumps by UVA light. n = 7 worms. Data derived from analysis of behavioral videos

(G) Moving averages of animals from (B), indicating that the burst pumping phase consistent almost completely of "open" pumps.

(H) Graphical summary of feeding and spitting behavior. In a representative feeding cycle (left), bacterial food is drawn in as the pharynx contracts. At the peak of contraction, the anterior tip of the pharynx relaxes, forming a size-selective filter. As the pharynx relaxes, fluid passes through the filter but bacteria are trapped. In a representative spitting cycle (right), food is drawn in as during a feeding pump. However, in spitting worms the anterior filtering region of the pharynx remains contracted while the main body of the pharynx relaxes. Thus, food is expelled rather than being retained.

Shading around traces indicates SEM.

Figure 2.2

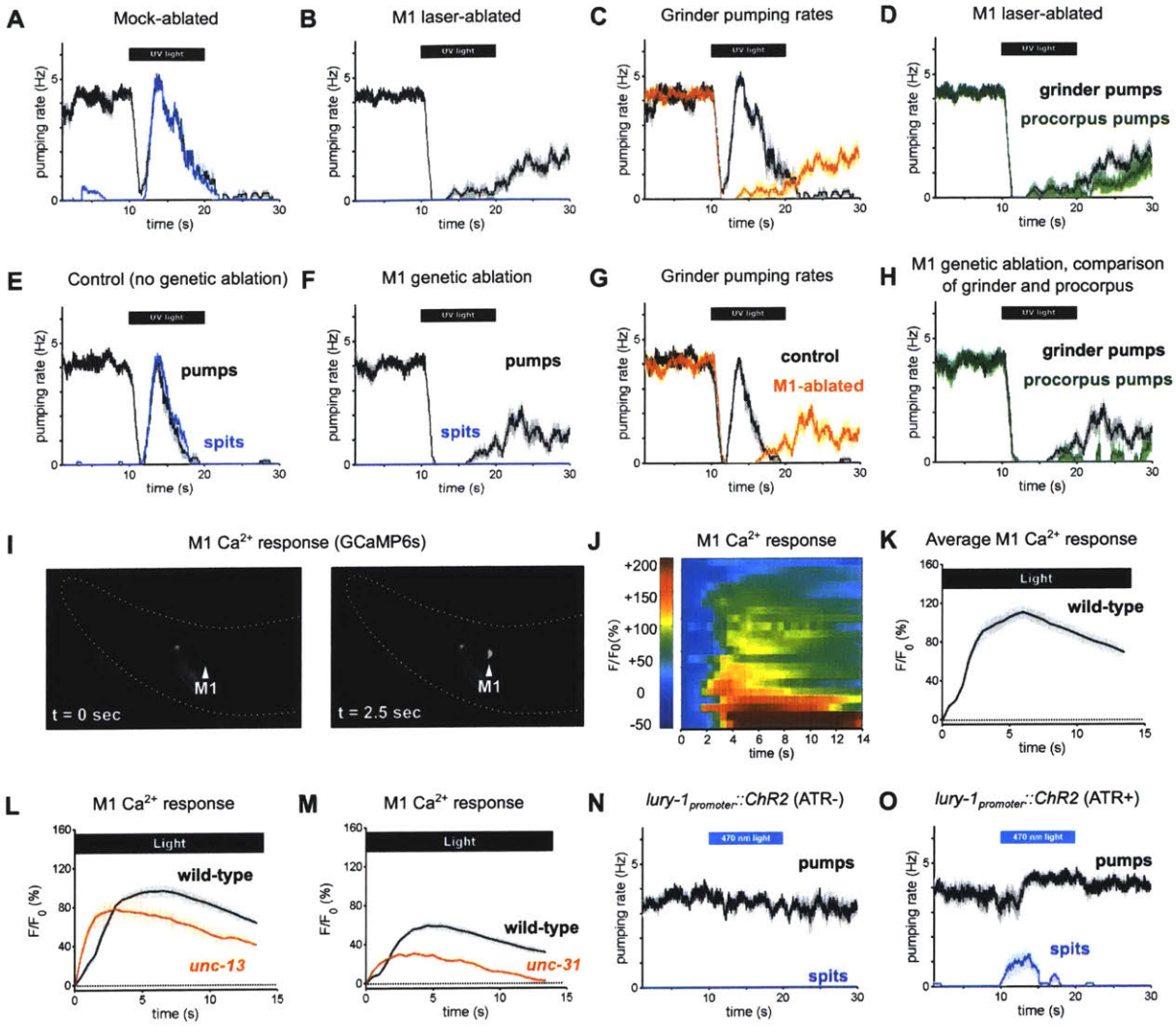
A
Mock-ablated
B
M1 laser-ablated
C
Grinder pumping rates
D
M1 laser-ablated
grinder pumps
procorpus pumps
E
Control (no genetic ablation)
pumps
spits
F
M1 genetic ablation
pumps
spits
G
Grinder pumping rates
control
M1-ablated
H
M1 genetic ablation, comparison of grinder and procorpus
grinder pumps
procorpus pumps
I
M1 Ca2+ response (GCaMP6s)
M1
t = 0 sec
M1
t = 2.5 sec
J
M1 Ca2+ response
F/F0(%)
time (s)
K
Average M1 Ca2+ response
Light
wild-type
F/F0 (%)
time (s)
L
M1 Ca2+ response
Light
wild-type
unc-13
F/F0 (%)
time (s)
M
M1 Ca2+ response
Light
wild-type
unc-31
F/F0 (%)
time (s)
N
lury-1promoter::ChR2 (ATR-)
470 nm light
pumps
spits
pumping rate (Hz)
time (s)
O
lury-1promoter::ChR2 (ATR+)
470 nm light
pumps
spits
pumping rate (Hz)
time (s)

Figure 2.2: UVA light induces M1-dependent burst pumping and spitting behavior.

(A) Mock-ablated animals are wild-type in UVA light-induced spitting. n = 12.

(B) Laser ablation of M1 eliminates spitting and burst pumping. n = 13.

(C) Comparison of grinder pumping rates of mock-ablated animals from (A) and M1-ablated animals from (B). In addition to eliminating burst pumping and spitting, M1-ablation enhances the rate of pumping recovery after UVA illumination.

(D) Laser-ablated animals from (B) exhibit unusual "uncoupled" pumps, during which the grinder pumps while the procorpus does not.

(E) Control animals lacking the M1 genetic ablation transgene (*lury-1*$_{promoter}$*::csp-1b::SL2::mCherry*) are indistinguishable from wild-type animals. n = 10.

(F) Genetic ablation of M1 eliminates spitting and burst pumping. n = 10.

(G) Comparison of grinder pumping rates of control animals from (E) and M1-ablated animals from (F). In addition to eliminating burst pumping and spitting, M1-ablation enhances the rate of pumping recovery after UVA illumination.

(H) As in (G), M1 genetically ablated animals from (I) exhibit unusual "uncoupled" pumps, during which the grinder pumps while the procorpus does not.

(I) Representative example of UVA light-induced GCaMP6s fluorescence increase in M1 (see experimental procedures).

(J) M1 somatic calcium, as measured by GCaMP6s fluorescence increases (F/F_0) in response to UVA light. Each row represents a different worm. n = 20.

(K) Average response of animals shown in (J).

(L) UVA light-induced calcium increases in M1 were largely preserved in *unc-13(s69)* mutants. n = 20.

(M) UVA light-induced calcium increases in M1 were largely preserved in *unc-31(u280)* mutants. n = 20.

(N) Animals expressing an M1-specific ChR2 transgene grown in the absence of ATR do not spit in response to 470 nm light. n = 10 worms.

(O) A subset (~25%) of animals expressing an M1-specific ChR2 transgene grown in the presence of ATR spit in response to 470 nm light. n = 11 worms.

Shading around traces indicates SEM. All data derived from analysis of behavioral or calcium imaging videos.

Figure 2.3

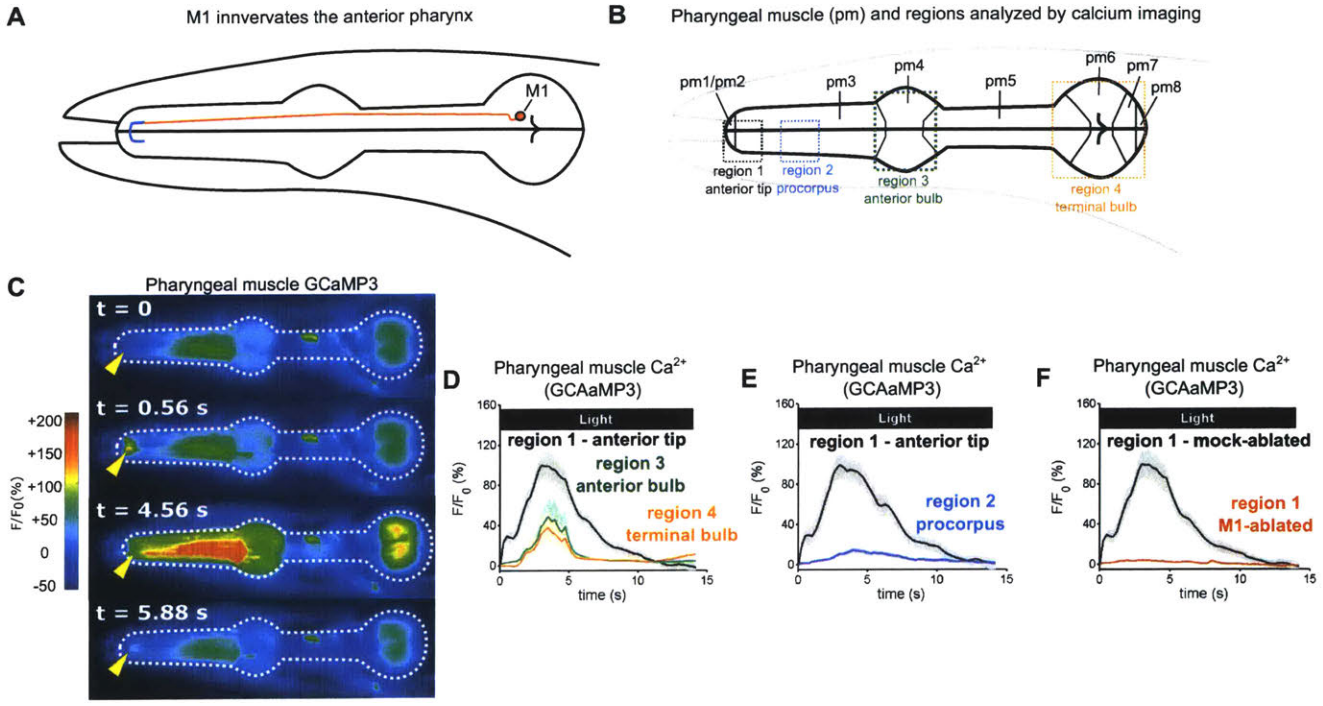
A
M1 innvervates the anterior pharynx
M1
B
Pharyngeal muscle (pm) and regions analyzed by calcium imaging
pm1/pm2
pm3
pm4
pm5
pm6
pm7
pm8
region 1
anterior tip
region 2
procorpus
region 3
anterior bulb
region 4
terminal bulb
C
Pharyngeal muscle GCaMP3
t = 0
t = 0.56 s
t = 4.56 s
t = 5.88 s
+200
+150
+100
+50
0
-50
F/F0(%)
D
Pharyngeal muscle Ca2+
(GCAaMP3)
Light
region 1 - anterior tip
region 3
anterior bulb
region 4
terminal bulb
F/F0 (%)
time (s)
E
Pharyngeal muscle Ca2+
(GCAaMP3)
Light
region 1 - anterior tip
region 2
procorpus
F/F0 (%)
time (s)
F
Pharyngeal muscle Ca2+
(GCAaMP3)
Light
region 1 - mock-ablated
region 1
M1-ablated
F/F0 (%)
time (s)

Figure 2.3: Spitting is accompanied by spatially restricted calcium increases in pharyngeal muscle.

(A) M1's anatomy (red) suggests that it might control spitting directly, as it is the only neuron to make neuromuscular junctions (blue) with the region of pharyngeal muscle that undergoes sustained contraction during spitting.

(B) Graphical depiction of the eight classes of pharyngeal muscle (pm1-8; borders indicated by solid black lines). Dashed boxes indicate regions analyzed for calcium increases based on GCaMP3 fluorescence.

(C) Representative images from video pharyngeal muscle calcium imaging using GCaMP3 expressed in pharyngeal muscle (*gpa-16*$_{promoter}$*::GCaMP3*). Yellow arrowhead indicates site of spatially restricted calcium increases.

(D) UVA light induces increases in pharyngeal muscle calcium. Regions analyzed are indicated in (B). n = 13 worms.

(E) Muscles of the anterior tip of the pharynx (pm1, pm2, and pm3) undergo sustained and spatially restricted increases in calcium at the same location as the pharyngeal valve and M1's synapses with pharyngeal muscles. Posteriorly adjacent regions of the procorpus do not exhibit sustained calcium signals. Regions analyzed are indicated in (B). n = 9 worms.

(F) Spatially restricted calcium signals depend on M1. Region analyzed is indicated in (B). n ≥ 11 worms.

Shading around traces indicates SEM. All data derived from analysis of calcium imaging videos.

Figure 2.4

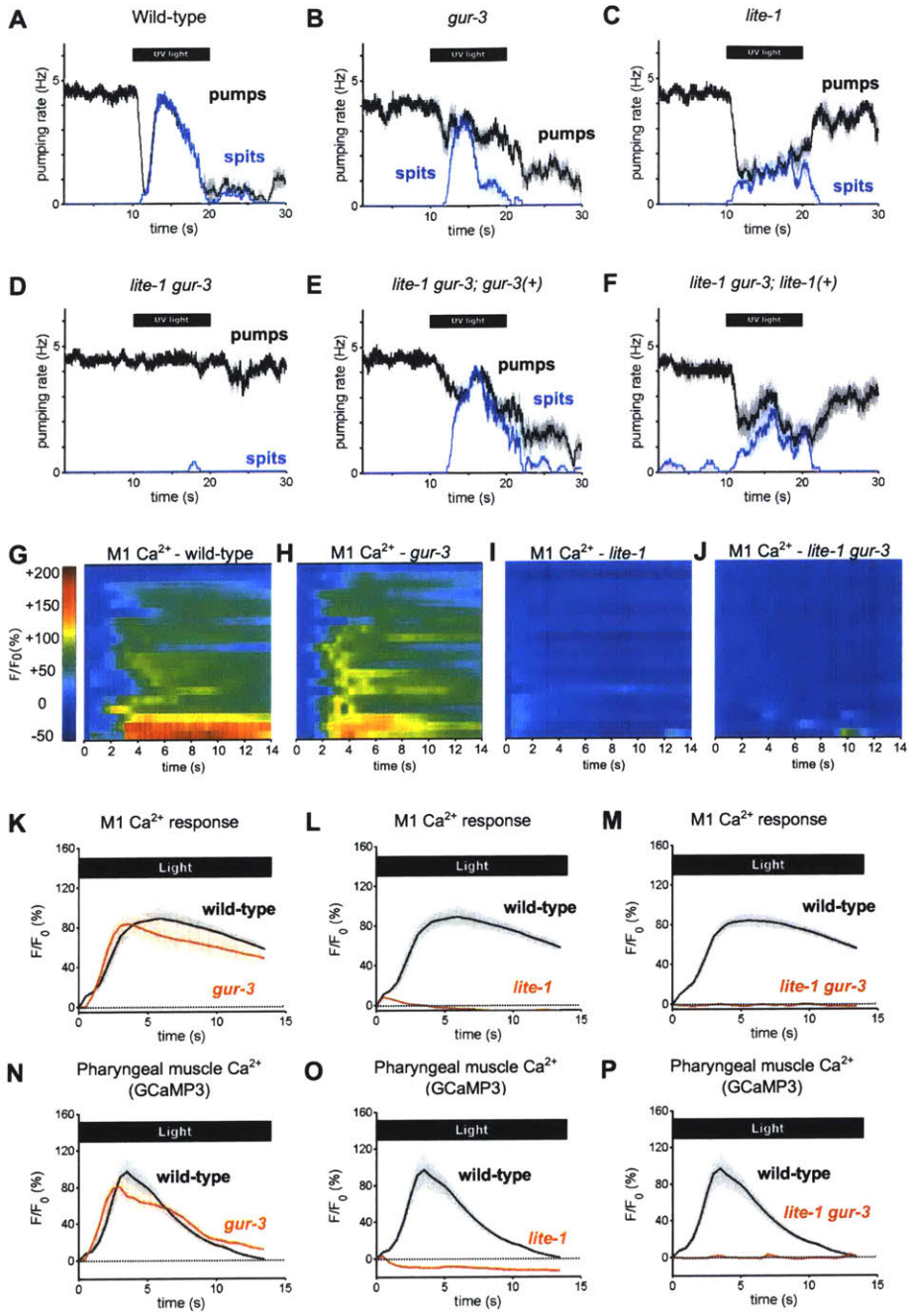
A
Wild-type
B
gur-3
C
lite-1
D
lite-1 gur-3
E
lite-1 gur-3; gur-3(+)
F
lite-1 gur-3; lite-1(+)
UV light
pumps
spits
pumping rate (Hz)
time (s)
G
M1 Ca2+ - wild-type
H
M1 Ca2+ - gur-3
I
M1 Ca2+ - lite-1
J
M1 Ca2+ - lite-1 gur-3
F/F0(%)
+200
+150
+100
+50
0
-50
K
M1 Ca2+ response
L
M1 Ca2+ response
M
M1 Ca2+ response
Light
wild-type
gur-3
lite-1
lite-1 gur-3
F/F0 (%)
N
Pharyngeal muscle Ca2+ (GCaMP3)
O
Pharyngeal muscle Ca2+ (GCaMP3)
P
Pharyngeal muscle Ca2+ (GCaMP3)

Figure 2.4: Gustatory-receptor orthologs *lite-1* and *gur-3* control UVA light-induced spitting.

(A-D) While UVA light-induced spitting is preserved in *gur-3(ok2245)* single mutants, it is reduced in *lite-1(ce314)* single mutants and eliminated in *lite-1(ce314) gur-3(ok2245)* double mutants. n = 10 worms except $n_{gur\text{-}3}$ = 9 worms.

(E-F) Expression of wild-type *gur-3* or *lite-1* restores partial or wild-type spitting to *gur-3(ok2245)* and *lite-1(ce314)* mutants respectively. n = 10 worms.

(G-J) Representative GCaMP6s ($glr\text{-}2_{promoter}$::*GCaMP6s*) calcium imaging data showing the M1 calcium response to UVA light in individual animals. Each row is a unique animal; fluorescence changes are indicated by the heatmap. n = 20 worms.

(K-M) Light-induced calcium increases in M1 depend on *lite-1* (which accounts for 99% of the response) and *gur-3,* which makes a small but significant contribution to M1's initial activation. n ≥ 60 worms.

(N-P) Light-induced calcium increases in pharyngeal muscle also depend on *lite-1* and *gur-3* (see experimental procedures). n ≥ 20 worms.

Shading around traces indicates SEM. All behavioral data derived from analysis of behavioral videos.

Figure 2.5

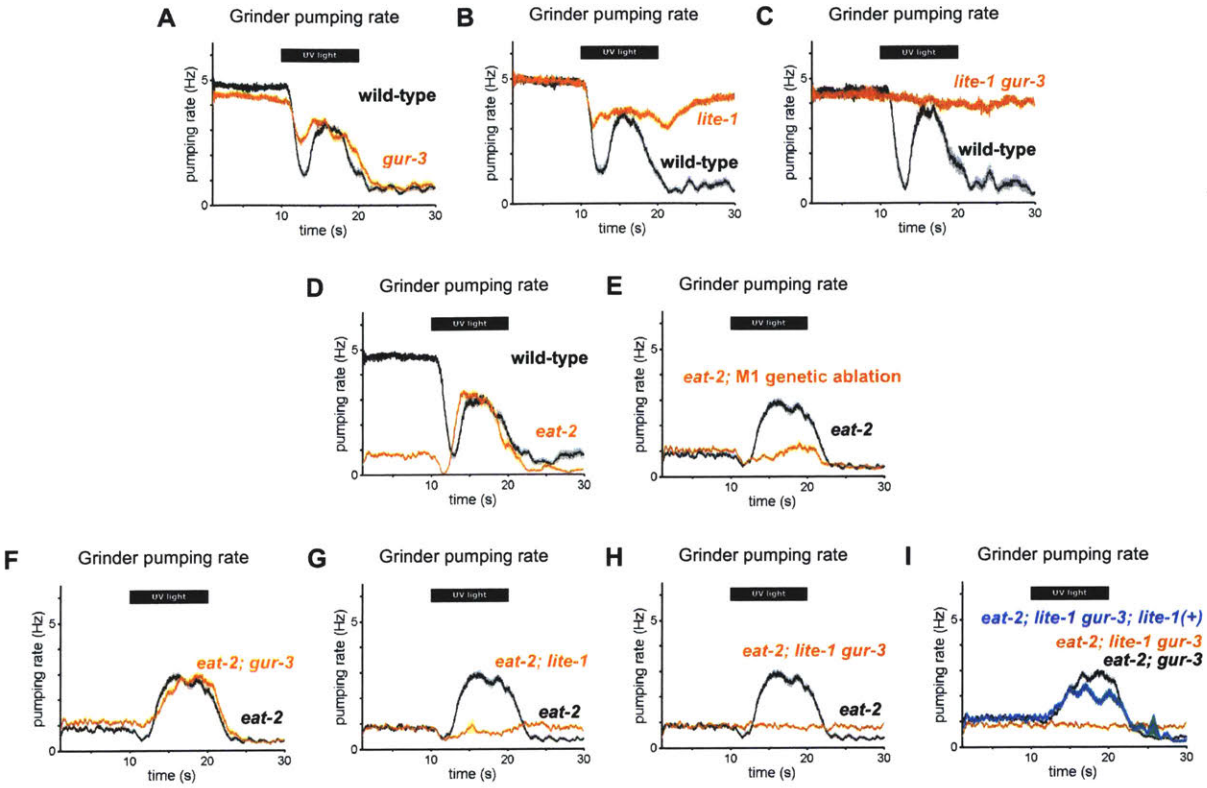
A
Grinder pumping rate
UV light
wild-type
gur-3
pumping rate (Hz)
time (s)
B
Grinder pumping rate
UV light
lite-1
wild-type
pumping rate (Hz)
time (s)
C
Grinder pumping rate
UV light
lite-1 gur-3
wild-type
pumping rate (Hz)
time (s)
D
Grinder pumping rate
UV light
wild-type
eat-2
pumping rate (Hz)
time (s)
E
Grinder pumping rate
UV light
eat-2; M1 genetic ablation
eat-2
pumping rate (Hz)
time (s)
F
Grinder pumping rate
UV light
eat-2; gur-3
eat-2
pumping rate (Hz)
time (s)
G
Grinder pumping rate
UV light
eat-2; lite-1
eat-2
pumping rate (Hz)
time (s)
H
Grinder pumping rate
UV light
eat-2; lite-1 gur-3
eat-2
pumping rate (Hz)
time (s)
I
Grinder pumping rate
UV light
eat-2; lite-1 gur-3; lite-1(+)
eat-2; lite-1 gur-3
eat-2; gur-3
pumping rate (Hz)
time (s)

Figure 2.5: *lite-1* controls burst pumping.

(A) *gur-3* is not required for light-induced burst pumping. n = 60 worms.

(B-C) *lite-1*'s contribution to burst pumping cannot be evaluated because *lite-1* mutants do not inhibit pumping. $n_{lite\text{-}1}$ = 40 and $n_{lite\text{-}1\ gur\text{-}3}$ = 20 worms.

(D) *eat-2(ad1ThiFig113)* mutants are defective in feeding pumping rate (t = 0-10) such that burst pumping can be assayed in the absence of pumping inhibition. n = 40 worms.

(E) M1 is required for burst pumping in the *eat-2* background. n = 60 worms.

(F-H) Burst pumping in the *eat-2* mutant background depends on *lite-1* but not *gur-3*. n = 60 worms.

(I) A $lite\text{-}1_{promoter}$*::lite-1::GFP* integrated transgene rescued the burst pumping defects of *lite-1 gur-3* mutants in the *eat-2* mutant background. n = 60 worms.

Shading around traces indicates SEM. All data recorded by eye in real time.

Figure 2.6

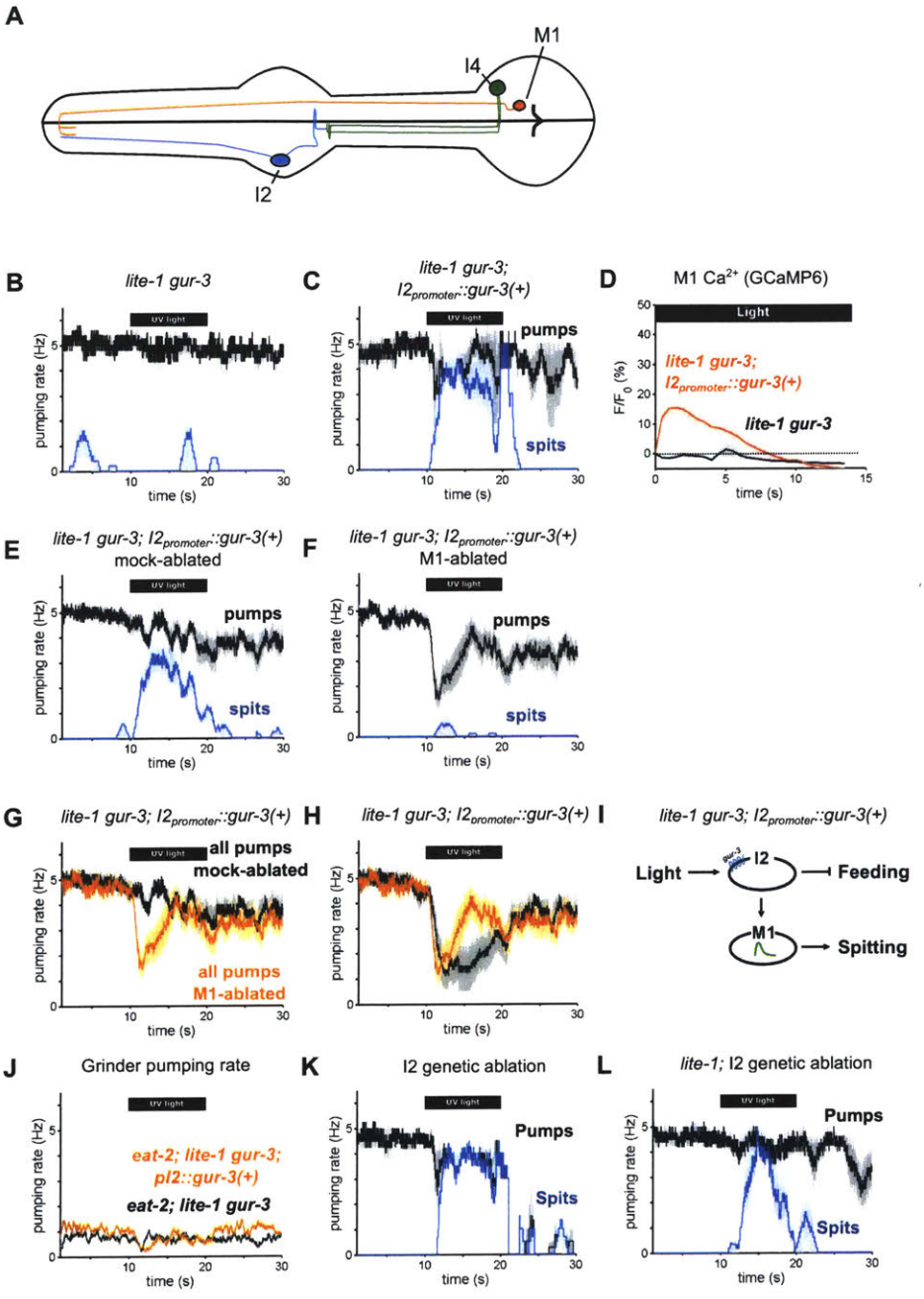
A
M1
I4
I2
B
lite-1 gur-3
C
lite-1 gur-3;
I2promoter::gur-3(+)
D
M1 Ca2+ (GCaMP6)
Light
lite-1 gur-3;
I2promoter::gur-3(+)
lite-1 gur-3
F/F0 (%)
time (s)
pumping rate (Hz)
UV light
pumps
spits
E
lite-1 gur-3; I2promoter::gur-3(+)
mock-ablated
F
lite-1 gur-3; I2promoter::gur-3(+)
M1-ablated
G
lite-1 gur-3; I2promoter::gur-3(+)
all pumps
mock-ablated
all pumps
M1-ablated
H
lite-1 gur-3; I2promoter::gur-3(+)
I
lite-1 gur-3; I2promoter::gur-3(+)
Light
I2
Feeding
M1
Spitting
J
Grinder pumping rate
eat-2; lite-1 gur-3;
pI2::gur-3(+)
eat-2; lite-1 gur-3
K
I2 genetic ablation
Pumps
Spits
L
lite-1; I2 genetic ablation
Pumps
Spits

Figure 2.6: Rescue of *gur-3* in the I2s permits light-induced spits via M1.

(A) Diagram indicating the cellular morphology of M1 and the *gur-3*-expressing I2s and I4 in the pharynx.

(B) *lite-1 gur-3* double mutants are defective in light-induced spitting. n = 5 worms. Data derived from analysis of behavioral videos.

(C) I2-specific expression of *gur-3* via the *flp-15*$_{promoter}$*::mCherry::gur-3(+)* transgene restores light-induced spitting to *lite-1 gur-3* mutants. n = 5 worms. Data derived from analysis of behavioral videos.

(D) I2-specific expression of *gur-3* via the *flp-15*$_{promoter}$*::mCherry::gur-3(+)* transgene restores the light-induced M1 calcium response *lite-1 gur-3* mutants. n ≥ 26 worms.

(E) Mock-ablated *lite-1 gur-3* animals bearing the I2-specific *flp-15*$_{promoter}$*::mCherry::gur-3(+)* transgene spit in response to light as in (B). n = 11 worms. Data derived from analysis of behavioral videos.

(F) Laser ablation of M1 suppressed the I2-specific *gur-3* rescue of *lite-1 gur-3* spitting. n = 11 worms. Data derived from analysis of behavioral videos.

(G) Comparison of grinder pumping rate from (D) and (E). While mock-ablated *lite-1 gur-3; P*$_{I2}$*::gur-3* animals from (D) do not inhibit pumping in response to light, M1-ablated animals from (E) exhibit robust light-induced inhibition, indicating that I2's promotion of pumping via M1 overpowers its inhibition of pumping. Data derived from analysis of behavioral videos.

(H) Comparison of feeding pumping rate from (D) and (E). By inhibiting feeding pumps and promoting spitting pumps via M1, the I2 neurons reduce overall feeding.

(I) Model for the I2s' effects on M1 and pumping. Data derived from analysis of behavioral videos.

(J) I2-specific expression of *gur-3* via the *flp-15*$_{promoter}$*::mCherry::gur-3(+)* transgene does not rescue the burst pumping defect of *eat-2; lite-1 gur-3* animals. n = 20 worms. Data recorded by eye in real time.

(K) The I2 neurons are not required for light-induced spitting in a wild-type background. n = 5 worms. Data derived from analysis of behavioral videos.

(L) The I2 neurons are not required for light-induced spitting in a *lite-1* background. n = 6 worms. Data derived from analysis of behavioral videos.

Shading around traces indicates SEM.

Figure 2.7

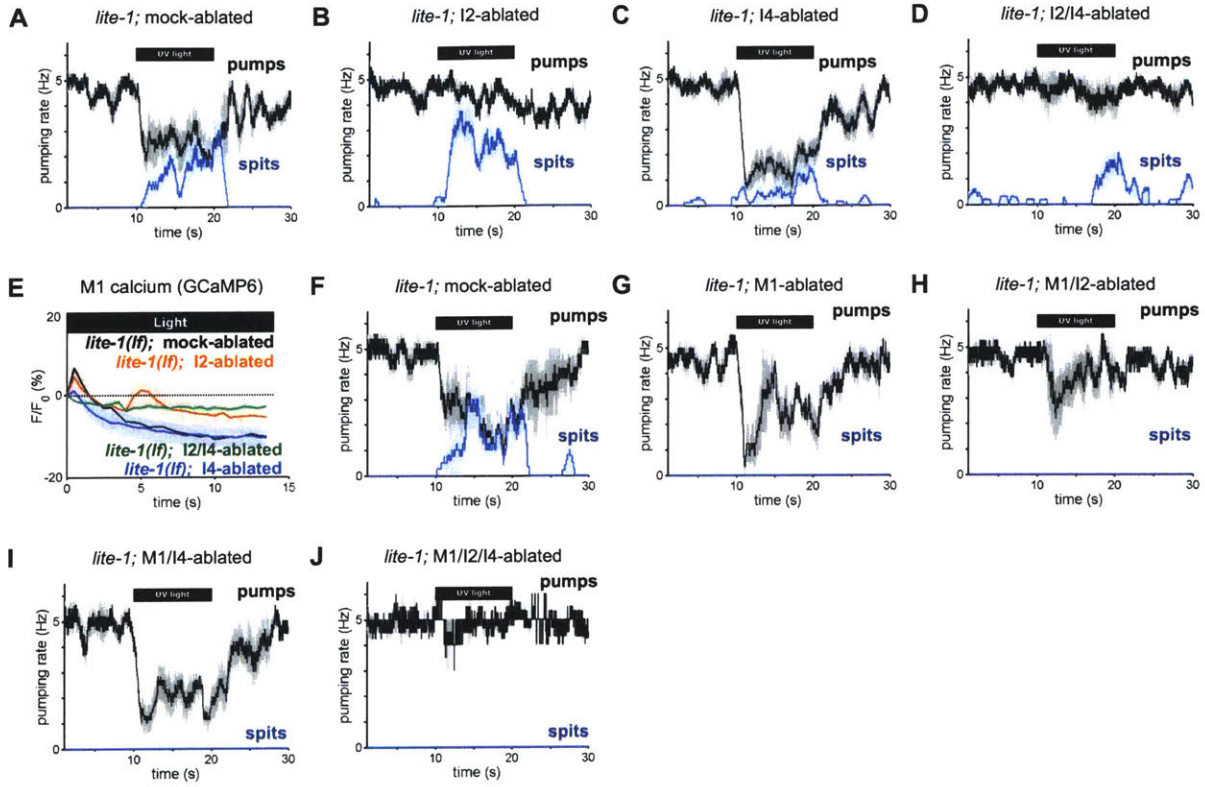
A
lite-1; mock-ablated
B
lite-1; I2-ablated
C
lite-1; I4-ablated
D
lite-1; I2/I4-ablated
UV light
pumps
spits
pumping rate (Hz)
time (s)
E
M1 calcium (GCaMP6)
Light
lite-1(lf); mock-ablated
lite-1(lf); I2-ablated
lite-1(lf); I2/I4-ablated
lite-1(lf); I4-ablated
F/F0 (%)
F
lite-1; mock-ablated
G
lite-1; M1-ablated
H
lite-1; M1/I2-ablated
I
lite-1; M1/I4-ablated
J
lite-1; M1/I2/I4-ablated

Figure 2.7: I4 functions with the I2s in the light-induced spitting of *lite-1* mutants.

(A) Mock-ablated *lite-1* animals inhibit pumping and spit in response to light. n = 8 worms.

(B) I2-ablated *lite-1* animals spit in response to light but do not inhibit pumping. n = 8 worms.

(C) I4-ablated *lite-1* animals inhibit pumping and spit in response to light. n = 10 worms.

(D) I2/I4 double-ablated *lite-1* animals exhibit delayed spitting and do not inhibit pumping in response to light. n = 8 worms.

(E) I2- and I4-ablated *lite-1* animals exhibit residual M1 calcium responses; I2/I4 double-ablated animals do not have detectable M1 calcium responses. n ≥ 8 worms.

(F) Mock-ablated *lite-1* animals inhibit pumping and spit in response to light. n = 5 worms.

(G) M1-ablated *lite-1* animals inhibit pumping, but do not spit, in response to light. n = 6 worms.

(H) M1/I2 double-ablated *lite-1* animals inhibit pumping, but do not spit, in response to light. n = 6 worms.

(I) M1/I4 double-ablated *lite-1* animals inhibit pumping, but do not spit, in response to light. n = 7 worms.

(J) M1/I2/I4 triple-ablated *lite-1* animals neither inhibit pumping nor spit in response to light. n = 4 worms.

All data derived from analysis of behavioral or calcium imaging videos. Shading around traces indicates SEM.

Figure 2.8

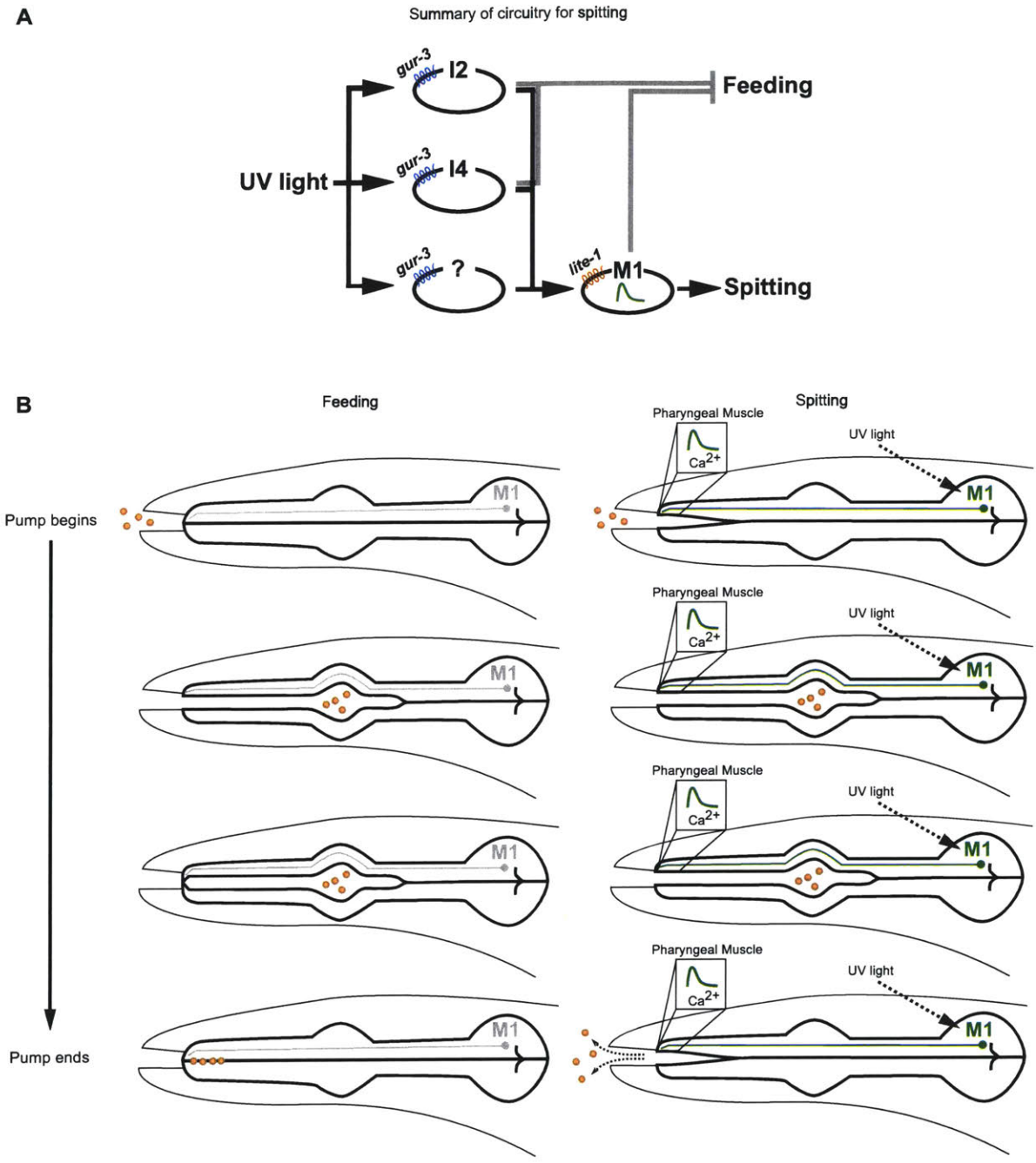
A
Summary of circuitry for spitting
gur-3
I2
gur-3
I4
gur-3
?
UV light
Feeding
lite-1
M1
Spitting
B
Feeding
Spitting
Pump begins
Pump ends
M1
Pharyngeal Muscle
Ca2+
UV light

Figure 2.8: Summary and model of spitting circuitry and behavior.

(A) Summary of circuitry controlling spitting. Multiple *gur-3*-expressing neurons converge on M1, acts as a hub in the functional network for spitting. Neurons in the spitting circuit also inhibit feeding independently of M1. Black pointed arrows indicate excitation and grey blunted arrows indicate inhibition.

(B) Model for biomechanics of spitting behavior. In feeding, M1 is inactive. The contraction of pharyngeal muscles opens the pharynx and draws material inward. Prior to the onset of pharyngeal muscle relaxation, the pharyngeal valve closes, sealing the anterior end of the lumen and acting as a filter to retain bacteria in the pharynx while fluid is ejected. In spitting, M1 is active, resulting in sustained contraction of the pharyngeal muscles that control the pharyngeal valve. As in feeding, the contraction of pharyngeal muscles opens the pharynx and draws material inward. However, due to the sustained contraction of the muscles operating the valve, the anterior end of the pharnx remains open, causing material to be ejected into the environment when the pharynx relaxes.

Supplemental Figure 2.1

A

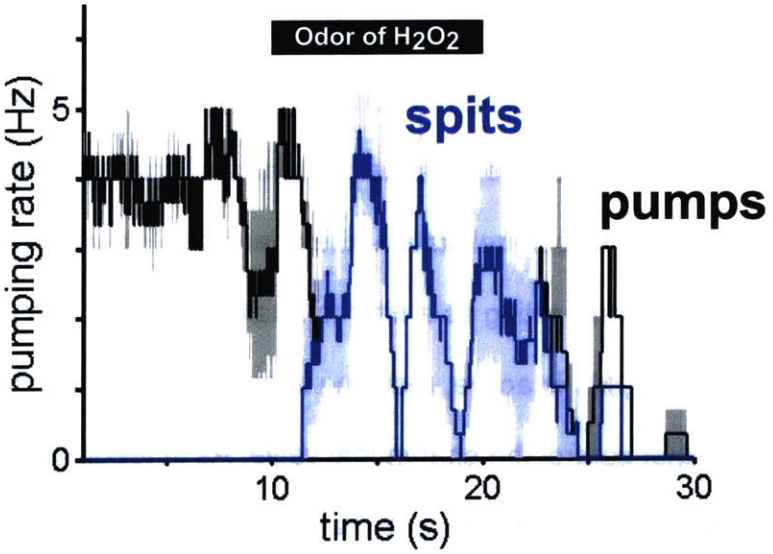

Supplemental Figure 2.1: Odor of hydrogen peroxide induces spitting.

(A) The odor of 9M hydrogen peroxide induces spitting by slow-moving *unc-29(e1072)* mutants. n = 4 worms. Data derived from analysis of behavioral videos. Shading around traces indicates SEM.

Supplemental Figure 2.2

A

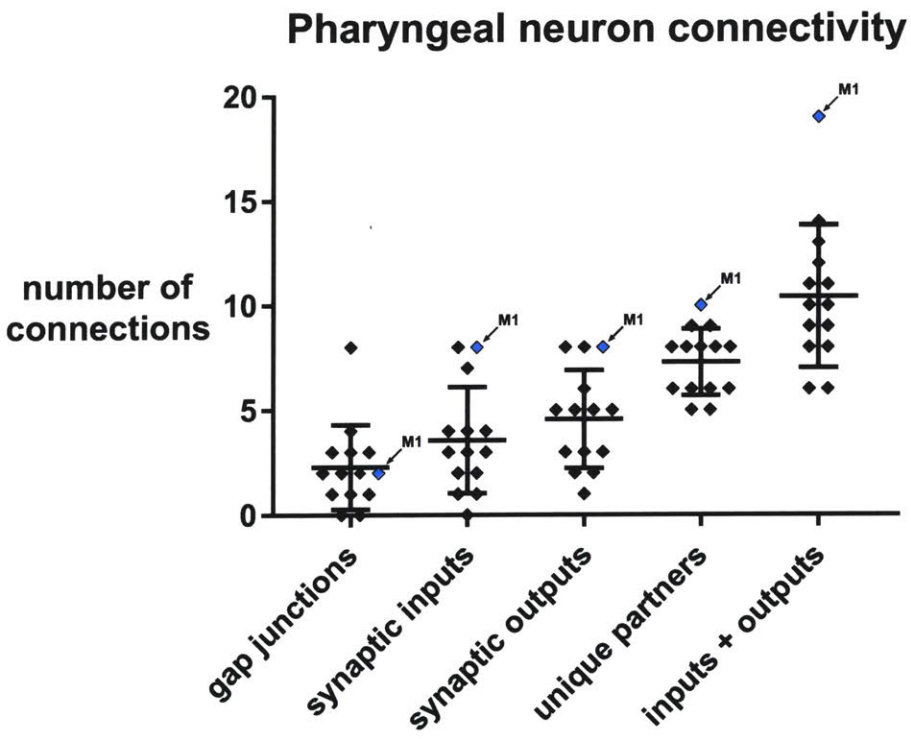

Supplemental Figure 2.2: Pharyngeal neuron connectivity from Albertson and Thompson, 1976.

(A) Summary of the connectivity of pharyngeal neurons. Each neuron is plotted as a dot based on the number of neuron classes with which it forms connections. M1, shown in blue and indicated with an arrow, makes a greater diversity of ingoing and outgoing synaptic connections than other pharyngeal neurons. Y-axis indicates the number of neuron classes forming connections, not the number of synapses. "Unique partners" refers to the sum of neurons giving input or output for a given cell, while "inputs + outputs" is the sum of the number of neuron classes providing inputs and the number of neuron classes receiving outputs for a given cell.

Supplemental Figure 2.3

A

Neuron	Percent ablated
M1	100% (30/30)
M2	53% (17/32)

B

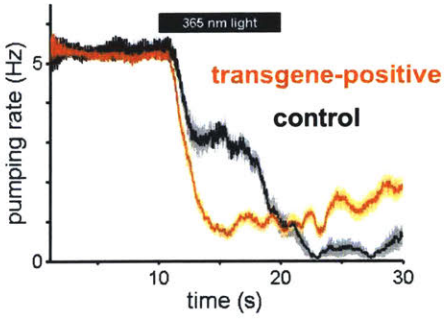

C

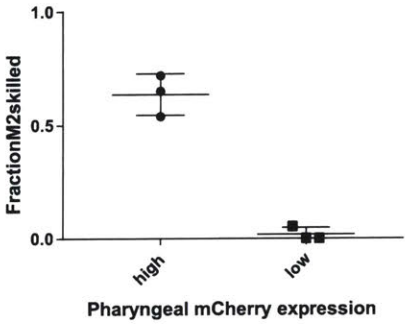

Supplemental Figure 2.3: M1 genetic ablation.

(A) Expression of mammalian caspase ICE kills M1 with high-efficiency and the M2 neurons with moderate efficiency. The presence of the neurons was determined by the expression of *glr-2*$_{promoter}$*: GFP* and *nlp-13*$_{promoter}$*::GFP* transgenes, respectively.

(B) M1 genetic ablation transgene eliminates burst pumping. n = 40 worms. Data recorded by eye in real time. Shading around traces indicates SEM.

(C) Screening animals based on the brightness of pharyngeal mCherry expression allows the selection M2-positive animals. When pharyngeal mCherry expression is high, animals are more likely to lack the M2s. Bars are mean ± SEM, n = 3 days, with 19-26 animals per condition per day.

Supplemental Figure 2.4

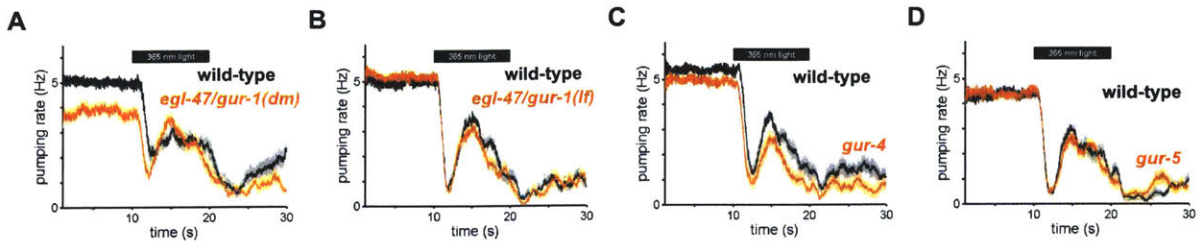

Supplemental Figure 2.4: response of gustatory receptor mutants to 365 nm light

(A) *egl-47(n1082dm)* mutants were normal in burst pumping. n = 20 worms.

(B) *egl-4ThSupFig 2.7(ok677)* mutants were normal in burst pumping. n = 20 worms.

(C) *gur-4(ok672)* mutants were normal in burst pumping. n = 20 worms.

(D) *gur-5(tm6169)* mutants were normal in burst pumping. n = 20 worms.

Shading around traces indicates SEM. All data recorded by eye in real time.

Class I: defective feeding, wild-type burst pumping	***eat-1:*** unknown ***eat-2:*** nAChR subunit ***eat-3:*** mitochondrial dynamin ***eat-8:*** solute carrier family 22 superfamily transporter ***eat-18:*** nAChR function
Class II: wild-type feeding and defective burst pumping	***eat-6:*** K+/Na+ ATPase ***eat-10:*** RNA-binding protein - glutamate receptor expression ***eat-12/egl-19:*** voltage-gated calcium channel ***eat-14:*** 50 kb deletion ***eat-15:*** serine protease inhibitor
Class III: generally defective pumping	***eat-5:*** innexin ***eat-11/gpb-2:*** $G_{\beta}5$ ***eat-13:*** 70 kb deletion ***eat-16:*** RGS ***eat-20:*** adherens junction biogenesis
Class IV: wild-type pumping	***eat-4:*** vesicular glutamate transporter ***eat-7/egl-4:*** cGMP-dependent kinase ***eat-17:*** Rab GAP

Supplemental Table 2.1: categorization of *eat* mutants by defects in rates of feeding and burst pumping.

Supplementary Figure 2.5

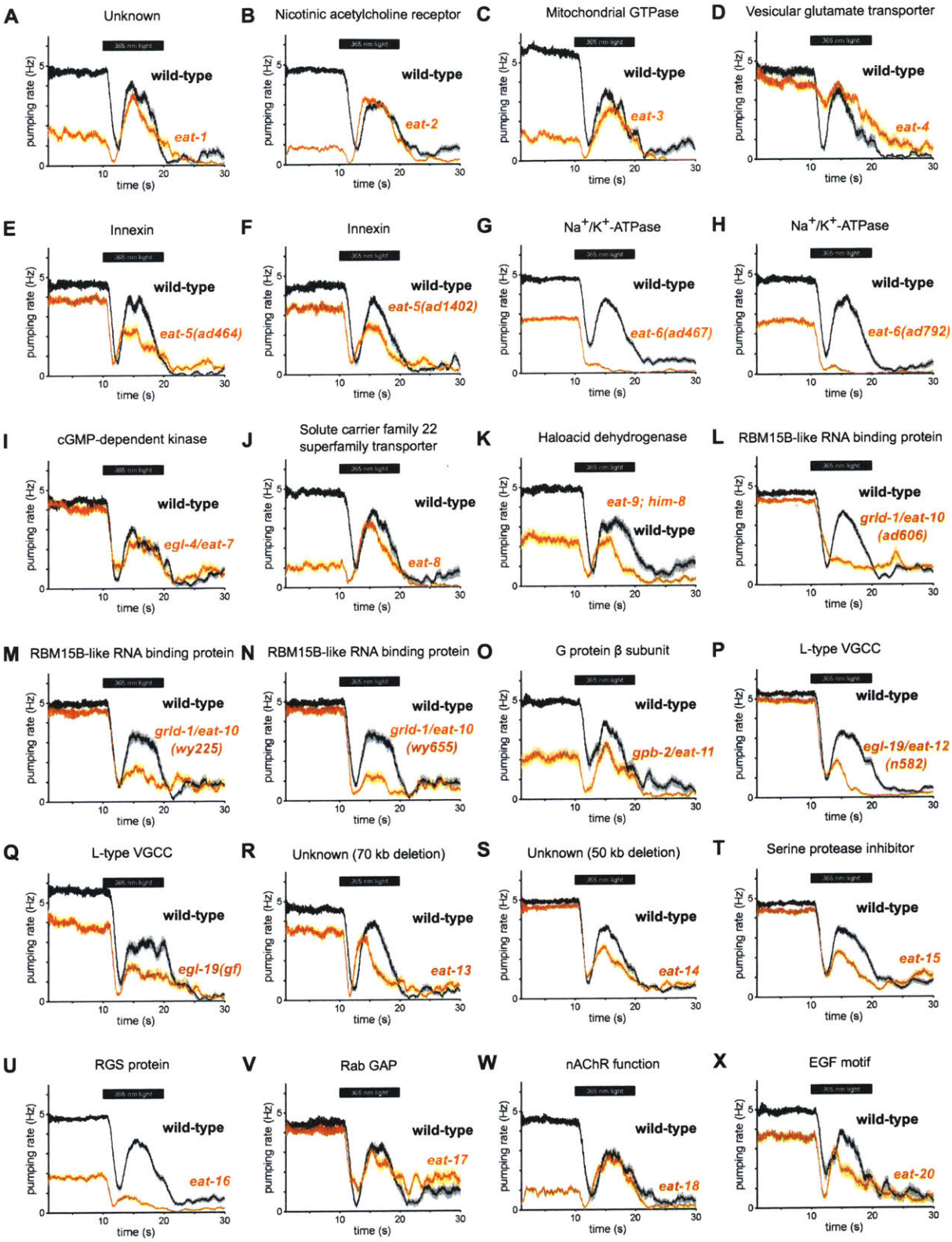

Supplemental Figure 2.5: candidate screen of *eat* mutants.

(A) *eat-1(ad427)* mutants were severely defective in feeding but not burst pumping. n = 20 worms.

(B) *eat-2(ad1113)* nicotinic acetylcholine receptor subunit mutants were severely defective in feeding but not burst pumping. n = 40 worms.

(C) *eat-3(tm1107)* mitochondrial GTPase mutants were defective in feeding but not burst pumping. n = 20 worms.

(D) *eat-4(ky6)* vesicular glutamate transporter mutants were not defective in feeding or burst pumping. n = 20 worms.

(E) *eat-5(ad464)* innexin mutants were generally defective in pumping. n = 20 worms.

(F) *eat-5(ad1402)* innexin mutants were generally defective in pumping. n = 20 worms.

(G) *eat-6(ad467)* Na^+/K^+-ATPase mutants were defective in feeding and severely defective in burst pumping. n = 60 worms.

(H) *eat-6(ad792)* Na^+/K^+-ATPase mutants were defective in feeding and severely defective in burst pumping. n = 60 worms.

(I) *egl-4/eat-7(n478)* cGMP-dependent kinase mutants were not defective in feeding or burst pumping. n = 20 worms.

(J) *eat-8(ad599)* solute carrier family 22 superfamily transporter mutants were severely defective in feeding but not burst pumping. n = 20 worms.

(K) *eat-9(e2337); him-8(1489)* haloacid dehydrogenase mutants were generally defective in pumping. n = 20 worms.

(L) *grld-1/eat-10(ad606)* RBM15B-like RNA binding protein mutants were defective in burst pumping but not feeding. n = 60 worms.

(M) *grld-1/eat-10(wy225)* RBM15B-like RNA binding protein mutants were defective in burst pumping but not feeding. n = 20 worms.

(N) *grld-1/eat-10(wy655)* RBM15B-like RNA binding protein mutants were defective in burst pumping but not feeding. n = 20 worms.

(O) *gpb-2/eat-11(ad541)* G protein β subunit mutants were generally defective in pumping. n = 20 worms.

(P) *egl-19/eat-12(n582)* L-type voltage gated calcium channel mutants were defective in burst pumping but not feeding. n = 60 worms

(Q) *egl-19/eat-12(n2386)* gain-of-function L-type voltage gated calcium channel mutants were generally defective in pumping. n = 20 worms.

(R) *eat-13(ad522)* mutants were generally defective in pumping. n = 20 worms.

(S) *eat-14(ad573)* mutants were not defective in feeding and were mildly defective in burst pumping. n = 60 worms.

(T) *eat-15(ad602)* serine protease inhibitor mutants were not defective in feeding and were mildly defective in burst pumping. n = 60 worms.

(U) *eat-16(sa609)* RGS protein mutants were generally and severely defective in pumping. n = 60 worms.

(V) *eat-17(ad707)* Rab GAP mutants were not defective in feeding or burst pumping. n = 20 worms.

(W) *eat-18(ad1110)* nAChR function mutants were severely defective in feeding but normal in burst pumping. n = 20 worms.

(X) *eat-20(nc4)* EGF motif mutants were generally defective in pumping. n = 20 worms. Shading around traces indicates SEM. All data recorded by eye in real time.

References

Albertson D.G., Thomson J.N., and Brenner, S. (1976). The pharynx of *Caenorhabditis elegans*. Philosophical Transactions of the Royal Society of London. B, Biological Sciences *275*, 299–325.

Avery, L. (1993). The genetics of feeding in *Caenorhabditis elegans*. Genetics *133*, 897–917.

Avery, L., and Horvitz, H.R. (1989). Pharyngeal pumping continues after laser killing of the pharyngeal nervous system of *C. elegans*. Neuron *3*, 473–485.

Avery, L., and You, Y. (2012). *C. elegans* feeding. WormBook, ed. The *C. elegans* Research Community, WormBook, doi/10.1895/wormbook.1.150.1, http://www.wormbook.org.

Bargmann, C.I. (1998). Neurobiology of the *Caenorhabditis elegans* genome. Science *282*, 2028–2033.

Bassett, D.S., and Bullmore, E.T. (2009). Human brain networks in health and disease. Curr. Opin. Neurol. *22*, 340–347.

Bedford, T.H.B. (1927). The nature of the action of ultra-violet light on micro-organisms. Br J Exp Pathol *8*, 437–441.

Berwin, B., Floor, E., and Martin, T.F.J. (1998). CAPS (mammalian UNC-31) protein localizes to membranes involved in dense-core vesicle exocytosis. Neuron *21*, 137–145.

Bhatla, N., and Horvitz, H.R. (2015). Light and hydrogen peroxide inhibit *C. elegans* feeding through gustatory receptor orthologs and pharyngeal neurons. Neuron *85*, 804–818.

Bhattacharya, A., Aghayeva, U., Berghoff, E.G., and Hobert, O. (2019). Plasticity of the electrical connectome of *C. elegans*. Cell *176*, 1174–1189.

de Bono, M., and Villu Maricq, A. (2005). Neuronal substrates of complex behaviors in *C. elegans*. Annual Review of Neuroscience *28*, 451–501.

Boyden, E.S., Zhang, F., Bamberg, E., Nagel, G., and Deisseroth, K. (2005). Millisecond-timescale, genetically targeted optical control of neural activity. Nat Neurosci *8*, 1263–1268.

Brockie, P.J., Madsen, D.M., Zheng, Y., Mellem, J., and Maricq, A.V. (2001). Differential expression of glutamate receptor subunits in the nervous system of *Caenorhabditis elegans* and their regulation by the homeodomain protein UNC-42. J. Neurosci. *21*, 1510–1522.

Buckholtz, J.W., and Meyer-Lindenberg, A. (2012). Psychopathology and the human connectome: toward a transdiagnostic model of risk for mental illness. Neuron *74*, 990–1004.

Bullmore, E., and Sporns, O. (2009). Complex brain networks: graph theoretical analysis of structural and functional systems. Nature Reviews Neuroscience *10*, 186–198.

Cerretti, D.P., Kozlosky, C.J., Mosley, B., Nelson, N., Ness, K.V., Greenstreet, T.A., March, C.J., Kronheim, Druck, T., Cannizzaro, L.A., et al. (1992). Molecular cloning of the interleukin-1 beta converting enzyme. Science *256*, 97–100.

Chen, T., Wardill, T.J., Sun, Y., Pulver, S.R., Renninger, S.L., Baohan, A., Schreiter, E.R., Kerr, R.A., Orger, M.B., Jayaraman, V., et al. (2013). Ultrasensitive fluorescent proteins for imaging neuronal activity. Nature *499*, 295–300.

Ciche, T. (2007). The biology and genome of *Heterorhabditis bacteriophora*, WormBook, ed. The *C. elegans* Research Community, WormBook, doi/10.1895/wormbook.1.135.1, http://www.wormbook.org.

Cronin, T.W., and Bok, M.J. (2016). Photoreception and vision in the ultraviolet. Journal of Experimental Biology *219*, 2790–2801.

Du, E.J., Ahn, T.J., Wen, X., Seo, D.-W., Na, D.L., Kwon, J.Y., Choi, M., Kim, H.-W., Cho, H., and Kang, K. (2016). Nucleophile sensitivity of *Drosophila* TRPA1 underlies light-induced feeding deterrence. Elife *5*, e18425.

ECETOC (1996). Special Report 10 - Hydrogen Peroxide OEL Criteria Document. (Brussels, Belgium: ECETOC).

Edwards, S.L., Charlie, N.K., Milfort, M.C., Brown, B.S., Gravlin, C.N., Knecht, J.E., and Miller, K.G. (2008). A novel molecular solution for ultraviolet light detection in *Caenorhabditis elegans*. PLOS Biology *6*, e198.

Emmons, S.W. (2018). Neural circuits of sexual behavior in *Caenorhabditis elegans*. Annual Review of Neuroscience *41*, 349–369.

Euler, T., Detwiler, P.B., and Denk, W. (2002). Directionally selective calcium signals in dendrites of starburst amacrine cells. Nature *418*, 845–852.

Fang-Yen, C., Avery, L., and Samuel, A.D.T. (2009). Two size-selective mechanisms specifically trap bacteria-sized food particles in *Caenorhabditis elegans*. PNAS *106*, 20093–20096.

Finkel, T. (2011). Signal transduction by reactive oxygen species. The Journal of Cell Biology *194*, 7–15.

Ghosh, D.D., Jin, X., and Nitabach, M. (2017). *C. elegans* discriminate colors without eyes or opsins. BioRxiv 092072.

Gong, J., Yuan, Y., Ward, A., Kang, L., Zhang, B., Wu, Z., Peng, J., Feng, Z., Liu, J., and Xu, X.Z.S. (2016). The *C. elegans* taste receptor homolog LITE-1 is a photoreceptor. Cell *167*, 1252-1263.e10.

Grefkes, C., and Fink, G.R. (2014). Connectivity-based approaches in stroke and recovery of function. Lancet Neurol *13*, 206–216.

Griffith, L.C. (2012). Identifying behavioral circuits in *Drosophila melanogaster:* moving targets in a flying insect. Current Opinion in Neurobiology *22*, 609–614.

Guntur, A.R., Gu, P., Takle, K., Chen, J., Xiang, Y., and Yang, C. (2015). *Drosophila* TRPA1 isoforms detect UV light via photochemical production of H_2O_2. Proc Natl Acad Sci USA *112*, E5753–E5761.

Guntur, A.R., Gou, B., Gu, P., He, R., Stern, U., Xiang, Y., and Yang, C. (2017). H_2O_2-sensitive isoforms of *Drosophila melanogaster* TRPA1 act in bitter-sensing gustatory neurons to promote avoidance of UV during egg-laying. Genetics *205*, 749–759.

Hannawi, Y., and Stevens, R.D. (2016). Mapping the connectome following traumatic brain injury. Curr Neurol Neurosci Rep *16*, 44.

Hendricks, M., Ha, H., Maffey, N., and Zhang, Y. (2012). Compartmentalized calcium dynamics in a *C. elegans* interneuron encode head movement. Nature *487*, 99–103.

van den Heuvel, M.P., and Fornito, A. (2014). Brain networks in schizophrenia. Neuropsychol Rev *24*, 32–48.

van den Heuvel, M.P., and Yeo, B.T.T. (2017). A spotlight on bridging microscale and macroscale human brain architecture. Neuron *93*, 1248–1251.

van den Heuvel, M.P., Bullmore, E.T., and Sporns, O. (2016). Comparative connectomics. Trends in Cognitive Sciences *20*, 345–361.

Higley, M.J., and Sabatini, B.L. (2008). Calcium signaling in dendrites and spines: practical and functional considerations. Neuron *59*, 902–913.

Hill, K., and Schaefer, M. (2009). Ultraviolet light and photosensitising agents activate TRPA1 via generation of oxidative stress. Cell Calcium *45*, 155–164.

Hockberger, P.E. (2002). A history of ultraviolet photobiology for humans, animals and microorganisms. Photochemistry and Photobiology *76*, 561–579.

Hockberger, P.E., Skimina, T.A., Centonze, V.E., Lavin, C., Chu, S., Dadras, S., Reddy, J.K., and White, J.G. (1999). Activation of flavin-containing oxidases underlies light-induced production of H_2O_2 in mammalian cells. PNAS *96*, 6255–6260.

Jansen, G., Thijssen, K.L., Werner, P., van der Horst, M., Hazendonk, E., and Plasterk, R.H.A. (1999). The complete family of genes encoding G proteins of *Caenorhabditis elegans*. Nature Genetics *21*, 414.

Kang, K., Panzano, V.C., Chang, E.C., Ni, L., Dainis, A.M., Jenkins, A.M., Regna, K., Muskavitch, M.A.T., and Garrity, P.A. (2012). Modulation of TRPA1 thermal sensitivity enables sensory discrimination in *Drosophila*. Nature *481*, 76–80.

Kim, M., and Johnson, W.A. (2014). ROS-mediated activation of *Drosophila* larval nociceptor neurons by UVC irradiation. BMC Neurosci *15*, 14.

Kim, E., Sun, L., Gabel, C.V., and Fang-Yen, C. (2013a). Long-term imaging of *Caenorhabditis elegans* using nanoparticle-mediated immobilization. PLoS ONE *8*, e53419.

Kim, M.J., Ainsley, J.A., Carder, J.W., and Johnson, W.A. (2013b). Hyperoxia-triggered aversion behavior in *Drosophila* foraging larvae is mediated by sensory detection of hydrogen peroxide. Journal of Neurogenetics *27*, 151–162.

Kral, A., Kronenberger, W.G., Pisoni, D.B., and O'Donoghue, G.M. (2016). Neurocognitive factors in sensory restoration of early deafness: a connectome model. The Lancet Neurology *15*, 610–621.

Liu, J., Ward, A., Gao, J., Dong, Y., Nishio, N., Inada, H., Kang, L., Yu, Y., Ma, D., Xu, T., et al. (2010). *C. elegans* phototransduction requires a G protein–dependent cGMP pathway and a taste receptor homolog. Nature Neuroscience *13*, 715–722.

Marder, E. (2012). Neuromodulation of neuronal circuits: back to the future. Neuron *76*, 1–11.

Maruyama, I.N., and Brenner, S. (1991). A phorbol ester/diacylglycerol-binding protein encoded by the *unc-13* gene of *Caenorhabditis elegans*. PNAS *88*, 5729–5733.

McCormick, J., Fischer, Pachlatko, J., and Eisenstark, A. (1976). Characterization of a cell-lethal product from the photooxidation of tryptophan: hydrogen peroxide. Science *191*, 468–469.

McKay, J.P., Raizen, D.M., Gottschalk, A., Schafer, W.R., and Avery, L. (2004). *eat-2* and *eat-18* are required for nicotinic neurotransmission in the *Caenorhabditis elegans* pharynx. Genetics *166*, 161–169.

Nagel, G., Szellas, T., Huhn, W., Kateriya, S., Adeishvili, N., Berthold, P., Ollig, D., Hegemann, P., and Bamberg, E. (2003). Channelrhodopsin-2, a directly light-gated cation-selective membrane channel. PNAS *100*, 13940–13945.

Ohno, H., Yoshida, M., Sato, T., Kato, J., Miyazato, M., Kojima, M., Ida, T., and Iino, Y. (2017). Luqin-like RYamide peptides regulate food-evoked responses in *C. elegans*. ELife *6*, e28877.

Raizen, D.M., Lee, R.Y., and Avery, L. (1995). Interacting genes required for pharyngeal excitation by motor neuron MC in *Caenorhabditis elegans*. Genetics *141*, 1365–1382.

Rengarajan, S., and Hallem, E.A. (2016). Olfactory circuits and behaviors of nematodes. Current Opinion in Neurobiology *41*, 136–148.

Rhee, S.G. (1999). Redox signaling: hydrogen peroxide as intracellular messenger. Exp Mol Med *31*, 53–59.

Richardson, A. (1893). The action of light in preventing putrefactive decomposition; and in inducing the formation of hydrogen peroxide in organic liquids. J. Chem. Soc., Trans. *63*, 1109–1130.

Richmond, J.E., Davis, W.S., and Jorgensen, E.M. (1999). UNC-13 is required for synaptic vesicle fusion in *C. elegans*. Nat Neurosci *2*, 959–964.

Richmond, J.E., Weimer, R.M., and Jorgensen, E.M. (2001). An open form of syntaxin bypasses the requirement for UNC-13 in vesicle priming. Nature *412*, 338–341.

Romanowski, A., Garavaglia, M.J., Goya, M.E., Ghiringhelli, P.D., and Golombek, D.A. (2014). Potential conservation of circadian clock proteins in the phylum Nematoda as revealed by bioinformatic searches. PLoS One *9*.

Schafer, W. (2016). Nematode nervous systems. Current Biology *26*, R955–R959.

Schröter, M., Paulsen, O., and Bullmore, E.T. (2017). Micro-connectomics: probing the organization of neuronal networks at the cellular scale. Nature Reviews Neuroscience *18*, 131–146.

Schuch, A.P., Moreno, N.C., Schuch, N.J., Menck, C.F.M., and Garcia, C.C.M. (2017). Sunlight damage to cellular DNA: Focus on oxidatively generated lesions. Free Radical Biology and Medicine *107*, 110–124.

Starich, T.A., Lee, R.Y., Panzarella, C., Avery, L., and Shaw, J.E. (1996). *eat-5* and *unc-7* represent a multigene family in *Caenorhabditis elegans* involved in cell-cell coupling. The Journal of Cell Biology *134*, 537–548.

Terakita, A. (2005). The opsins. Genome Biology *6*, 213.

Thornberry, N.A., Bull, H.G., Calaycay, J.R., Chapman, K.T., Howard, A.D., Kostura, M.J., Miller, D.K., Molineaux, S.M., Weidner, J.R., Aunins, J., et al. (1992). A novel heterodimeric cysteine protease is required for interleukin-1β processing in monocytes. Nature *356*, 768.

Tian, L., Hires, S.A., Mao, T., Huber, D., Chiappe, M.E., Chalasani, S.H., Petreanu, L., Akerboom, J., McKinney, S.A., Schreiter, E.R., et al. (2009). Imaging neural activity in worms, flies and mice with improved GCaMP calcium indicators. Nature Methods *6*, 875–881.

Van Essen, D.C., and Barch, D.M. (2015). The human connectome in health and psychopathology. World Psychiatry *14*, 154–157.

Ward, A., Liu, J., Feng, Z., and Xu, X.Z.S. (2008). Light-sensitive neurons and channels mediate phototaxis in *C. elegans*. Nature Neuroscience *11*, 916–922.

White, J.G., Southgate, E., Thomson J. N., and Brenner, S. (1986). The structure of the nervous system of the nematode *Caenorhabditis elegans*. Philosophical Transactions of the Royal Society of London. B, Biological Sciences *314*, 1–340.

Xiang, Y., Yuan, Q., Vogt, N., Looger, L.L., Jan, L.Y., and Jan, Y.N. (2010). Light-avoidance-mediating photoreceptors tile the *Drosophila* larval body wall. Nature *468*, 921–926.

Yan, G., Vértes, P.E., Towlson, E.K., Chew, Y.L., Walker, D.S., Schafer, W.R., and Barabási, A. (2017). Network control principles predict neuron function in the *Caenorhabditis elegans* connectome. Nature *550*, 519–523.

Yang, H.H., StPierre, F., Sun, X., Ding, X., Lin, M.Z., and Clandinin, T.R. (2016). Subcellular imaging of voltage and calcium signals reveals neural processing in vivo. Cell *166*, 245–257.

Zheng, Y., Brockie, P.J., Mellem, J.E., Madsen, D.M., and Maricq, A.V. (1999). Neuronal control of locomotion in *C. elegans* is modified by a dominant mutation in the GLR-1 ionotropic glutamate receptor. Neuron *24*, 347–361.

Chapter 3

Future directions

I. Behavioral analysis of a novel *C. elegans* gulping behavior

Having characterized pharyngeal circuitry that generates spitting in response to 365 nm (UV) light when the worm is in the presence of food (Chapter 2), I wondered how these circuits might function in different contexts. One such context of likely relevance to the pharynx is when food is absent from the environment.

Another group analyzed the pumping behavior of worms in the absence of food and found that worms removed from food inhibited pumping over the course of minutes and hours (Dallière *et al.*, 2016). This chronic inhibition of pumping depends in part on the I2s (Nicolas Dallière, personal communication). Previous work in our lab found that the pharyngeal I2 neurons rapidly inhibit pumping on food in response to light (Bhatla and Horvitz, 2015).

I previously showed that the I2s of worms on food promote M1-dependent spitting in response to light (Figure 2.6, B-F), and wondered whether a similar 'inhibit-feeding-and-spit' circuit might function in the absence of food, perhaps as a foraging behavior (as discussed below, spitting rinses material in and out of the pharynx), which might allow the worm to better sample the environment for food. Consistent with the hypothesis that similar circuitry might underlie responses to light and food deprivation, I

found that worms on 1 μM beads without food do indeed spit significantly more than worms on beads with food (data not shown).

Most interestingly, this experiment led me to identify new pump types. In my previous work, I categorized pumps based on whether they retained or released food. In my observation of worms pumping in the absence of food, I noticed an additional dimension of pumping behavior. During a feeding pump, food is drawn through the buccal cavity, a channel that connects the anterior opening of the pharynx to the environment (Figure 3.1, A). The buccal cavity is separated from the pharynx by the metastomal flaps, cuticular structures that protrude from the anterior pharynx into the buccal cavity (Figure 3.1, A). A previous study observed that the metastomal flaps restrict the flow of food from the buccal cavity into the pharynx and hypothesized that the flaps might be passive structures that limit food-intake to prevent over-ingestion (Fang-Yen *et al.*, 2009).

I observed variation in how efficiently food passes from the buccal cavity into the pharynx itself. During the low-intake feeding pumps described previously (Fang-Yen *et al.*, 2009), food trickles gradually (i.e., filters) from the buccal cavity into the pharyngeal lumen such that only a small number of particles are ingested (Figure 3.1, B). During spitting, however, this filtering mechanism is disengaged, likely by 'opening' the flaps, and material flushes freely into and out of the pharynx. Interesting, some feeding pumps also seemed to interrupt this filtering mechanism. Because the influx of food is not regulated by the metastomal flaps, these high-intake (or 'gulping') pumps trap and ingest large quantities of food (Figure 3.1, B).

Thus, pumps can be categorized by their effects on both influx (i.e., filtering versus non-filtering) and efflux (i.e., retaining versus releasing) of particles, leading to four possible pump types (Figure 3.1, C), three of which I have commonly observed in the contexts of UV light administration and removal from food. Like spits, gulping pumps occurred at a greater frequency in the absence of food, suggesting they are behaviorally regulated (Figure 3.2, A).

How might the pharyngeal nervous system control the configuration of the metastomal flaps and thus the rate of food intake? The metastomal flaps are mounted on pharyngeal muscles 1 and 2 (pm1/2) such that differential contraction of these muscles might adjust the angle of the flaps and thus the degree to which they block incoming particles (Figure 3.1, A). The pharyngeal connectome indicates that these muscles are in turn innervated by M1 and no other neuron. This anatomical connectivity suggests that, in addition to producing spits by opening the pharyngeal valve, M1 might control gulping pumps by exciting pm1 and/or pm2 and thus opening the metastomal flaps.

How might a single neuron generate multiple, opposite types of motor output? A simple hypothesis is that one flow regulator (e.g., flap or valve) might be more sensitive to M1 activity than the other, such that a graded increase in M1 activity opens first one regulator and then the other. Specifically, I hypothesized that pm1 and pm2, the small pharyngeal muscles from which the metastomal flaps project, might be more sensitive to M1 activity than pm3, the large pharyngeal muscle from which the pharyngeal valve projects. A prediction of this model is that a graded increase in M1 activity will evoke

first gulping pumps (opening the metastomal flaps but not the valve) and subsequently spits (opening both the metastomal flaps and the valves).

In collaboration with Eugene Lee, who analyzed behavioral videos, I attempted to test this model, but the reagents I generated were unable to manipulate M1 activity with the required reliability. Additionally, I was unable to find conditions in which M1 was necessary for gulping. Thus, additional work is required to characterize this interesting pharyngeal behavior and clarify M1's potential role in it.

II. Behavioral and circuit analysis of a novel *C. elegans* vomiting behavior

The spitting behavior described in Chapter 2 produces reversal of flow in the procorpus, but not in the isthmus and terminal bulb regions posterior to the procorpus (for anatomy, see, Figure 2.1, A). Additionally, the intestinal contents remain in the intestine during spitting. In other words, light makes worms spit, but it does not make them vomit.

In the course of exploratory experiments, I noticed on several occasions that, strikingly, light induced true vomiting of intestinal contents, which were pumped backwards through the length of the pharynx and then ejected into the environment (Figure 3.3, A). This observation was made using starved, *gur-3(ok2245)* mutant animals carrying an unidentified bacterial contaminant in their intestines, so multiple variables might account for this exceptional behavior. Entomopathogenic nematodes can vomit to infect host insects with pathogenic bacteria (Chiche, 2007), so this behavior is not unprecedented in nematodes. If this behavior could be reliably replicated

in the lab, it would afford a fascinating opportunity to observe how the pharyngeal nervous system orchestrates a functional inversion of a multi-compartmental neuromuscular system.

III. Identification of M1's neurotransmitter and downstream receptors

To determine the neurotransmitter or neurotransmitters used by M1 to produce spitting and burst pumping behavior, I performed a burst-pumping candidate screen of mutant animals defective in the production or release of a variety of neurotransmitters (Figure 3.4, A-J). Most mutants were grossly normal in their UV-induced burst pumping behavior. Mutants defective in the production or release of acetylcholine were severely defective for both feeding and burst pumping (Figure 3.4, A,B). Consistent with M1 being cholinergic, it expresses *unc-17,* the *C. elegans* vesicular acetylcholine transporter (Franks *et al.*, 2009). Additionally, *ric-3* mutants, which are defective in the maturation of nicotinic acetylcholine receptors (Halevi *et al.*, 2012), also resemble *unc-17* and *cha-1* mutants (Figure 3.4, C). The 5 Hz rate of feeding in the presence of food is controlled by the MC pacemaker neurons of the pharynx, which are likely cholinergic (Raizen *et al.*, 1995; McKay *et al.*, 2004). The burst-pumping defect is unlikely to be consequence of impaired MC function causing a general reduction in muscle excitability, because mutation of *eat-2*, a nicotinic acetylcholine receptor (nAChR) subunit required downstream of the MCs' for MC-dependent stimulation of pumping, leaves burst pumping intact (see Figure 2.5, D). Future M1-specific rescue experiments of *unc-17* and *cha-1* will clarify this question.

To determine the identity of acetylcholine receptors potentially functioning downstream of M1, I performed a burst-pumping candidate screen of animals mutant for each of 36 predicted acetylcholine receptors (Figure 3.5, A-Q') (*acr-9*, which encodes a nAChR subunit, was not tested because null mutations result in lethality). Mutations in no single receptor subunit produced a striking defect, but mutations in *acr-6*, *acr-7*, and *acr-24*, which encode nAChR subunits, and in *gar-1*, which encodes a muscarinic acetylcholine receptor subunit, produced modest defects in burst pumping rates (Figure 3.5, F,G,H,Z,A',O') . Future efforts in this area will require making double-, triple-, and quadruple-mutants amongst these genes to look for enhancement of their burst pumping defects. Identifying receptors downstream of M1 would facilitate the analysis of the effects of M1 on pharyngeal muscle activity and could clarify some aspects of the spatially restricted calcium signals reported in Chapter 2.

IV. Determination of the molecular sensory transduction pathway that controls the M1 response to light

The sensory transduction mechanisms downstream of LITE-1 and GUR-3 function are incompletely understood (see Chapter 1). I performed a preliminary candidate screen of putative LITE-1 effectors based on genes that were found to be required for phototransduction in the putative photoreceptor ASJ (Figure 3.6) (Ward *et al.*, 2008; Liu *et al.*, 2010). This screen identified significant burst pumping defects in triple-mutant animals lacking the CNG channel subunit-encoding genes *cng-1*, *cng-3*, and *tax-4,* with minor defects in *cng-4* and *tax-4* single mutants (Figure 3.6, G,I,J). Further genetic verification and analysis of these results might allow the burst pumping

phenotype to be developed into an expedient method of testing the function of genes potentially acting in the LITE-1 phototransduction pathway, which could inform our understanding of *lite-1*'s function in sensory biology.

Figure 3.1

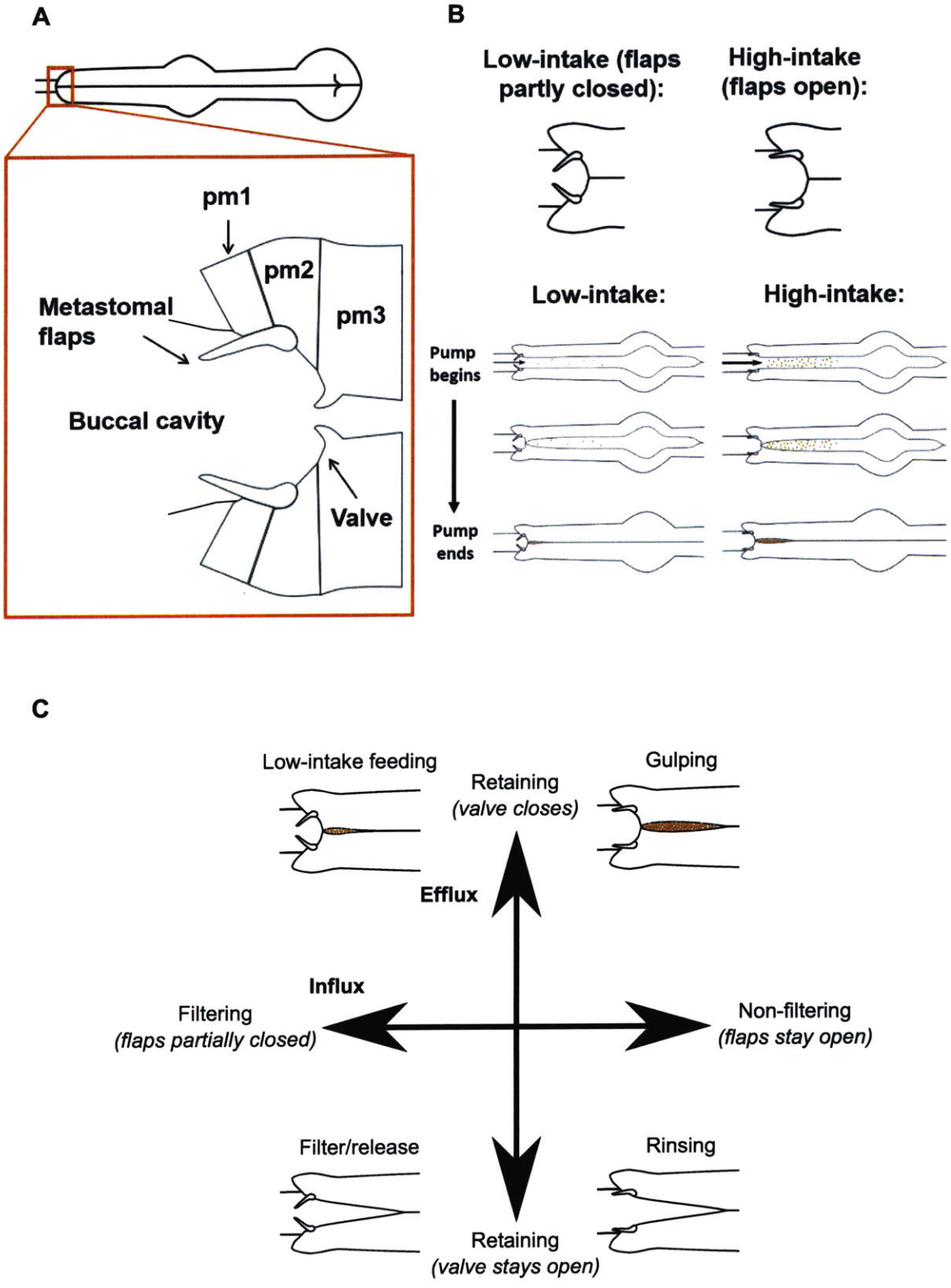
A
pm1
pm2
pm3
Metastomal flaps
Buccal cavity
Valve
B
Low-intake (flaps partly closed):
High-intake (flaps open):
Low-intake:
High-intake:
Pump begins
Pump ends
C
Low-intake feeding
Retaining
(valve closes)
Gulping
Efflux
Influx
Filtering
(flaps partially closed)
Non-filtering
(flaps stay open)
Filter/release
Rinsing
Retaining
(valve stays open)

Figure 3.1: consequences of metastomal flap position for food intake.

A) Anatomy of the anterior pharynx illustrating the buccal cavity, metastomal flaps, pharyngeal valve, and pharyngeal muscles pm1, pm2, and pm3.

B) Illustration of metastomal flap positions in low- and hight-intake pumping and consequences for food intake. During low-intake pumps, the metastomal flaps are partially closed and food gradually filters into the pharyngeal lumen. During high-intake pumps, the metastomal flaps are opened such that food passes freely through the buccal cavity into the pharyngeal lumen, resulting in the ingestion of many particles.

(C) Categorization of pumps based on the state of the pharyngeal valve and metastomal flaps and subsequent consequences for food intake.

Figure 3.2

A

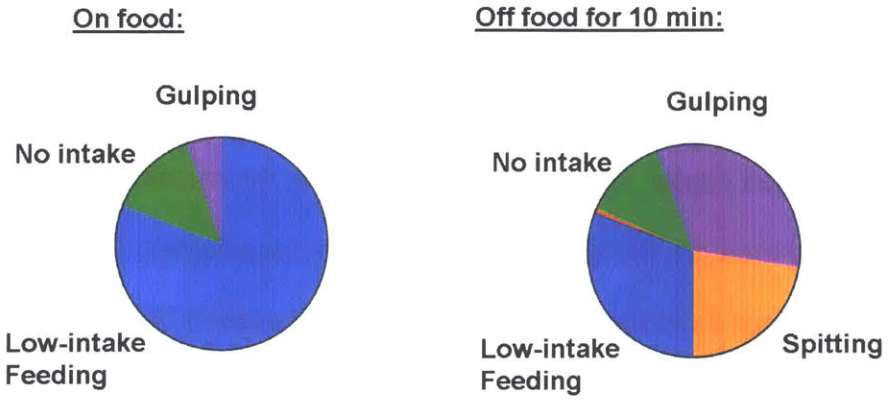
On food:
Gulping
No intake
Low-intake Feeding
Off food for 10 min:
Gulping
No intake
Low-intake Feeding
Spitting

Figure 3.2: Pump-type distribution changes when worms are removed from food.

(A) the distribution of pump types changes when animals are removed from food. n_{OnFood}= 9 worms, 394 pumps; $n_{OffFood}$= 8 worms, 150 pumps. p=0.0001, Chi-squared test.

Figure 3.3

A

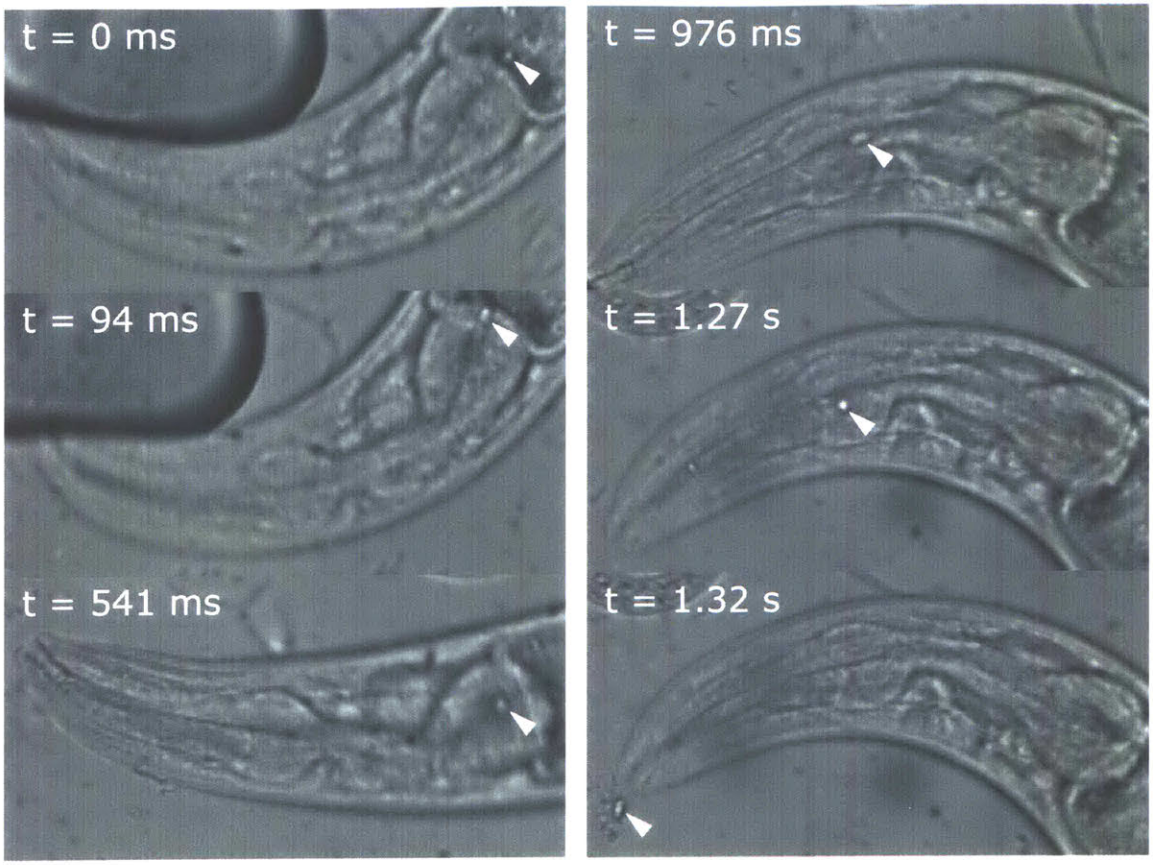

Figure 3.3: *C. elegans* vomiting behavior.

(A) Selected frames from a video of a *gur-3(ok2245)* animal vomiting. The white arrowheads indicate an object that begins in the intestine, is pumped backward through each pharyngeal compartment, and is ultimately expelled.

Figure 3.4

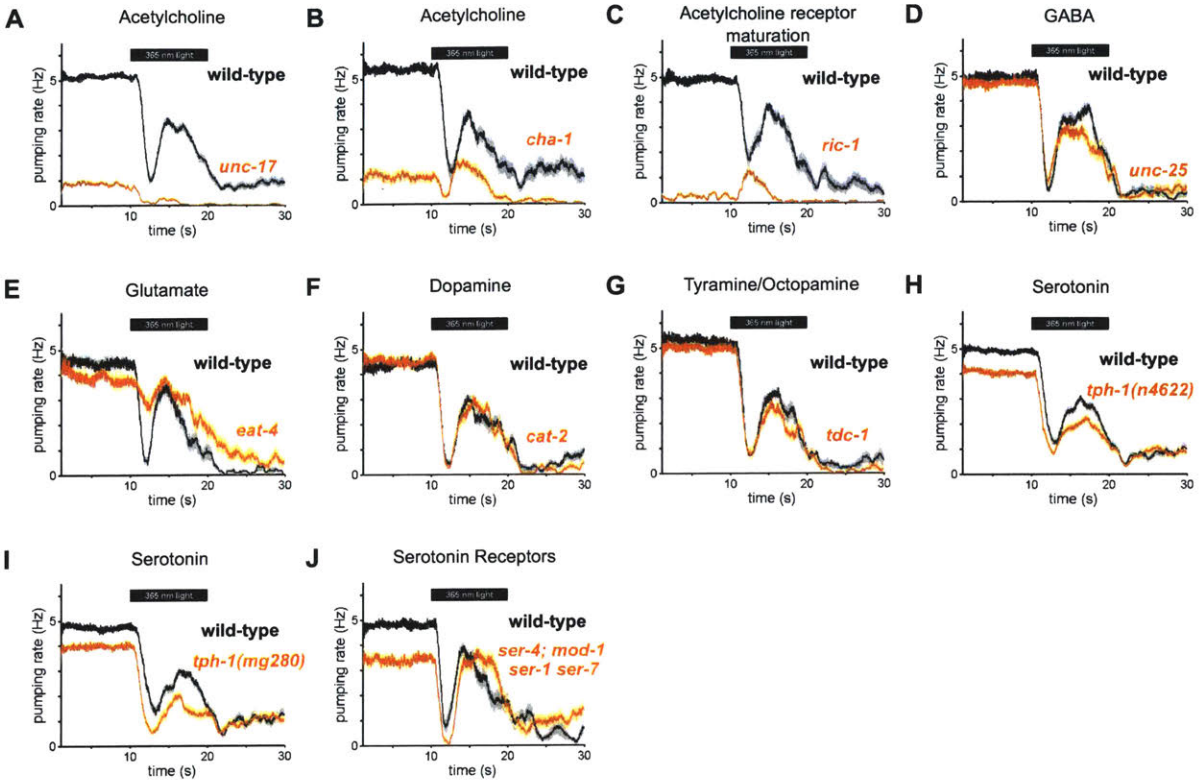
A
Acetylcholine
wild-type
unc-17
B
Acetylcholine
wild-type
cha-1
C
Acetylcholine receptor maturation
wild-type
ric-1
D
GABA
wild-type
unc-25
E
Glutamate
wild-type
eat-4
F
Dopamine
wild-type
cat-2
G
Tyramine/Octopamine
wild-type
tdc-1
H
Serotonin
wild-type
tph-1(n4622)
I
Serotonin
wild-type
tph-1(mg280)
J
Serotonin Receptors
wild-type
ser-4; mod-1
ser-1 ser-7
pumping rate (Hz)
time (s)

Figure 3.4: response of neurotransmitter mutants to 365 nm light.

(A) *unc-17(e245)* vesicular acetylcholine transporter mutants defective in vesicular acetylcholine import were severely defective in both feeding and burst pumping. n = 60 worms.

(B) *cha-1(p1152)* choline acetyltransferase mutants defective in acetylcholine synthesis were severely defective in both feeding and burst pumping. n = 20 worms.

(C) *ric-3(md158)* mutants defective in nicotinic acetylcholine receptor maturation were severely defective in both feeding and burst pumping. n = 20 worms.

(D) *unc-25(e156)* glutamate decarboxylase mutants defective in GABA synthesis were normal in burst pumping. n = 20 worms.

(E) *eat-4(ky6)* vesicular glutamate transporter mutants defective in vesicular glutamine import were defective in acute inhibition but normal in burst pumping. n = 20 worms.

(F) *cat-2(e1113)* tyrosine hydroxylase mutants defective in dopamine synthesis were normal in burst pumping. n = 20 worms.

(G) *tdc-1(n3420)* tyrosine decarboxylase mutants defective in tyramine and octopamine synthesis were normal in burst pumping. n = 20 worms.

(H) *tph-1(n4622)* tryptophan hydroxylase mutants defective in serotonin synthesis were mildly defective in both feeding and burst pumping. n = 20 worms.

(I) *tph-1(mg280)* tryptophan hydroxylase mutants defective in serotonin synthesis were mildly defective in both feeding and burst pumping. n = 20 worms.

(J) *ser-4(ok512); mod-1(ok103); ser-1(ok345) ser-7(tm1325)* quadruple serotonin receptor mutants were defective in feeding but wild type burst pumping. n = 20 worms.

Figure 3.5, p. 1

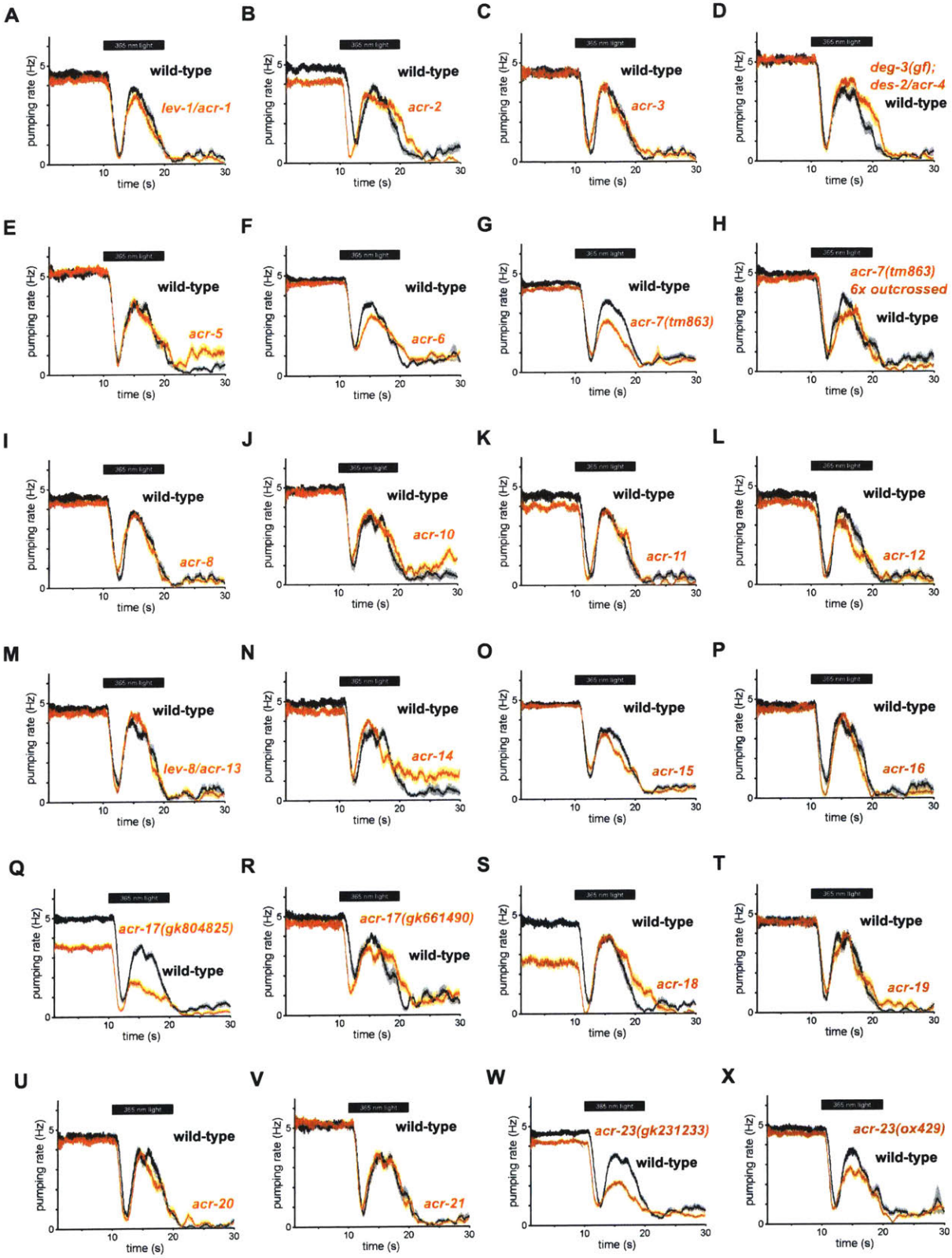
A
wild-type
lev-1/acr-1
B
wild-type
acr-2
C
wild-type
acr-3
D
deg-3(gf);
des-2/acr-4
wild-type
E
wild-type
acr-5
F
wild-type
acr-6
G
wild-type
acr-7(tm863)
H
acr-7(tm863)
6x outcrossed
wild-type
I
wild-type
acr-8
J
wild-type
acr-10
K
wild-type
acr-11
L
wild-type
acr-12
M
wild-type
lev-8/acr-13
N
wild-type
acr-14
O
wild-type
acr-15
P
wild-type
acr-16
Q
acr-17(gk804825)
wild-type
R
acr-17(gk661490)
wild-type
S
wild-type
acr-18
T
wild-type
acr-19
U
wild-type
acr-20
V
wild-type
acr-21
W
acr-23(gk231233)
wild-type
X
acr-23(ox429)
wild-type
pumping rate (Hz)
time (s)

Figure 3.5, p. 2

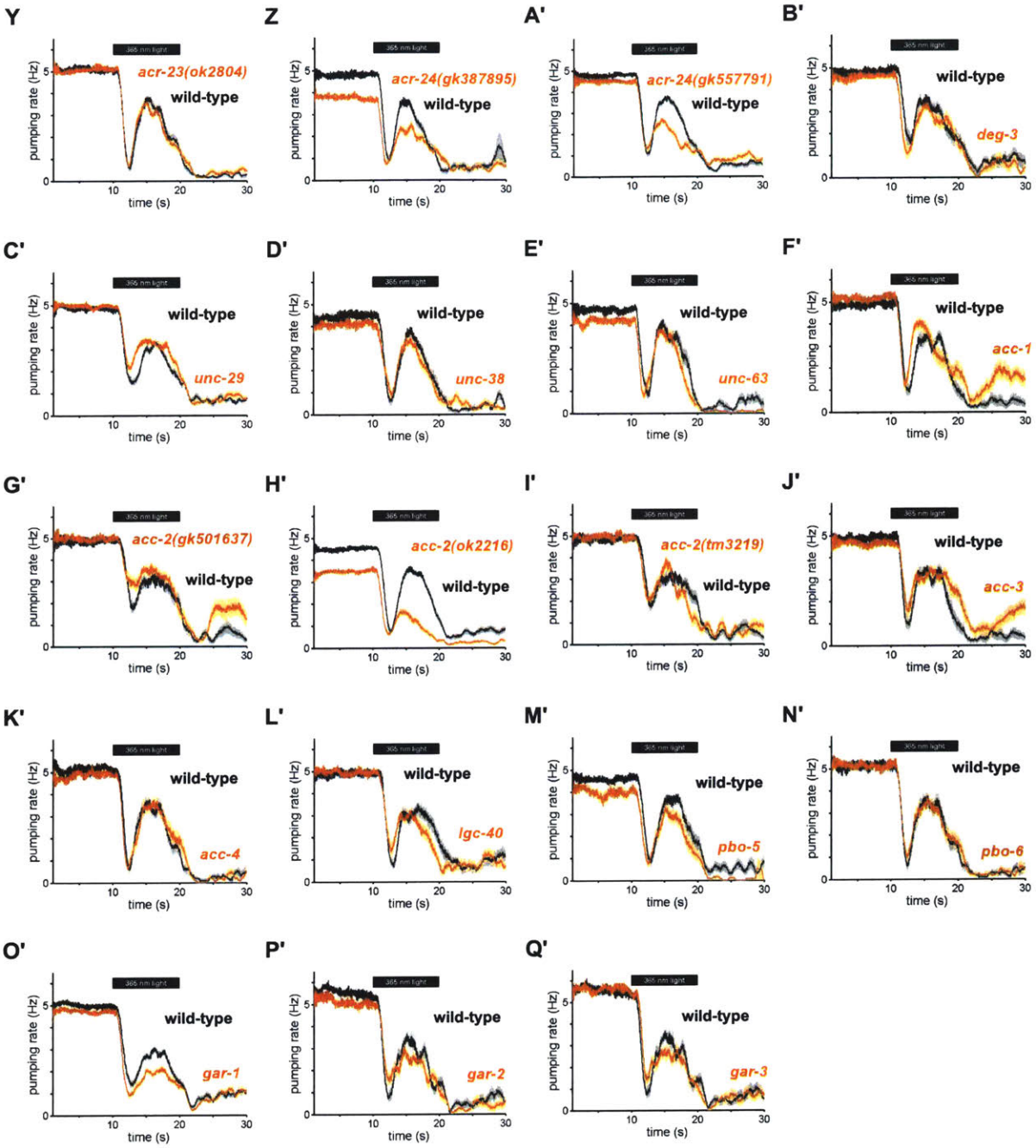
Y
acr-23(ok2804)
wild-type
Z
acr-24(gk387895)
wild-type
A'
acr-24(gk557791)
wild-type
B'
wild-type
deg-3
C'
wild-type
unc-29
D'
wild-type
unc-38
E'
wild-type
unc-63
F'
wild-type
acc-1
G'
acc-2(gk501637)
wild-type
H'
acc-2(ok2216)
wild-type
I'
acc-2(tm3219)
wild-type
J'
wild-type
acc-3
K'
wild-type
acc-4
L'
wild-type
lgc-40
M'
wild-type
pbo-5
N'
wild-type
pbo-6
O'
wild-type
gar-1
P'
wild-type
gar-2
Q'
wild-type
gar-3
365 nm light
pumping rate (Hz)
time (s)

Figure 3.5: Response of acetylcholine receptor mutants to 365 nm light.

(A) *lev-1(e211)* nicotinic acetylcholine receptor mutants were normal in burst pumping. n = 20 worms.

(B) *acr-2(n2595 n2420)* nicotinic acetylcholine receptor mutants were normal in burst pumping. n = 20 worms.

(C) *acr-3(ok2049)* nicotinic acetylcholine receptor mutants were normal in burst pumping. n = 20 worms.

(D) *deg-3(u662); des-2/acr-4* nicotinic acetylcholine receptor mutants were normal in burst pumping. n = 20 worms.

(E) *acr-5(ok180)* nicotinic acetylcholine receptor mutants were normal in burst pumping. n = 20 worms.

(F) *acr-6(3723)* nicotinic acetylcholine receptor mutants were subtly defective in burst pumping. n = 60 worms.

(G) *acr-7(tm863)* nicotinic acetylcholine receptor mutants were modestly defective in burst pumping. n = 60 worms.

(H) *acr-7(tm863)* nicotinic acetylcholine receptor mutants (6x outcrossed) were subtly defective in burst pumping. n = 20 worms.

(I) *acr-8(ok1240)* nicotinic acetylcholine receptor mutants were normal in burst pumping. n = 20 worms.

(J) *acr-10(tm2515)* nicotinic acetylcholine receptor mutants were normal in burst pumping. n = 20 worms.

(K) *acr-11(gk827759)* nicotinic acetylcholine receptor mutants were normal in burst pumping. n = 20 worms.

(L) *acr-12(ok367)* nicotinic acetylcholine receptor mutants were normal in burst pumping. n = 20 worms.

(M) *lev-8/acr-13(x15)* nicotinic acetylcholine receptor mutants were normal in burst pumping. n = 20 worms.

(N) *acr-14(tm5819)* nicotinic acetylcholine receptor mutants were normal in burst pumping. n = 20 worms.

(O) *acr-15(ok1214)* nicotinic acetylcholine receptor mutants were normal in burst pumping. n = 20 worms.

(P) *acr-16(ok789)* nicotinic acetylcholine receptor mutants were normal in burst pumping. n = 20 worms.

(Q) *acr-17(gk804825)* nicotinic acetylcholine receptor mutants were defective in both eating and burst pumping. n = 40 worms.

(R) *acr-17(gk661490)* nicotinic acetylcholine receptor mutants were normal in burst pumping. n = 20 worms.

(S) *acr-18(gk324494)* nicotinic acetylcholine receptor mutants were defective and feeding but normal in burst pumping. n = 20 worms.

(T) *acr-19(ok967)* nicotinic acetylcholine receptor mutants were normal in burst pumping. n = 20 worms.

(U) *acr-20(gk161737)* nicotinic acetylcholine receptor mutants were normal in burst pumping. n = 20 worms.

(V) *acr-21(ok1314)* nicotinic acetylcholine receptor mutants were normal in burst pumping. n = 20 worms.

(W) *acr-23(gk231233)* nicotinic acetylcholine receptor mutants were subtly defective in feeding and defective in burst pumping. n = 60 worms.

(X) *acr-23(ox429)* nicotinic acetylcholine receptor mutants were subtly defective in burst pumping. n = 60 worms.

(Y) *acr-23(ok2804)* nicotinic acetylcholine receptor mutants were normal in burst pumping. n = 20 worms.

(Z) *acr-24(gk387895)* nicotinic acetylcholine receptor mutants were defective in both feeding and burst pumping. n = 40 worms.

(A') *acr-24(gk557791)* nicotinic acetylcholine receptor mutants were defective in burst pumping. n = 60 worms.

(B') *deg-3(u773)* nicotinic acetylcholine receptor mutants were normal in burst pumping. n = 20 worms.

(C') *unc-29(e1072)* nicotinic acetylcholine receptor mutants were normal in burst pumping. n = 60 worms.

(D') *unc-38(e264)* nicotinic acetylcholine receptor mutants were normal in burst pumping. n = 20 worms.

(E') *unc-63(x13)* nicotinic acetylcholine receptor mutants were normal in burst pumping. n = 20 worms.

(F') *acc-1(tm3268)* acetylcholine-gated chloride channel mutants were normal in burst pumping. n = 20 worms.

(G') *acc-2(gk501637)* acetylcholine-gated chloride channel mutants were normal in burst pumping. n = 20 worms.

(H') *acc-2(ok2216)* acetylcholine-gated chloride channel mutants were defective in feeding and burst pumping. n = 60 worms.

(I') *acc-2(tm3219)* acetylcholine-gated chloride channel mutants were normal in burst pumping. n = 20 worms.

(J') *acc-3(tm3674)* acetylcholine-gated chloride channel mutants were normal in burst pumping. n = 20 worms.

(K') *acc-4(ok2371)* acetylcholine-gated chloride channel mutants were normal in burst pumping. n = 20 worms.

(L') *lgc-40(tm3377)* acetylcholine-gated chloride channel mutants were normal in burst pumping. n = 20 worms.

(M') *pbo-5(gk963058)* nicotinic acetylcholine receptor family mutants were normal in burst pumping. n = 20 worms.

(N') *pbo-6(ok1564)* nicotinic acetylcholine receptor family mutants were normal in burst pumping. n = 20 worms.

(O') *gar-1(ok755)* muscarinic acetylcholine receptor mutants were defective in burst pumping. n = 60 animals.

(P') *gar-2(ok520)* muscarinic acetylcholine receptor mutants were normal in burst pumping. n = 20 worms.

(Q') *gar-3(gk337)* muscarinic acetylcholine receptor mutants were normal in burst pumping. n = 20 worms.

Figure 3.6

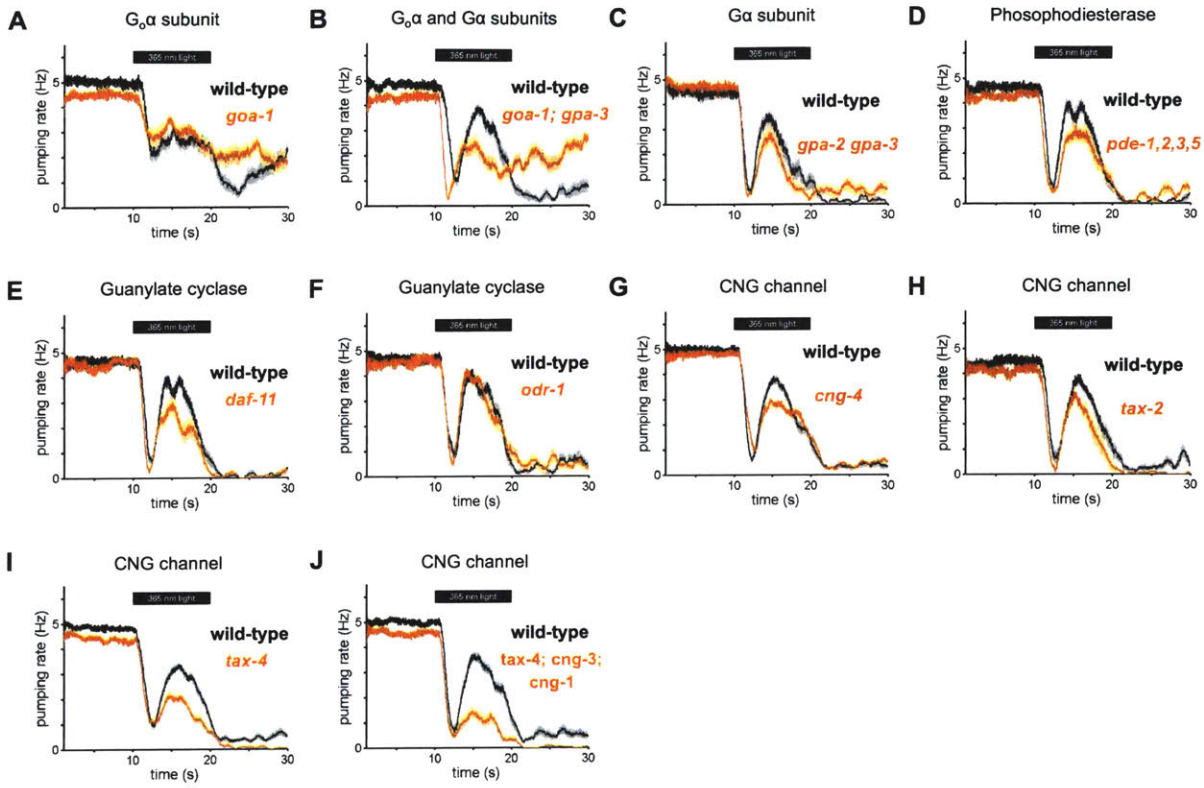
A
G$_o$α subunit
wild-type
goa-1
B
G$_o$α and Gα subunits
wild-type
goa-1; gpa-3
C
Gα subunit
wild-type
gpa-2 gpa-3
D
Phosphodiesterase
wild-type
pde-1,2,3,5
E
Guanylate cyclase
wild-type
daf-11
F
Guanylate cyclase
wild-type
odr-1
G
CNG channel
wild-type
cng-4
H
CNG channel
wild-type
tax-2
I
CNG channel
wild-type
tax-4
J
CNG channel
wild-type
tax-4; cng-3; cng-1
pumping rate (Hz)
time (s)

Figure 3.6: candidate testing of potential *lite-1* effectors.

(A) *goa-1(n1134)* mutants were not defective in their response to light. n = 20 worms.

(B) *goa-1(n1134); gpa-3(gk35)* double mutants might have a subtly defective response to light. n = 20 worms.

(C) *gpa-2(pk16); gpa-3(gk35)* mutants might have a subtly defective response to light. n = 20 worms.

(D) *pde1(nj57) pde5(nj49); pde3(nj59); pde2(tm3098)* quadruple phosphodiesterase mutants might be subtly defective in the response to light. n = 20 worms.

(E) *daf-11(m47ts)* guanylate cyclase mutants were mildly defective in their response to light. n=20 worms.

(F) *odr-1(n1936)* guanylate cyclase mutants were not defective in their response to light. n = 20 worms.

(G) *cng-4(tm5036)* cyclic-nucleotide gated channel mutants were mildly defective in their response to light. n = 40 worms.

(H) *tax-2(p671)* cyclic-nucleotide gated channel mutants might have a subtle defect in their response to light. n = 20 worms.

(I) *tax-4(p678)* mutants were moderately defective in their response to light. n = 60 worms.

(J) *tax4(p678); cng3(jh113); cng1(jh111)* triple cyclic-nucleotide gated channel mutants were defective in their response to light. n = 40 worms.

References

Bhatla, N., and Horvitz, H.R. (2015). Light and hydrogen peroxide inhibit *C. elegans* feeding through gustatory receptor orthologs and pharyngeal neurons. Neuron *85*, 804–818.

Ciche, T. (2007). The biology and genome of *Heterorhabditis bacteriophora*, WormBook, ed. The *C. elegans* Research Community, WormBook, doi/10.1895/wormbook.1.135.1, http://www.wormbook.org.

Dallière, N., Bhatla, N., Luedtke, Z., Ma, D.K., Woolman, J., Walker, R.J., Holden-Dye, L., and O'Connor, V. (2015). Multiple excitatory and inhibitory neural signals converge to fine-tune *Caenorhabditis elegans* feeding to food availability. The FASEB Journal *30*, 836–848.

Fang-Yen, C., Avery, L., and Samuel, A.D.T. (2009). Two size-selective mechanisms specifically trap bacteria-sized food particles in *Caenorhabditis elegans*. PNAS *106*, 20093–20096.

Franks, C.J., Murray, C., Ogden, D., O'Connor, V., and Holden-Dye, L. (2009). A comparison of electrically evoked and channel rhodopsin-evoked postsynaptic potentials in the pharyngeal system of Caenorhabditis elegans. Invert Neurosci *9*, 43–56.

Halevi, S., McKay, J., Palfreyman, M., Yassin, L., Eshel, M., Jorgensen, E., and Treinin, M. (2002). The C.elegans ric-3 gene is required for maturation of nicotinic acetylcholine receptors. The EMBO Journal *21*, 1012–1020.

Liu, J., Ward, A., Gao, J., Dong, Y., Nishio, N., Inada, H., Kang, L., Yu, Y., Ma, D., Xu, T., et al. (2010). *C. elegans* phototransduction requires a G protein–dependent cGMP pathway and a taste receptor homolog. Nature Neuroscience *13*, 715–722.

McKay, J.P., Raizen, D.M., Gottschalk, A., Schafer, W.R., and Avery, L. (2004). *eat-2* and *eat-18* are required for nicotinic neurotransmission in the *Caenorhabditis elegans* pharynx. Genetics *166*, 161–169.

Raizen, D.M., Lee, R.Y., and Avery, L. (1995). Interacting genes required for pharyngeal excitation by motor neuron MC in *Caenorhabditis elegans*. Genetics *141*, 1365–1382.

Ward, A., Liu, J., Feng, Z., and Xu, X.Z.S. (2008). Light-sensitive neurons and channels mediate phototaxis in *C. elegans*. Nature Neuroscience *11*, 916–922.